ARYLOXY TUNGSTEN-BASED CLASSICAL CATALYTIC SYSTEMS AND GROUP 14 METAL-CONTAINING DIENES IN ACYCLIC DIENE METATHESIS POLYMERIZATION

By

FERNANDO JOSE GOMEZ

A DISSERTATION PRESENTED TO THE GRADUATE SCHOOL
OF THE UNIVERSITY OF FLORIDA IN PARTIAL FULFILLMENT
OF THE REQUIREMENTS FOR THE DEGREE OF
DOCTOR OF PHILOSOPHY

UNIVERSITY OF FLORIDA

2000

A mi madre,
por soltar siempre mi mano
para que yo recogiera canelitas.

A la memoria de mi abuelo Mario
quien me enseñó que un hombre debe ser
honesto, trabajador y buen amigo.

To my mother,
for she always let my hand go
so I could pick up canelitas.

To the memory of my grandfather Mario,
who taught me that a man should be
honest, a hard worker and a good friend.

ACKNOWLEDGMENTS

Near or far, the infinite confidence and support I found in my family made every day possible. No words can describe the way in which their hands helped mine to get things done through optimism, strength, and the promise of better times for all of us.

This learning experience could have not been possible without the constant scientific and personal interaction with the past and present members of the Butler Polymer Research Laboratory, especially with those in the Wagener group who kept alive my interests in our chemistry. Special thanks go to Dr. Mark Watson, Dr. Shane Wolfe, Dr. Jason Portmess, and Dr. Debra Tindall for turning into friendship their support, guidance, and acceptance. Very special gratitude is expressed to Dr. Tammy Davidson, for she was a caring and supportive friend in the hardest of times. The cultural and racquetball experiences with Gayanga Weeraserekera are also appreciated.

A large group of friends from every corner of Latin America and especially from my missed Colombia were my home away from home and helped me tremendously through these years. Our experiences together made me proud of our culture and heritage. Among these, the support and unconditional friendship of Roberto Bravo, Edwin Saldarriaga, and María and Mauricio Ospina will always be remembered.

Thanks to Claudia Madrigal, for offering me the caring hands, companionship, and love that made the end of my graduate career much easier.

The contributions to the scientific work described herein by Dr. Andrew Bell (BF Goodrich), Dr. Jerry Feldman (DuPont), Dr. Kirk Abbey (LORD Corp.), Michael Manak, Nelson Guzmán, Gabriela Feldberg, and Dr. Carlos Ortiz were instrumental for the execution of this research. Thanks also to Professors Lisa McElwee-White, James Boncella, William Dolbier, and Christopher Batich for serving on my graduate committee and for sharing with me their experiences every time I wanted to *talk chemistry* with them. The prompt and invaluable help of the spectroscopic services staff, especially Dr. Khalil Abboud, Dr. David Powell, and Dr. Ion Ghiviriga, is also acknowledged.

Thanks also to the polymer chemistry office staff, and very especially to Mrs. Lorraine Williams, for always having the answers to my questions.

The financial support provided by LORD Corporation (Cary, NC) and the National Science Foundation is highly appreciated.

Finally, eternal gratitude is extended to Professor Kenneth B. Wagener, for being a true mentor, for giving me the appropriate amount of opportunity and advice I needed, and for sharing with me his exemplary research, teaching, and life philosophy.

TABLE OF CONTENTS

Abstract of Dissertation Presented to the Graduate School
of the University of Florida in Partial Fulfillment of the
Requirements for the Degree of Doctor of Philosophy

ARYLOXY TUNGSTEN-BASED CLASSICAL CATALYTIC SYSTEMS AND GROUP 14 METAL-CONTAINING DIENES IN ACYCLIC DIENE METATHESIS POLYMERIZATION

By

Fernando José Gómez

May 2000

Chairman: Kenneth B. Wagener
Major Department: Chemistry

The design of a methodology for the acyclic diene metathesis (ADMET) polymerization of hydrocarbon and ester dienes using classical catalytic systems composed of aryloxide complexes of tungsten and tin-based activators is presented. The experimental conditions explored afford clean, linear polymers of high molecular weight.

The attributes of the tungsten complexes investigated were extrapolated to include new precatalyst structures, which demonstrated their applicability not only in ADMET polymerization, but also in other metathesis processes such as ring opening metathesis polymerization and ring closing metathesis.

The nature of the formation of the actual catalytic species in the mentioned classical systems motivated the investigation of a synthetic scheme towards ADMET

polycarbostannanes in which stannadienes act as both monomers and activators of the catalytic systems, and its results are also presented. This synthetic approach afforded tin-containing ADMET polymers that exhibit interesting thermal properties such as high ceramic yields and low glass transition temperatures.

ADMET polymerization was used in the synthesis of new tin-containing polymers, in an effort to investigate the effect of structure modification on their physicochemical properties. These include unsaturated polymers containing the dimethyl- or diphenylstannane moiety along the polymer backbone. A methodology for the synthesis of organometallic polymers containing oligostannane segments was devised and used in their preparation.

Complementing the organometallic polymer structures studied, ADMET polymers were also synthesized from germanadienes, providing access to linear, unsaturated germanium-containing polymers.

CHAPTER 1
INTRODUCTION

Synthetic polymeric materials occupy a privileged position in modern society, for they have become indispensable. From commodity plastics to specialty polymers, the field of polymer synthesis is challenged everyday with demands for new materials and efficient polymerization processes. The interaction between the commercial, engineering and scientific activities involved in polymer technology seems to be shaped as a constant quest for developments, and as chemists we are responsible for discovery.

Long before our time others set the frame-theory onto which macromolecular science is inscribed. The fact that a group of substances behaved uniquely when compared to chemicals known at the time and the fact that the similarities with respect to known natural polymers were not clear, were instrumental for the birth of a new science: polymer science. Within this field, nature is the greatest *maker*, and natural structures such as polysaccharides, proteins, and even human tissue are its masterpieces of polymer synthesis.

With functions and properties as essential as those exhibited by natural polymers, a parallel exploration of sources and targets for synthetic polymers was to be expected at a point of chemical maturity in the development of scientific knowledge. With a little help from serendipity, several polymerization schemes towards synthetic polymers were

developed following the acceptance of macromolecular theory, and as a result synthetic polymers can be found in virtually every aspect of modern life.

This dissertation can be contemplated within the general field of polymer synthesis from both of the approaches described above, namely the synthesis of new materials and the exploration of alternatives to known polymerization processes.

Addition and Condensation Polymerization, Chain and Step Polymerization

Macromolecule Formation: The Concepts

The terms *addition* and *condensation* refer to the *propagation* reaction, and describe the *type of reaction* involved in linking molecules for polymer formation. By classifying a polymerization reaction as addition or condensation, we are making use of the same concepts used in organic chemistry. Some straightforward examples of addition reactions are the hydrosilation of olefins, cycloadditions (e.g., Diels-Alder) and hydrogenation of alkynes. The most relevant characteristic of addition reactions to our discussion is the fact that all of the fragments present in the reactant molecules can be found in the product. No formation of byproducts is observed. In a similar way, recurrence to some organic reactions classified as condensations is a helpful tool, and reactions such as esterifications and some coupling reactions (e.g., McMurray) exemplify this concept properly. In this case, a byproduct (condensate) is removed from the intended product (either by itself or as a conjugate).

Analogously, the terms *chain* and *step* also refer to the mode of propagation of a certain polymerization but describes *how macromolecules grow from monomers*. In the literature since as early as 1927 (Carothers 1927), this is arguably the most important classification of polymerization processes. It is essential for the understanding of not only the mechanistic details of a given polymerization scheme, but also for the effective prediction of some of the physical properties and possible applications of polymeric materials. It is imperative to describe and compare the main features of these two different propagation modes prior to the discussions of polymerization processes included in further sections of this work. For a comprehensive presentation of step and chain polymerization see Odian (1991).

In chain polymerization, an active species (e.g., a cation, a free radical) is generated in the first reaction called initiation. This active species reacts with the first monomer unit that gets incorporated, and a new active entity is generated. The reaction of this new species is the basic propagation phenomenon, and subsequent reactions of the growing chain with monomers will generate species with similar reactivities to that of the prior propagating species. For the sake of clarity, other important phenomena in chain polymerization (chain transfer, termination) will not be discussed.

In step polymerization no initiation step needs to be defined and with few exceptions, propagation reactions mark the beginning of the polymerization scheme. The first propagation event involves the reaction between two monomer units to yield a dimer, a molecule of increased size which contains the same functional groups that were present in the monomer, available for further reaction. Reactions of this dimer with another molecule of monomer yields a trimer, and the polymer size increases slowly as the

reaction proceeds. It is safe to assume that all of the species present in the reaction mixture at any given time exhibit the same functional group reactivity towards each other; this identical reactivity ensures the growth of the polymer after every propagation step produces a new molecule. A general scheme for step and chain (initiation and) propagation reactions is shown in Figure 1-1.

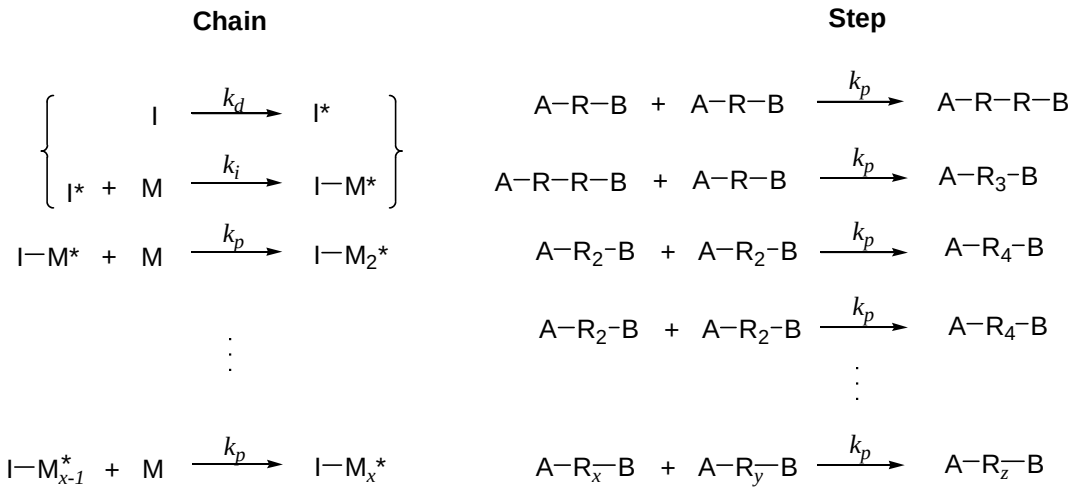

Figure 1-1. General schemes for propagation in chain and step polymerization.

The first evident and important difference between the two schemes is the time at which monomer disappears from the reaction. While in chain polymerization monomer units are present in the reaction mixture until the polymerization is completed, they disappear at very early stages in step polymerization. Analysis of a polymerizing mixture following a chain process reveals that monomer and (usually high molecular weight) polymer are present at any given time, while in the step polymerization case, the mixture consists of exclusively molecules of low to medium molecular weight. This is a

characteristic feature of the polymerization mechanisms, and is often used to distinguish between the two.

The average chain length is another significant difference between chain and step polymerization. High molecular weight polymer is formed at low % conversion in chain polymerization, while only until very high functional group conversion can it be found in a step process. This fact prompts for very specific experimental conditions for each process, and often has a significant effect on the molecular weight of the final product. It also suggests that since very high percentages of functional group conversion are needed in order to reach high molecular weight in step polymers, only a few organic reactions proceeding almost quantitatively can be used in the synthesis of macromolecules via step polymerization.

Among the organic reactions used in the synthesis of step polymers, condensation reactions are very common. In fact, most of the processes employed for step polymerizations involve condensations in their propagation reactions, and this stands as the reason why the terms condensation and step polymers are often –and sometimes carelessly– interchanged. The rationale behind the application of condensations in step polymerization is simple: condensation reactions are often equilibrium processes, and the removal of the condensate from the mixture ensures high conversion through shifting the equilibrium towards product.

From Small to Large Molecules: Functionality

The concept of functionality (f) in polymer chemistry helps understand the transition from small to large molecules. Functionality can be seen as an index, which

describes the *maximum number of possible connections a substrate can make when involved in the polymerization reaction,* whether the mechanism is chain or step polymerization. In order to yield a linear polymer, the value of f must be at least 2 for all the monomers in a specific polymerization scheme. As an example consider benzoic acid and methanol in an esterification reaction. Benzoic acid has only one carboxyl group which can be involved in the esterification: only one ester linkage could be formed with a molecule of benzoic acid (f =1). It is the same case for methanol: one is the maximum number of ester groups that can be formed in its esterification (f =1). As a consequence, the reaction of these two species will yield a small molecule (methyl benzoate) and not a polymer. The same analysis can be performed on terephthalic acid (f =2) and methanol (f =1), and it reveals that the product (dimethyl terephthalate) is not a polymeric structure. The number of ester linkages was given by the maximum value of f found. However, when two difunctional molecules (f =2) are reacted (e.g., terephthalic acid and ethyleneglycol) at very high functional group conversion, the result is a large macromolecule. This is the case for polymerization of hydroxyacids which contain one alcohol and one carboxyl functional group in the same molecule, yielding a difunctional monomer (f =2).

As mentioned before, a molecule's functionality depends on the polymerization scheme in which it is considered. For addition polymers (e.g., the free radical polymerization of styrene) the olefin bond has a functionality of 2, since two new (covalent) bonds can be formed upon its reaction.

From the analysis described above, it is easy to understand the effects of adding monomers with f values other than 2 to polymerization mixture. For example, the

reaction of a growing chain with a monofunctional molecule causes the chain growth to stop by incorporating a fragment contained in the monofunctional molecule at the chain termini. This monofunctional adduct is known as a *chain limiter*, and the technology based on its usage is widely used as a molecular weight control procedure. In a similar way, polymerizing systems with average functionalities greater than 2 causes branching and the inter-chain linkages are responsible for the formation of network and crosslinked structures. This phenomenon can be used in a systematic way, and synthetic strategies towards interesting polymer architectures such as star polymers can be devised. Odian (1991) presents an interesting and comprehensive treatise on functionality and its effect on polymer synthesis.

Olefin Metathesis

One of the most attractive transition metal-catalyzed processes available to today's chemist is olefin metathesis. Modern synthesis strategies of specialty polymers, fine chemicals, natural products, and even protein mimics reported in the last decade are just some representative examples of the fields in which olefin metathesis is finding its applications.

Several (almost simultaneous) observations led the way to realizing that olefin metathesis was the reaction operating in a series of chemical processes reported in the chemical literature between 1960 and 1964 (Truett 1960, Banks 1964), with precedent reports as early as 1957 in the patent literature (Eleuterio 1957). The pioneering work of

Calderon (1967,a,b) is attributed to be fundamental to this realization, as well as to coining the expression *olefin metathesis* to describe such reaction.

In a general way, olefin metathesis can be described as the apparent exchange of carbon moieties between a pair of double bonds in two alkene molecules. This is a true equilibrium process, which in some cases can be attained in seconds. A simple example is illustrated in Figure 1-2.

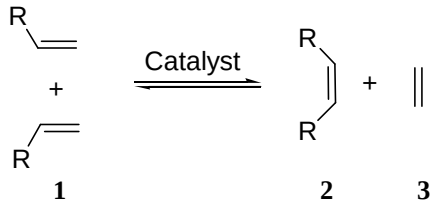

Figure 1-2. Olefin metathesis of a terminal alkene.

Although elusive at first, a consistent mechanistic scheme known today as the carbene/metallacyclobutane mechanism, was proposed by Hèrrison and Chauvin in 1971 (Hèrrison 1971). This proposal suggests that the active catalytic species is a metal carbene (an organometallic species containing a metal-carbon double bond), which mediates the exchange of the alkylidene portions between the two reactant olefins. The most important step in Chauvin's proposal, consists in the formation of a metallacyclobutane intermediate from the reaction of the metal carbene and an olefin. As an illustration, the mechanism by which the conversion depicted in Figure 1-2 proceeds is shown in Figure 1-3.

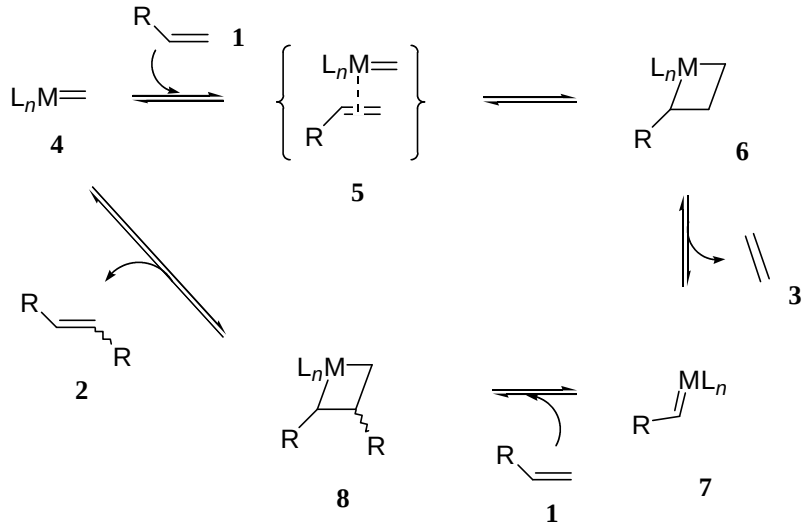

Figure 1-3. The carbene/metallacyclobutane mechanism illustrating the metathesis of a terminal alkene **1**.

The mechanism shown in Figure 1-3, begins with the methylidene **4**, which is believed to be the actual catalytic species and is generated in previous steps of the reaction (not shown). The reaction of a substrate molecule (**1**) with this alkylidene in a fashion that resembles a [2+2] cycloaddition forms the metallacycle **6**, a key intermediate present in the mechanism of every olefin metathesis process. (The formation of **6** is believed to proceed through the π-complex **5** (Tallarico 1997, Dias 1997) and the presence of this intermediate in our mechanistic discussion will be of significant importance in further sections of this work. In an analogous way, cleavage and formation of every metallacycle may involve π-complexes such as **5**, and their formation will be implied for the rest of our discussion.) The *productive* cleavage of **6** yields ethylene and the new alkylidene **7**, which upon reaction with a second molecule of substrate forms metallacycle **8** with a stereoselectivity mainly determined by the steric interactions

between the substituent R and the ligand set. The disproportionation of **8** produces the new internal olefin and regenerates methylidene **4**, which begins another catalytic cycle.

Several features are instrumental to understand both the outcome of metathesis processes in terms of the final structure and properties of the reaction products and the implications that both catalyst and substrate have on this mechanism. Ivin and Mol (Ivin 1997) have presented these in depth. Two key factors are of utmost importance in our discussion: the equilibrium nature of every step has to be considered, and the formation of the metallacyclobutane intermediates is considered to be the rate-determining step in every olefin metathesis application.

Exchange Metathesis

The reaction depicted in Figure 1-2 is the most basic example of one type of olefin metathesis known as *exchange metathesis*, in which two molecules of a terminal (monosubstituted) olefin react to yield ethylene and the disubstituted olefin **2**. This reaction proceeds with ease due to the low steric constraints imposed by only one substituent on the double bond, and it becomes of synthetic importance when the disubstituted olefin obtained as one of the products is of greater value than the starting material. The second olefin produced (ethylene) is in most cases treated as a byproduct, because of its low cost and of being a gas at standard conditions, which facilitates its removal from the reaction mixture ensuring not only essentially quantitative conversions but also very high product purity. The stereochemical outcome is in most cases determined by the type of catalyst used (geometry, ligand set, etc.,) as well as by the

extent of isomerization (also known as *cis : trans* equilibration) processes that may follow product formation.

Exchange metathesis can also take place with two disubstituted olefins as substrates. Its synthetic utility is given by the identity of the species formed in the equilibrium, as well as by the ease of separation of the olefins formed. This is a field of growing interest in the fields of fine chemicals and natural products.

The equilibration of more than one type of starting olefin is known as *cross metathesis*. Depending of the extent of substitution of the starting materials and considering all the possible stereoisomers obtainable, this reaction may lead to a very complex mixture of olefins coexisting at the equilibrium. This phenomenon which appears to render the reaction of low synthetic value, makes it a valuable tool in the construction of libraries for combinatorial chemistry (Brandli 1999, Giger 1999). Cross metathesis is also used when one of the equilibrium components is an olefin of very high value or otherwise very difficult to synthesize by other means. The exploration of selectivity issues associated with both sterics and electronics of the reacting olefins is a field of active research (Randall 1998).

Ring Closing Metathesis

Ring closing metathesis is arguably today's most important application of olefin metathesis. The advances in the field have been recently reviewed by Armstrong (1998), Furstner (1997), Grubbs (1998), Schuster (1997), and Wright (1999). It consists of the reaction of two tethered olefins to yield carbo- and heterocyclic structures, mainly from terminal dienes. A general scheme is shown in Figure 1-4.

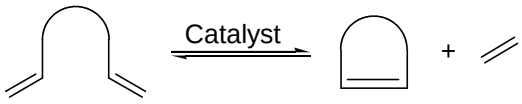

9 **10**

Figure 1-4. General scheme for ring closing metathesis (RCM)

Two factors of interest should be highlighted. First, in order to ensure an intramolecular reaction the experimental conditions often include high dilution. Second, the feasibility of a specific conversion must be analyzed taking into account kinetic and thermodynamic parameters given by the ring size (and thus ring strain), the effect of substituents, both from the steric and electronic point of view, and finally the compatibility between the functional groups present in the starting diene and the catalyst employed.

Ring Opening Metathesis Polymerization

As mentioned in the previous sections, olefin metathesis can be employed in the synthesis of ring systems of different sizes by the proper choice of experimental conditions and whenever the ring strain is sufficiently low (or virtually none) so that the equilibrium shown in Figure 1-4 favors the cyclic species **10**. Strained olefins (represented by **11** in Figure 1-5) are engaged in a different type of chemical equilibrium when exposed to a metathesis catalyst, and this process is known as ring opening metathesis polymerization (ROMP), chronologically the first method of polymer

synthesis that involves olefin metathesis. The general scheme for the conversion of a strained olefin into a polymer is shown in Figure 1-5.

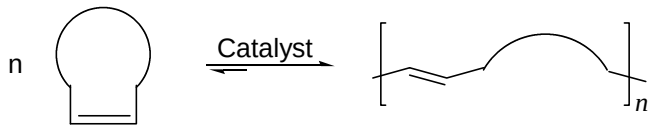

11 **12**

Figure 1-5. General scheme for ring opening metathesis polymerization (ROMP)

Although an equilibrium in principle, it is the case for most ROMPs to be considered irreversible. This is the consequence of a very favorable forward reaction due to the release of ring strain, making the overall conversion an exothermic process. The product of this chain polymerization is a macromolecule containing a double bond every repeat unit. Because of its widespread applications and its mechanistic beauty, ROMP has received a great deal of attention since its discovery in the fifties –in fact, some of the first examples of olefin metathesis were polymerizations of cycloolefins. Examples of common ROMP polymers include polynorbornene and polynorbornene derivatives and polydicyclopentadiene (PDCPD), a thermoset resin of high volume production in the United States.

The mechanism by which the ring opening metathesis polymerization of a cycloolefin proceeds is shown in Figure 1-6. First, the interaction between the cycloalkene **11** and a carbene (e.g., the methylidene **4**) yields the fused bicyclic structure **13**, which can be visualized as a substituted metallacyclobutane. When this ring cleaves productively, breakage of the σ bonds opens the two rings in a virtually irreversible step.

The ring strain is released and a new carbene is formed, this time at the termini of a linear unsaturated structure (**14**). It is at this point where the *chain* nature of the process should be noticed, since an active center is attaching at the chain end after the propagation step. From this point of view, it is also useful to visualize the carbene used (e.g., **4**) as an *initiator* and not as a *catalyst* since its original structure is not regenerated after the propagation cycle: a totally new chemical species is formed.

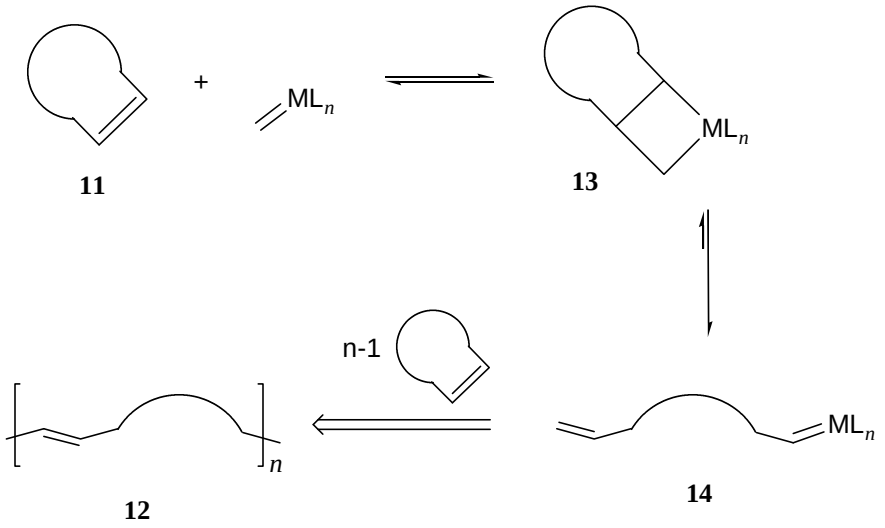

Figure 1-6. Mechanism of the ring opening metathesis polymerization (ROMP) of a strained cycloolefin.

In summary, ROMP is a chain polymerization that involves the olefin metathesis reaction in every propagation event and a metal carbene as the initiator. In depth discussion of this topic can be found in Odian (1997), as well as in reviews by Grubbs and Khosravi (Grubbs 1999), and Schrock (1990, 1993).

Acyclic Diene Metathesis Polymerization

ADMET (acyclic diene metathesis) polymerization is another method that provides access to linear, unsaturated hydrocarbon polymers and materials containing a wide variety of functionalities along the polymer backbone. Two recent reviews provide a comprehensive view of the ADMET chemistry (Tindall 1998, Davidson 1999). In general, ADMET polymerization can be described as the condensation of terminal dienes into unsaturated polymers, yielding a molecule of ethylene in every propagation step. Based on this description, ADMET falls in the category of *step-propagation condensation-type* polymerization (Odian 1991).

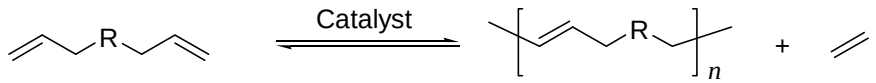

Figure 1-7. General scheme for acyclic diene metathesis polymerization.

Both hydrocarbon and functionalized polymers can be produced following the same synthetic scheme. As suggested by Figure 1-7, the incorporation of the functionality takes place at the monomer design step, making of ADMET a valuable tool in polymer synthesis. In addition, the rules that govern functional group tolerance as well as structure-reactivity relationships have been explored throughout the years and while obeyed, make useful monomers of a variety of terminal dienes. These have been used in the construction of interesting macromolecular architectures through grafting, hydrogenation, copolymerization and the condensation of telechelic dienes.

Mechanism and Kinetics

ADMET polymerization is an extension of an exchange metathesis reaction to terminal dienes, in which they are perfectly difunctional monomers (f =2). Because of being a step polymerization, ADMET requires high monomer purity and a single mechanistic event operating throughout the reaction in order to achieve the high conversion levels. Experimentally the polymerization is often run under bulk conditions in order to maximize the concentration of reactive functional groups, an essential requirement for the formation of high molecular weight polymer. These experimental conditions suggest that high monomer conversion is often associated with a dramatic increase in viscosity and with changes in the physical state of the polymerizing mixture which, in turn, affect the kinetic profile of the reaction.

With these two features in mind, we can analyze the proposed mechanism by which acyclic dienes are converted into unsaturated polymeric structures, illustrated in Figure 1-8. Again, for the sake of simplicity, we have illustrated the alkylidene in its most abbreviated form where the site L_nM refers to a moiety containing M, a transition metal, and a series of ligands (L_n). The *initiation* steps of the mechanism begin with the interaction between a metal alkylidene (**16**, top right corner) and an olefin site within the diene monomer (**14**). Consequently, a π-complex (**17** or **18**) forms between the metal alkylidene and the olefin site, which then collapses to a metallacyclobutane; both steps being reversible and thermoneutral in essence. Because of the two possible types of addition (α, in which the metal attaches to the *terminal* carbon of the double bond; or β, in which the metal attaches to the *internal* carbon of the olefin) two possible metallacyclobutanes (**19** and **20**) can be formed. Next, either metallacyclobutane

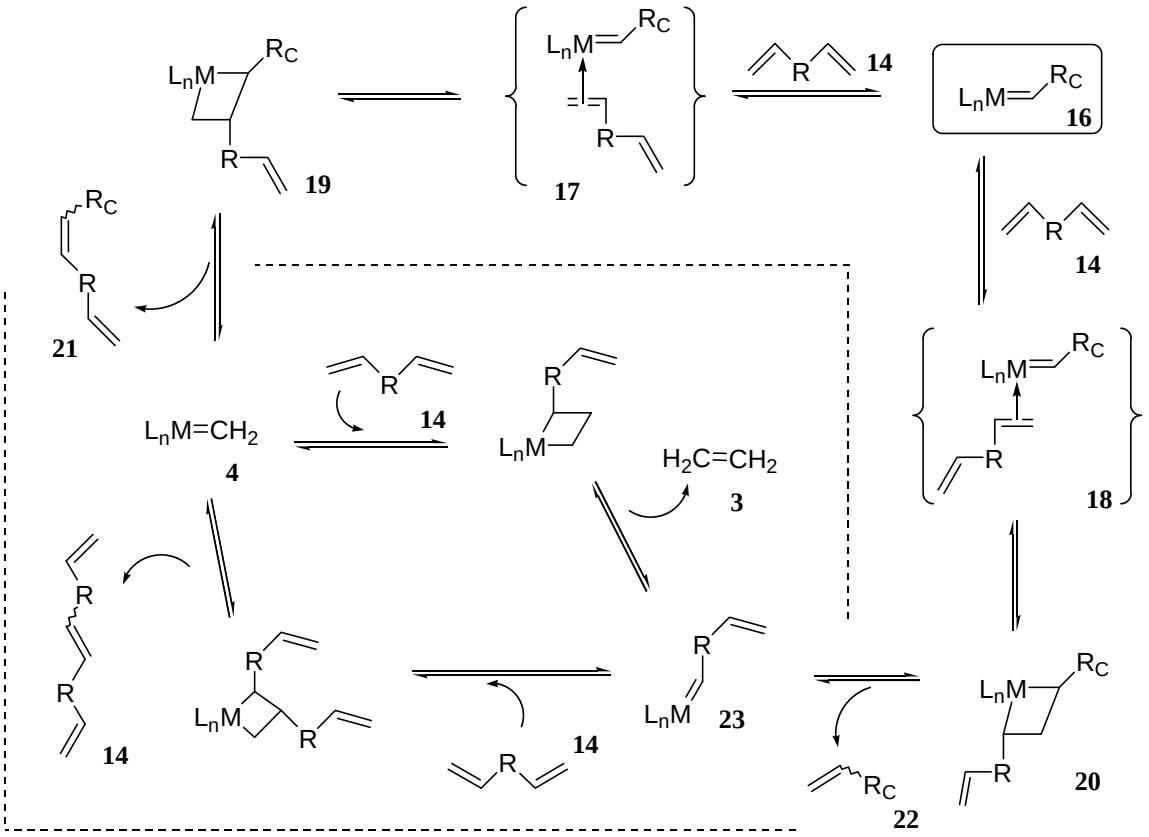

Figure 1-8. Mechanism for acyclic diene metathesis polymerization of a diene **14**.

ring disproportionates and in the case of α-addition, the new alkylidene is the methylidene **4**, eliminating part of the original complex as a new diene (**21**). In the case of β-addition, the metallacycle **20** cleaves to eliminate a new alkene containing a portion of the original complex (**22**), and placing the transition metal on the end of a propagating monomer structure (**23**).

It is at this point that the step condensation cycle (in the dotted inset) begins where another diene monomer (**14**) interacts with either alkylidene as has just been previously described: a π-complex is formed, rearranges into a metallacyclobutane, disproportionates eliminating either the condensate (**3**) or the propagating polymer chain (**15**), at the same

time regenerating either structure **4** or **23**, which continues the cycle. As shown in Figure 1-8, ethylene is ultimately evolved as the condensate in this reaction when α,ω-dienes are used, and polymer growth continues in a stepwise manner.

There is ample evidence for the validity of this mechanism. For example, the kinetics have been shown to be second order in monomer as is often observed in step polymerization chemistry (Wagener 1997b). Further, the molecular weight distribution that is obtained is in keeping with that statistically expected, i.e., a molecular weight distribution of 2.0 is often observed. In addition, steric factors play an important role, for if the olefin involved in π-complexation is sterically crowded, then the kinetics of the reactions are either dramatically slowed or polymerization is not observed at all. Finally, the presence of functional groups can alter the rates of reaction, again for reasons related to both the modification of the electronic properties of the transition metal found on the propagating monomer (i.e. structure **23** in Figure 1-8) and to inter- as well as intramolecular direct interactions between such functionality and the metal center (mostly of Lewis acid-base type).

From an enthalpic point of view (and as implied by the overall reaction shown in Figure 1-7) ADMET polymerization is essentially thermoneutral, making of this process an entropy-driven transformation. The observed kinetic parameters of ADMET polymerization strongly support the accepted mechanistic description. The reaction is second order in monomer resembling in this way other polycondensation reactions such as nylon or polyester synthesis (Wagener 1997b).

Functionality and ADMET Polymers

A wide variety of functionalities can be incorporated into ADMET polymers; and monomer design plays a crucial role in determining not only the feasibility of ADMET polymerization, but also the properties of the final product.

Ideally, any terminal diene can be homo- or copolymerized using ADMET chemistry. However, all of the transition metal complexes used in metathesis catalytic systems are inherently Lewis-acidic, and acid-base interactions may be of significant importance in terms of catalyst deactivation. Because of this, compatibility between the catalyst and the functional group contained in the monomer must be ensured through the exploration of different experimental conditions.

Another important factor to be considered is what is known as the *negative neighboring group effect*, which can be visualized as differences in reactivity exhibited by monomers that differ exclusively in the spacing between the reactive olefin and the functional group. This effect has been studied for a number of functionalities as well as quantified through kinetic studies (Wagener 1997b).

Last, of significant importance in any step polymerization is monomer purity. Besides the described effect of basic functionalities in catalyst decomposition, the presence of impurities containing groups that may become involved in metathesis chemistry (e.g. monoenes, alkynes) is detrimental to achieving high molecular weight polymer, and may lead to ill-defined structures.

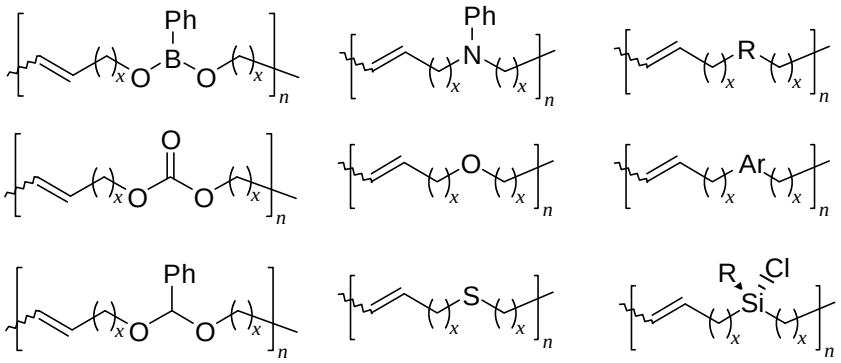

Figure 1-9. Representative structures of ADMET polymers synthesized to date.

The study of hydrocarbon monomers, both aliphatic and aromatic, has led to the understanding of many features of ADMET chemistry. Pure hydrocarbon monomers such as 1,9-decadiene are readily available and have been used as the standard for reactivity and compatibility mainly because of the absence of basic functionalities and their ease of purification.

Among the most interesting hydrocarbon ADMET polymers is 1,4-polybutadiene, obtained through the condensation of 1,5-hexadiene. ADMET polymerization offers the possibility of molecular weight control as well as easy end functionalization of this useful material. Other hydrocarbon ADMET polymers of interest include poly(*p*-phenylene)octylene and fully conjugated oligomers such as polyacetylene (Tao 1994) and poly(1,4-paraphenylenevinylene) (PPV) (Thorn-Csanyi 1999).

Several oxygenated functionalities have been incorporated in unsaturated polymers via ADMET. Among these, the synthesis and light induced crosslinking of polyethers, as well as the direct synthesis of polyalcohols via the condensation of hydroxydienes are of special importance from the materials point of view. ADMET polymerization can also provide novel synthetic approaches to other conventional step

polymers such as polycarbonate and polyesters. The utility of ADMET in the synthesis of otherwise hard to synthesize polymeric structures has been demonstrated in the synthesis of polymers bearing ketone and very especially, acetal functional groups. The liquid crystal properties of ADMET polyester-ethers containing mesogenic groups along the main chain have been explored, and constitute a very promising field for applications of ADMET polymers (Walba 1996).

The efficient incorporation of other heteroatoms along the backbone of unsaturated polymers via ADMET has led to a diversity of materials. For example, boronate- and amine-containing dienes have been efficiently converted to ADMET polymers. Polymers that contain silicon have been thoroughly explored, and constitute today an area of very active research towards useful materials. These include polycarbosilanes and polycarbosiloxanes, the latter being silicones with amount of hydrocarbon content along the backbone that are variable through monomer design, copolymerization and polymer modification. Another type of silicon-containing polymers synthesized using ADMET chemistry are polycarbochlorosilanes. This type of polymers are of special interest because of the possibility of accessing a variety of materials through polymer modification, mainly using macromolecular nucleophilic substitution.

Architectures and Modeling with ADMET

As mentioned earlier, monomer design plays a pivotal role in ADMET polymerization. Some structural features, polymer properties, and possible applications may be inferred as early as monomer conception and synthesis. Such predictability allows the use of ADMET chemistry in the synthesis of interesting macromolecular

architectures, as well as in the rational preparation of models for other polymerization schemes.

Among the different types of known copolymer structures, segmented copolymers are easily accessed using step-propagation chemistry. ADMET polymerization has been used in the preparation of this type of materials, which may exhibit unique properties such as microphase separation, ampiphilic behavior or increased blend compatibility. The synthetic scheme involves the design of diene-terminated oligomers (diene telechelomers) which can be homo- or copolymerized with other terminal dienes, either mono- or oligomeric. Representative examples of diene telechelomers include α,ω-diene terminated polytetrahydrofuran and polyisobutylene, two segments based on polymers with low glass transition temperatures. These telechelomers have been efficiently incorporated as the soft phase in copolymers with hard polyalkenylene, polyester and polyurethane segments (Wagener 1997a, Tindall 1999).

Another application is the synthesis of polyalkenylene telechelics by end functionalization of ADMET polymers through the addition of a chain limiter. Using this strategy, chlorosilane- and methoxysilane-terminated polyoctenylene has been synthesized and successfully copolymerized with hydroxy-terminated silicones yielding an ABA triblock copolymer (Brzezinska 1999). Along the same lines, acetoxy-terminated polyoctenylene and 1,4-polybutadiene has been synthesized using an unsaturated ester for functionalization (Nubel 1994). This material is a precursor for both ester- and hydroxy-terminated polyethylene, a building block of special importance in step polymerization (and very especially in polyester technology) which can be isolated upon hydrogenation (and hydrolysis) of the parent unsaturated polymer.

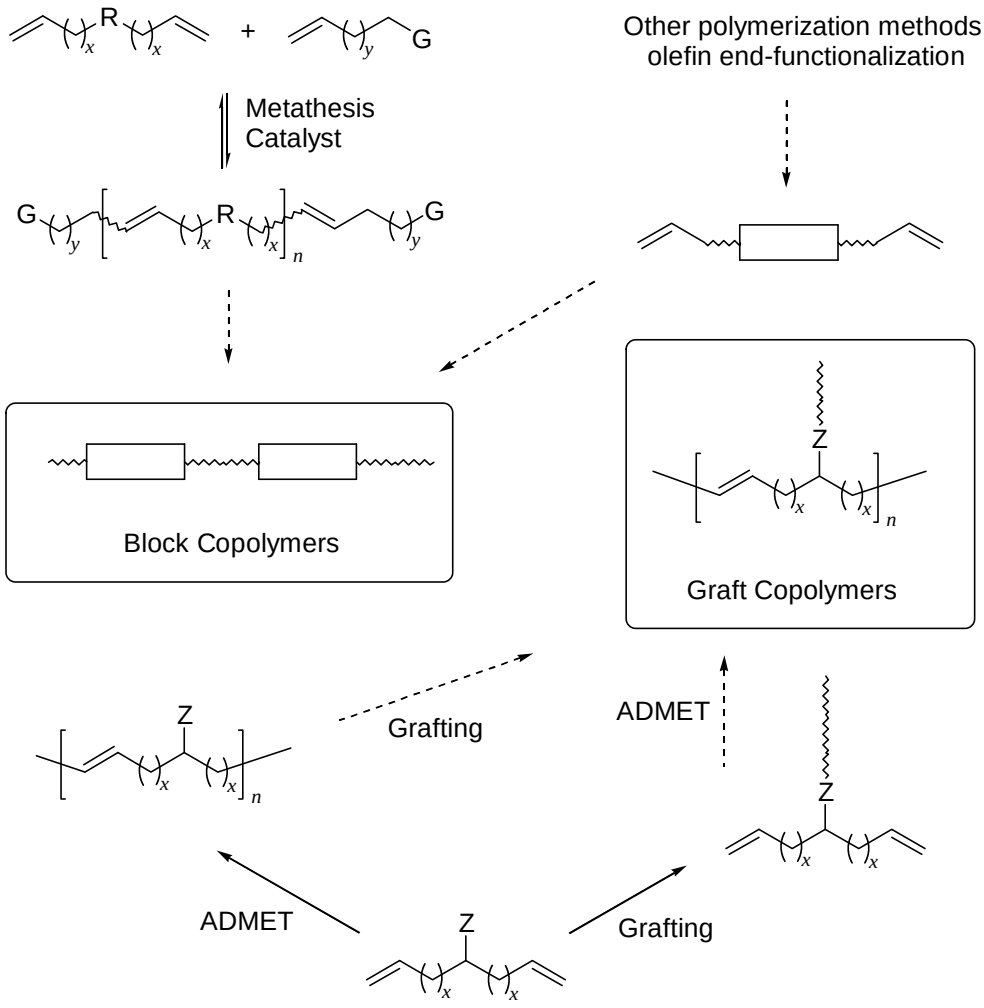

Figure 1-10. Examples of polymer architectures using ADMET polymerization.

Finally, the use of functionalized dienes as initiators for other type of polymerizations yields diene macromonomers which upon homo- or copolymerization, produce graft copolymers via the combination of two mechanisms. The ultimate composition and some of the architectural properties of such copolymers can be predicted by the choice of comonomer, the feed ratio, and the structure present in the diene macromonomer.

Polyoctenylene, the ADMET polymer produced from 1,9-decadiene, is a linear structure that contains a double bond every repeat unit separated from each other by six methylene groups. Hydrogenation of this polymer provides access to *perfectly linear polyethylene*. Structures of this type are step polymers that can be used to model polymers produced by chain chemistry.

Modeling polyolefin crystallization behavior using ADMET chemistry is currently an area of extensive research. The polymerization of symmetrical dienes containing an alkyl substituent (i.e. methyl) and its subsequent hydrogenation yields polyethylene with alkyl branches separated by a specific number of methylene groups. This strategy allows the side chain and the spacing between branches to be defined by the monomer structure. The case of methyl-substituted dienes is of significance since it is a model for a poly(ethylene-co-propylene) in which the frequency of propylene incorporation is controlled.

Along the same lines, ADMET polymerization serves as a route to precise models of copolymers of ethylene with a variety of olefins such as vinyl chloride, styrene, methyl acrylate and vinyl acetate, through the design and polymerization of dienes containing the corresponding substituent. Furthermore, the polymerization of dienes containing a reactive group such as hydroxyl or carboxylate facilitates the synthesis of graft copolymers with precise placement of the grafted segments.

As depicted in Figure 1-7, ADMET polymerization is an overall equilibrium. This suggests that once the experimental conditions are found, exposure of an unsaturated polymer to an excess olefin in the presence of a metathesis catalyst (ensuring 100 %

olefin conversion) should afford a low molecular weight diene. In the case of ethylene being used as the depolymerizing olefin, the theoretical product is the monomer.

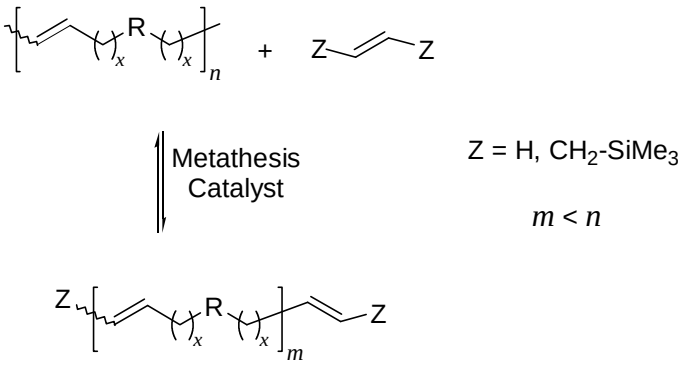

Figure 1-11. ADMET depolymerization.

ADMET chemistry is, in fact, an opportunity of recycling unsaturated polymers. Several studies have demonstrated the feasibility of ADMET depolymerization, leading to both functionalized telechelics or oligomeric terminal dienes. When this depolymerization scheme is applied to polyalkenylenes such as 1,4-polybutadiene, it becomes a new route towards telechelic polyolefins (e.g., polyethylene). Since the same reactivity rules apply for the reverse reaction, depolymerization of functionalized unsaturated polymers can also take place. ADMET depolymerization has been observed with allylsilanes and ethylene as depolymerizing agents (Watson 1999, Marmo 1997)

CHAPTER 2
ARYLOXIDE TUNGSTEN-BASED CLASSICAL CATALYSTS FOR ADMET POLYMERIZATION

Metal Carbenes and Olefin Metathesis Catalysts

Organometallic complexes containing a metal-carbon double bond are referred to as *metal carbenes*. The classification of metal carbenes is based on the identity of the atoms attached to the carbene carbon, which in many cases has a dramatic influence on the electronic properties (and thus the reactivity) of the complex itself. If such carbon bears a heteroatom, the name metal *carbene* or *Fischer carbene* is given to the complex. On the other hand, if only carbon or hydrogen is attached, the complex is designated as a metal *alkylidene* or a *Schrock carbene* Figure 2-1. Although the reactivity of the complex is determined by a collection of factors such as the electronic properties of the ligands and the type of metal-ligand interaction they exhibit, it is often observed that the carbene ligand in a Fisher carbene shows electrophilic behavior, while nucleophilic behavior is observed in Schrock carbenes. Today these features are well known and the reactivity of a determined complex can usually be rationally modified by the alteration of its ligand set (Elsenbroich 1992). A detailed comparison of the properties of Fisher and Schrock's carbenes is given in Crabtree (1994).

M in a low oxidation state
X = amines, alkoxides

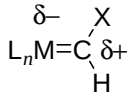

24

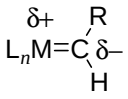

25

M in high oxidation states
R = alkyl, aryl, silyl

Figure 2-1. Structures of a Fischer (**24**) and a Schrock (**25**) carbene.

Early examples of olefin metathesis reactions employed ill-defined catalyst systems (Ivin 1997). Although these catalysts demonstrated very early their utility in metathesis chemistry, the mechanism was not only poorly understood but also difficult to study, mainly because of the heterogeneous nature of such systems. In 1971, Hèrrison and Chauvin were the first to propose metal carbenes as intermediates in the olefin metathesis mechanism, the same mechanistic proposal that is widely accepted today (Hèrrison 1971).

A number of transition metal carbenes are known to be active catalysts for olefin metathesis (Ivin 1997). These catalytic systems have been classified as *well-defined* or *classical* catalysts based on whether the carbene moiety is present from the beginning of the reaction or formed *in situ* by the reaction of a *precatalyst* with an *activator*. While all of the well-defined systems are soluble and have been thoroughly characterized, several examples of heterogeneous classical systems exist in the literature. These systems have been used extensively in the metathesis of olefins at elevated temperatures, and although much less is known about the mechanism by which they are converted to a metal carbene, supported metathesis catalysts continue to be the best alternative in industrial applications because of their robustness and reusability, albeit the side-reactions often induced by these ill-defined systems (Ivin 1983). However, since we are concerned with the issues surrounding the applicability of classical catalysts to ADMET chemistry, we will

concentrate our discussion on soluble classical systems. Because of the mechanistic and kinetic features already described (Chapter 1), only the most active and tolerant metathesis catalysts can be used in acyclic olefin metathesis and hence ADMET polymerization, but more importantly, only systems capable of polymerizing dienes in a clean fashion can be considered as alternative ADMET catalysts.

Well-Defined ADMET Catalysts

It was noticed early that the electronic properties of Fischer carbenes (coordinatively and electronically saturated metals in most cases) were not correct in order to induce most metathesis reactions, and not until the advent of the Schrock carbenes did metathesis chemistry using well-defined catalysts prove to be so remarkably active.

The isolation and characterization of the first alkylidene complexes led to early studies on olefin metathesis catalysis by well-defined systems. However, very poor reactivities were found, and the steady development of very active alkylidenes occurred parallel to major discoveries in the area of classical systems. In fact, the Schrock catalysts **26** and **27** illustrated in Figure 2-2 are the result of a lengthy period of research examining both steric and electronic issues (Schrock 1988, 1990a, Feldman 1991). motivated in part by the rapid evolution of alkylidyne complexes (Schrock 1983, Sharp 1981). While several transition metals have been explored, the molybdenum and tungsten versions of

Schrock catalysts have received the most attention and, in fact the use of Schrock alkylidenes led to the first successful ADMET reaction (Wagener 1991).

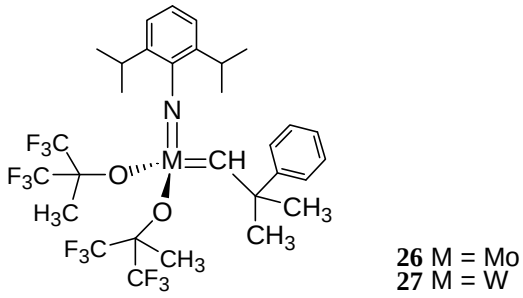

Figure 2-2. Two examples of Schrock carbenes, active catalysts for olefin metathesis.

Several features contribute to the high reactivity of complexes such as **26** and **27** towards olefin metathesis. First, the metal is in a high oxidation state (+6) and bears electron withdrawing ligands such as fluorinated alkoxides. This combination results in a very electropositive metal, which favors the metal-olefin interaction previously described as imperative (Chapter 1). At the same time, stabilization of the metal is a consequence of the π-donor ability of oxygenated and nitrogenated ligands, and especially of the bulkiness of all the ligands present, which prevents the decomposition of the catalyst by for example, bimetallic pathways. Finally, the complex is coordinatively unsaturated (a pseudo-tetrahedron) which allows the first event in the mechanism: olefin coordination. The ligand set on complexes **26** and **27** is the product of a careful exploration of the effect each ligand has on the complex activity, the results of which have set the guidelines for olefin metathesis catalysts design.

While Schrock's catalyst presented the opportunity to be definitive in terms of structure reactivity relationship for a number of ADMET monomers, it is an air-sensitive compound that requires handling under stringent conditions. Consequently the opportunity existed for the creation of catalyst structures more amenable to polymerization and workup procedures.

It was with this in mind that the development of ruthenium-based catalyst systems moved from their use in more classical catalyst arrangements to well-defined ones. In the early 1990's Grubbs and coworkers were able to generate well-defined ruthenium catalyst structures such as those illustrated in Figure 2-3 (Nguyen 1993, Schwab 1996, Dias 1998).

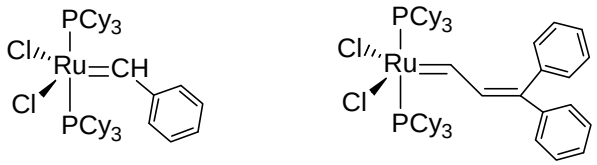

28 **29**

Figure 2-3. Two examples of ruthenium carbenes, well-defined catalysts for olefin metathesis.

Note that these indeed are well-defined metathesis catalyst structures where again tuning appropriate molecular features leads to higher degrees of reactivity. More importantly, these catalyst structures are active under conditions requiring less care in handling. These catalysts can actually be handled in air, and though kinetically they are approximately an order of magnitude slower than those observed for the Schrock alkylidenes, they still are quite useful systems.

The activity of the ruthenium system **28** in the metathesis of acyclic olefins can be explained following a different rationale than that of the Mo and W alkylidenes. The ruthenium systems are different in terms of their electronic properties: they are not in high oxidation states, and only halogens have been included as electron withdrawing ligands. Also, two phosphine ligands –excellent σ-donors– are present in the coordination sphere of the complex. A closer look at the trigonal-bipyramidal complex **28** reveals that the two phosphine ligands are coordinated in the apical positions, and that they are responsible for the steric bulk around the metal center.

In an effort to fine-tune the activity of ruthenium based systems, Grubbs and coworkers have carried out comprehensive studies of the effect of the ligand identity on the catalytic activity of a series of complexes, which revealed very interesting features of these systems. (Dias 1997, Schwab 1996) For example, activities decrease when moving from Cl to Br to I, an observation explained in terms of the *trans* effect of the halides as well as of the steric effect on olefin coordination and geometric rearrangement. It was also found that modification of the electronic properties of the phosphine ligand had a more dramatic effect than steric modifications; and even more surprising, that the activity towards acyclic alkene metathesis increased parallel to the electron donating ability of the phosphines (Dias 1997). The mechanistic proposal for ring closing metathesis derived by Grubbs reveals intimate details of these systems that can be extrapolated to ADMET polymerization, and constitutes the beginning of a new school of thought within the area of ruthenium carbenes as catalysts for ADMET.

In summary, two types of well-defined catalysts have been successfully employed in ADMET polymerization: the Schrock-type alkylidenes (**26** and **27**), and the

Grubbs-type Ru benzylidene **28**. Both types are useful ADMET catalysts and each type exhibits unique properties that make it suitable for specific monomer or polymer systems. The advantages of Schrock's systems over complexes like **26** are their higher activity (faster polymerization kinetics), their higher reactivity towards substituted olefins, and the endless possibilities for fine-tuning through ligand modification. At the same time, Grubbs' carbenes are synthesized in a very convenient and straightforward manner, which makes them the system of choice for many large-scale applications in polymer as well as in organic synthetic chemistry. Furthermore, these systems display high air and moisture resistance, as well as a superb tolerance to polar functionalities.

Olefin Metathesis Classical Catalytic Systems

The first olefin metathesis reactions were performed by the use of ill-defined catalysts, and the term *classical* has been commonly given to systems that fall into this category. By classical catalytic system we designate the mixture of a transition metal complex with an activator (also known as cocatalyst), which react to form a metal carbene *in situ*. These types of systems have been used in many applications of olefin metathesis, using either cyclic or acyclic substrates (Ivin 1997). The ease of synthesis and the robustness often exhibited by the transition metal complexes used as precatalysts make the classical systems of special interest, and some of these features are often considered advantageous for certain types of metathesis processes, especially at an industrial level where stringent conditions are undesired.

Transition Metal Halides and Alkoxides

Among the wide variety of soluble classical catalysts, halides and alkoxides of W, Mo, Ta, Nb, and Re, activated by main group alkyls constitute a subgroup of special interest. In fact, one of the most common catalytic systems consists of binary and ternary mixtures containing WCl_6, aluminum or tin-based activators, and sometimes other organic additives. Today, numerous of applications of metathesis chemistry are possible because of its availability, low cost and high efficiency. Some examples include the ring opening metathesis polymerization of dicyclopentadiene, carried out at a commercial scale using $EtAlCl_2$ as the activator, as well as the synthesis of polyacetylene derivatives involving Me_4Sn and other tin alkyls as cocatalysts (Balcar 1994, 1995, Masuda 1986, 1988).

In order to arrive at an agreement between the olefin metathesis catalytic cycle, and the identity of the ill-defined systems described, the activation mechanism by which metal halides are converted into metathesis catalyst should lead to the formation of a metal carbene. Figure 2-4 depicts a plausible activation route for the WCl_6/Me_4Sn system, as proposed by Thorn-Csanyi (1985). The first event in the mechanism is the double alkylation of the tungsten occurring through a transmetallation reaction, yielding a transition metal dialkyl complex (**30**). The existence of such an intermediate (although not always isolated or even observed) is in concert with the experimental data (Ivin 1987), and the extent of this reaction reflects in many cases the nucleophilicity (or alkylating ability) of the alkyl groups present in the main group metal complex (Ivin 1983). In the second step, the dialkyl complex **30**, is believed to undergo a (usually

thermally induced) α-abstraction reaction, eliminating the metal carbene **31** and an alkane molecule. This second part of the mechanism is in good agreement with the well known use of dialkyl complexes as precursors to alkylidenes, elegantly demonstrated and extensively supported in the literature (Schrock 1974, 1975, Feldman 1991, Elsenbroich 1992)

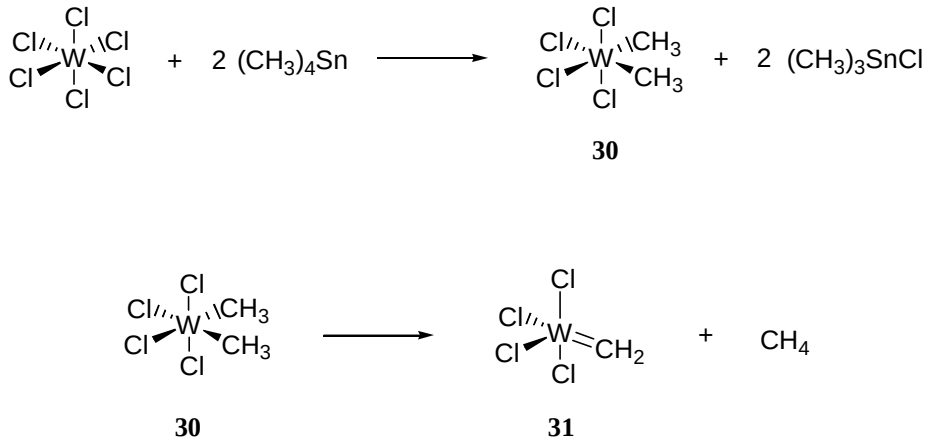

Figure 2-4. Proposed mechanism for the conversion of WCl_6 into a tungsten carbene.

A few characteristics of complex **31** should be mentioned. It not only contains the carbene moiety but also the tungsten atom in its highest oxidation state (+6). The latter fact and the available coordination site ensure the feasibility of the first mechanistic event in the olefin metathesis catalysis cycle: olefin coordination.

As noted by Ivin (1987) only a portion of the initial precatalyst is converted into a carbene, and only part of the formed carbene is responsible for the olefin metathesis catalysis. This finding was extrapolated from the calculated degree of polymerization of a sample of polynorbornene obtained when a 1:2:1 mixture of $WCl_6/(^{13}CH_3)_4Sn$/NBE was

reacted in an NMR experiment. A low extent of activation (as low as 0.7%) was observed, and this behavior can be expected for other similar systems.

In turn, organic compounds used as additives play a significant role in ternary catalytic systems. In some of the early examples the presence of a Lewis base (phosphines, ethers, nitrogenated bases) as the third component of the catalytic mixture resulted in increased stabilities with respect to the binary systems known, and this effect can be rationalized from an electronics point of view (Ivin 1997). The protection of the carbenes formed seems to have an observable effect on the apparent extent of conversion to (or the half-life of the) active catalyst (Masuda 1992).

The observed improvements in catalyst stability resulted in the introduction of protic Lewis bases, among which alcohols and phenols are well known examples. However, the reactivity of early transition metal halides with alcohols and water suggests that the formation of a new type of catalytic species was indeed taking place. Reasonable structures for the precatalysts formed include metal alkoxides (and phenoxides), generated though halide substitution reaction schemes.

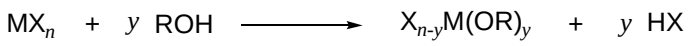

Figure 2-5. Metal alkoxides from metal halides.

The generation of alkoxide (or phenoxide) species then was proposed, and soon after the pioneering work of Dodd (1982) became the first report on olefin metathesis catalysis by systems generated from (tungsten) phenoxide precursors, thereby opening a door to systems with a many advantages with respect to their parent metal halides.

Among these, phenoxide derivatives of WCl_6, $WOCl_4$, and $MoOCl_4$ have found utility in the metathesis of acyclic olefins, both terminal (Dodd 1988) and internal (Quignard 1985, 1986), ring opening metathesis polymerization (Bell 1992, Barnes 1994, Dietz 1993), the polymerization of substituted acetylenes to yield π-conjugated structures (Nakayama 1993, 1996) and the ring closing metathesis of a variety of dienes to yield carbo-and heterocyclic structures (Nugent 1995). A summary of these applications is presented in Table 2-A.

The most notable consequences of halide substitution by an aryloxide group are – besides the already mentioned increase in stability/half-life– the modification of the electronic properties of both the precursor complex (and the aimed catalytic species synthesized therefrom) as well as an increased compatibility with organic substrates, an especially important feature in solvent-free processes. The third effect is related to the electronics of the complex, since the electron withdrawing properties of the aryloxide group are often different than those of halide ligands.

Classical Systems and ADMET Polymerization

As noted earlier, the original attempts to polymerize dienes by polycondensation chemistry met with difficulty primarily due to the fact that the classical catalysts that had been chosen ($WCl_6/EtAlCl_2$) resulted in more than one mechanistic event (e.g., Lewis acid-induced crosslinking) (Lindmark-Hamberg 1987, Wagener 1990). This has been attributed to the high Lewis acidity of the studied cocatalyst ($EtAlCl_2$) and/or of the actual catalytic species. Figure 2-6 illustrates a case of crosslinking *via* vinyl addition catalyzed by a Lewis acid (LA) in an attempted ADMET polymerization.

Table 2-A. Some examples of metathesis reactions catalyzed by metal aryloxide-based classical systems.

Transformation	Conditions[a]	Reference
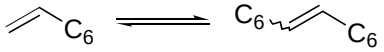	$WCl_2(OAr)_4$, $Et_3Al_2Cl_3$ or SnR_4, 20 to 140 °C	Dodd 1988
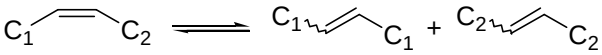 and some fatty acid esters	$WCl_4(OAr)_2$, R_4M,[b] 85 °C	Quignard 1986
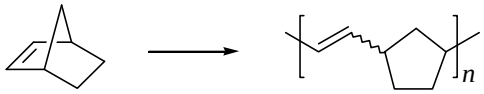	$WOCl_2(OArO)$, Et_2AlCl, 0 °C	Dietz 1993 Barnes 1994
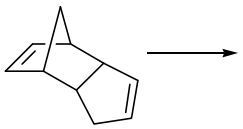 Crosslinked polydicyclopentadiene	$WOCl_2(OAr)_2$, Bu_3SnH, 80 °C	Bell 1992
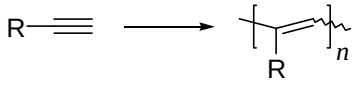	$M^tCl_x(dmp)_y$,[c] $AlEt_3$, -20 to 60 °C	Nakayama 1993
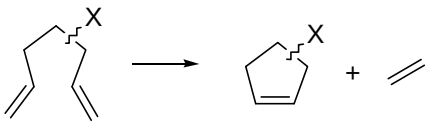	$WOCl_2(dbp)_2$,[c] Et_4Pb, 85 °C	Nugent 1995

a) OAr represents any monodentate, substituted phenoxide, while OArO represents a bidentate aryloxide (e.g., binaphtol derivatives). For specific examples, see the corresponding references.
b) A series of tin and lead-based activators were explored.
c) dmp=2,6-dimethylphenoxide, dbp=2,6-dibromophenoxide.

Here the presence of a mixed catalyst system probably allowed cationic vinyl addition chemistry at a rate competitive with metathesis polycondensation chemistry. Thus, it was initially thought that classical catalyst systems would never serve much of a purpose in condensing dienes to their polymers.

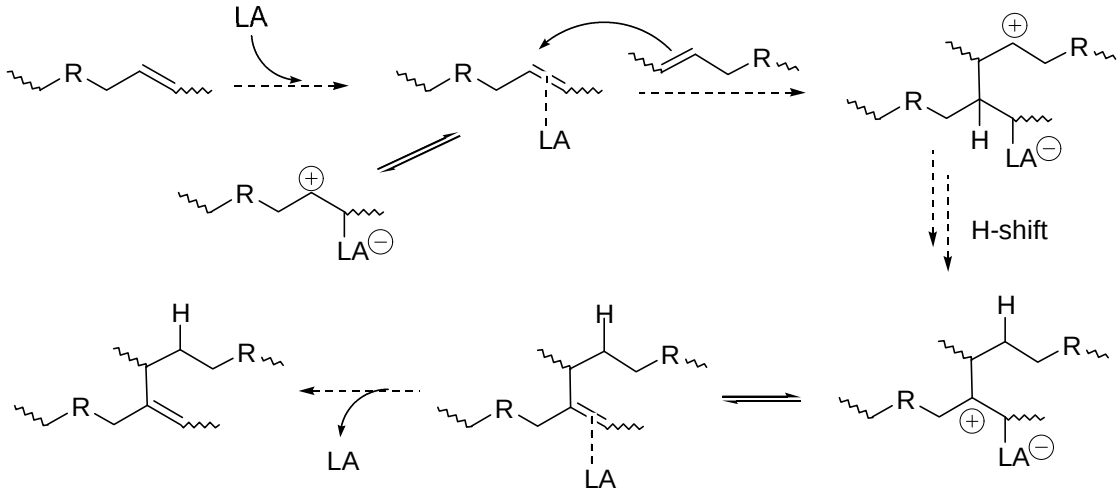

Figure 2-6. A plausible mechanism for the Lewis acid-induced crosslinking of an unsaturated polymer.

However, in 1994 Nubel, Lutman, and Yokelson demonstrated that a mixture of WCl_6 and Me_4Sn in the presence of propyl acetate would produce linear 1,4-polybutadiene through the clean ADMET polymerization of 1,5-hexadiene (Nubel 1994). In this case the use of a Lewis base like propyl acetate was pointed as the key to linear polymers, reducing the side reactions that could lead to crosslinked product, and this condensation became the first example of a clean ADMET polymerization catalyzed by a classical catalytic system.

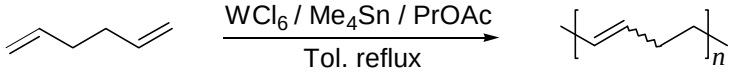

Figure 2-7. ADMET polymerization of 1,5-hexadiene.

Nubel's experiment prompted the exploration of other classical systems in order to develop a flexible polymerization methodology, especially in light of the possibility of applying such to the synthesis of high temperature ADMET polymers.

Tungsten Aryloxide Complexes and ADMET Polymerization

Three known aryloxide tungsten complexes were chosen for our initial studies on the ADMET polymerization of hydrocarbon dienes: $WOCl_2(O\text{-}2,6\text{-}C_3H_6Br_2)_2$ (**32**) $WCl_4(O\text{-}2,6\text{-}C_3H_6Ph_2)_2$ (**33**) and $WCl_4(O\text{-}2,6\text{-}C_3H_6Br_2)_2$ (**34**), whose structures are shown in Figure 2-8.

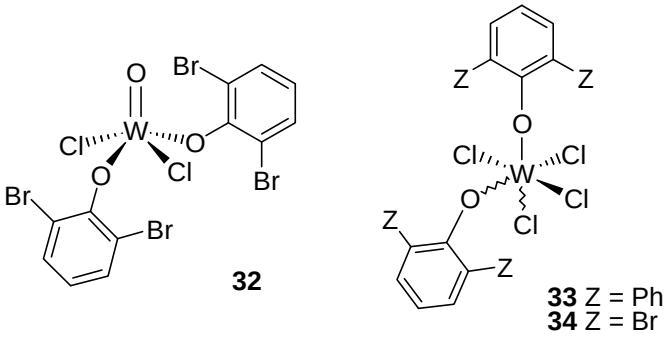

Figure 2-8. Structure of complexes **32**-**34** studied as precursors to classical catalysts for ADMET polymerization.

The polymerization studies were conducted using Bu_4Sn, Me_4Sn or Bu_3SnH, cocatalysts used in previous applications of systems **32**-**34** (Quignard 1986, Bell 1992).

ADMET Polymerization of 1,9-Decadiene

The exploration of tungsten aryloxide-based systems began in our hands with the bulk polymerization of 1,9-decadiene, and the first binary system studied was a 1:2 mixture of complex **32** and Bu_3SnH. Experimentally, a solution of complex **32** was heated to 65 °C under an argon atmosphere, and the hydride addition was performed using a microsyringe. A distinctive color change of the reaction mixture, from dark red to dark orange, was evident soon after the tungsten complex came in contact with the tin hydride, and the release of a gas was suggested by small bubbles formed in the reaction flask. As shown in Figure 2-4, one mole of alkane is produced in the α-abstraction step when the cocatalyst used is a tetraalkyltin complex. However, based on the differences of the reacting species, a different activation mechanism for the activation using metal hydrides has been proposed by Kelsey and coworkers (Kelsey 1997), and no efforts were made for the identification of this initial gaseous byproduct. The steady gas evolution under constant stirring can then be attributed to the release of ethylene, which is evidence for the propagation stages of the polymerization. After ca. 4-6 hours of reaction, the mixture was exposed to high vacuum in order to remove the condensate, and the reaction was continued for ca. 2 days. After 48 hours of reaction, the viscosity of the mixture was high enough to hinder magnetic agitation. The polymerization was now complete, and crude solid polyoctenylene was obtained upon cooling of the reaction flask. The study of other activators shows that a mixture of complex **32** and Bu_4Sn catalyzes the polymerization of 1,9-decadiene at 85-95 ºC, and a significant viscosity change can be observed in a shorter period of time than when Bu_3SnH is used as the activator. In a similar fashion, tetramethyltin was also capable of activating complex **32** to generate an

active catalyst and the polymerization of 1,9-decadiene in the presence of **32** and Me_4Sn at 110-120 ºC also yielded polyoctenylene (**35**).

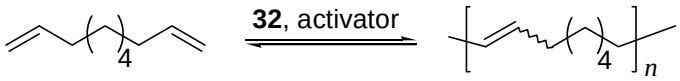

35

Figure 2-9. Synthesis of polyoctenylene from 1,9-decadiene.

Soluble, high molecular weight polyoctenylene can be isolated after the workup procedure in all cases, and no evidence for addition chemistry can be observed in any of the characterization steps for these polymers. The quantitative ^{13}C-NMR of the precipitated polymers (e.g., Figure 2-10) shows the expected signals for polyoctenylene and matches exactly the ^{13}C-NMR of a sample of the same polymer synthesized using either Schrock's molybdenum (**26**) or Grubbs' ruthenium (**28**) well-defined systems.

The experimental conditions described are the result of a series of reactions carried out in order to establish the optimum polymerization conditions, varying activation temperature and pressure conditions. The summarized results are shown in Table 2-B. The determination of molecular weight was performed by gel permeation chromatography (polystyrene standards) and by NMR end group analysis through the integration of the olefin signals.

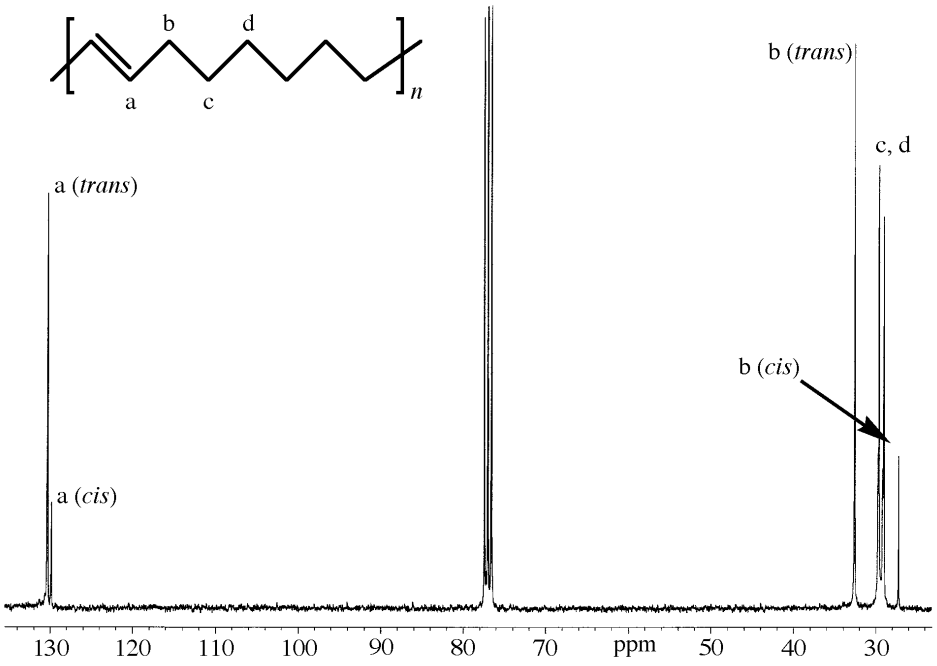

Figure 2-10. ^{13}C-NMR of polyoctenylene synthesized using complex **32** and Bu_4Sn.

From comparative experiments, it was found that among the three complexes studied Bu_4Sn is *apparently* the most active cocatalyst for complex **32** in ADMET polymerization. For example, high molecular weight polyoctenylene has been obtained using this catalytic system in the polymerization of 1,9-decadiene, even in polymerizations run at atmospheric pressure. (Table 2-B) However, the difference in reaction times cannot be directly associated with a difference in activity of the catalytic species reported in this study because of two factors. First, the three cocatalysts exhibit different activation temperatures with respect to the same precatalyst (e.g., several failed attempts to initiate the polymerization of 1,9-decadiene with complex **34** and Bu_4Sn at temperatures below 80 ºC confirmed this fact.) Secondly, this observation is based only

in the apparent changes in viscosity of the polymer obtained at different temperatures, which does not constitute a reliable indication of the percent conversion.

Table 2-B. Experimental conditions for the polymerization of 1,9-decadiene with complexes **32**-**34** and organotin activators.

Catalytic System	Reaction Conditions[a,d]	M_n		
		GPC[b]	^{1}H-NMR[c]	^{13}C-NMR[c]
32 + Bu_3SnH	65 ºC, 48 h	14,400	6,200	5,200
32 + Bu_3SnH	65 ºC, 72 h, 10^{-3} atm	6,100	2,700	2,500
32 + Bu_4Sn	65 ºC, >100 h	No reaction observed		
32 + Bu_4Sn	85 ºC, 48 h	50,000	neg	neg
32 + Bu_4Sn	85 ºC, 72 h, 1 atm Ar	50,300	neg	neg
32 + Me_4Sn	65 ºC, > 72 h	No reaction observed		
32 + Me_4Sn	120 ºC, 36 h	43,000	neg	neg
33 + Bu_3SnH	100 ºC, 48h	11,300	4,000	3,400
33 + Bu_4Sn	85 ºC, 24 h	26,900	neg	neg
34 + Bu_4Sn	85 ºC, 24 h	18,700	6,000	6,700

a) Monomer/Precatalyst/Cocatalyst ratio = 500:1:2-2.5, pressure = ca. 1×10^{-5} atm.
b) Solvent: THF, calibrated using polystyrene standards.
c) Determined by integration of the terminal vinyl and internal olefin signals. neg = no end groups observable.
d) High yields (75-97%) observed in all cases. Deviations from quantitative conversion are due to monomer loss at high temperatures and are not reproducible.

ADMET Polymerization of 1,8-Nonadiene

Although several hydrocarbon and functionalized dienes have been polymerized *via* ADMET chemistry, the polymerization of 1,8-nonadiene has not been reported previously. In order to expand the scope of this polycondensation, we decided to study the reaction of this diene not only with the classical systems **32**-**34** but also with the well-defined system **26** under bulk conditions.

When 1,8-nonadiene is heated to 85 ºC in the presence of a 1:2 mixture of (e.g.,) **33** and Bu_4Sn under an argon atmosphere, ethylene evolution is also observed for a period of 8 h, and continues for ca. 48 h under reduced pressure. Again, the formation of high molecular weight polymer hinders magnetic stirring of the reaction mixture and the polymerization is stopped. Linear, soluble polyheptenylene (**36**) can be isolated in good yields (77-87%) after dilution in toluene followed by precipitation into cold, stirring acetone (Figure 2-11). This behavior resembles that exhibited by the polymerization performed by Schrock's system **26**, which also effectively catalyzes the polymerization of 1,8-nonadiene in a much faster reaction. Solid polyheptenylene can be isolated after 0.5 h of reaction at room temperature followed by 1 h at 60 ºC, after which agitation becomes impossible. After similar purification, a polymer with the same characteristics as **36** is obtained.

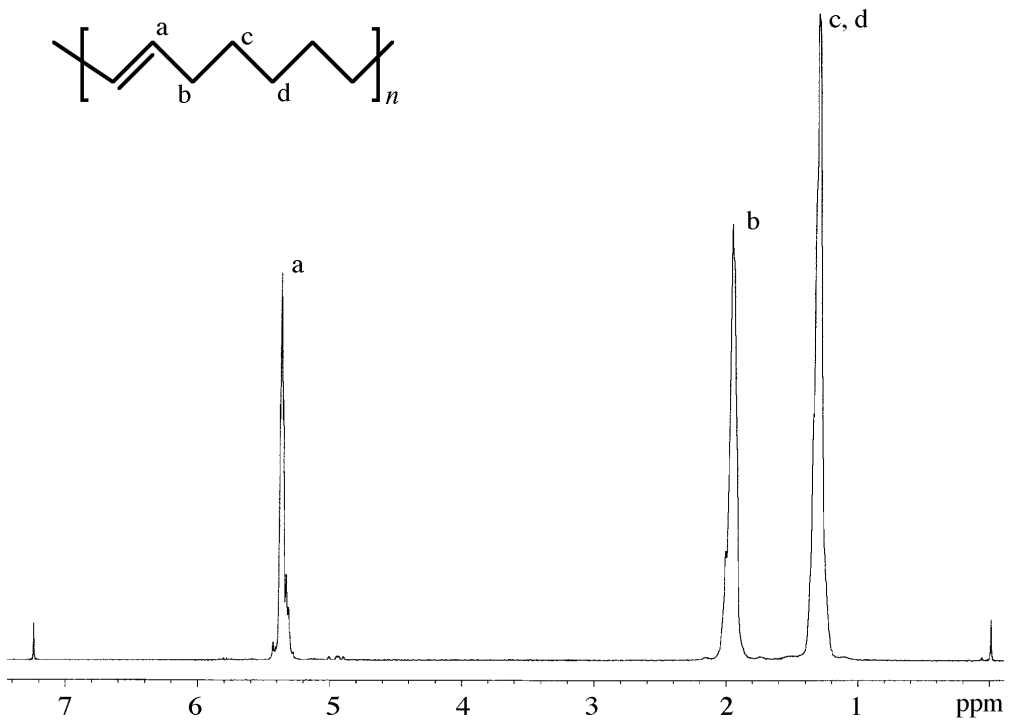

Figure 2-11. ^{1}H-NMR of polyheptenylene synthesized using complex **32** and Bu_4Sn.

In the characterization of the polymers synthesized using the aryloxy-tungsten systems **32-34**, we find that the *trans*/*cis* ratio approaches 80:20 in all cases (determined by integration of the olefin signals at e.g., 130.3 and 129.8 ppm in the quantitative ^{13}C-NMR of polymer **35**). This also is observed in the ADMET polymerization catalyzed by the well-defined complexes **26-28** and represents the expected equilibrium distribution of geometrical isomers, as a consequence of long reaction times. Similarly, the polydispersity of all the polymers synthesized with systems **32-34** ranged between 1.7 and 2.3, a range in concert with the step propagation-type ADMET mechanism.

The Reaction of Other Hydrocarbon Dienes

The reaction of other unsubstituted terminal dienes with complexes **32** and **33** in the presence of tetrabutyltin was studied in order to explore the behavior and selectivity of the reaction towards cyclization in the bulk.

The reaction of 1,7-octadiene with a 1:2 mixture of complex **32** and Bu_4Sn was initially investigated under different experimental conditions. Although Feldman and co-workers reported the synthesis of substituted cyclohexenes *via* the RCM of substituted octadienes catalyzed by a mixture of complex **32** and Et_4Pb in solution (Nugent 1995), the attempted cyclization in the bulk could not be driven to completion. However, analysis of the ^1H- and ^{13}C-NMR of the reaction mixture suggests not only the formation of cyclohexene but also of low molecular weight oligomers; combined conversions are <20 % in most of the cases. The highest % conversion (ca. 56 %) was observed with complex **34** and Bu_4Sn, which yielded a mixture consisting of ca. 55 % cyclohexene, 30 % linear oligomer and 10 % unreacted starting material.

On the other hand, 1,5-hexadiene has been previously utilized in the synthesis of linear 1,4-polybutadiene under different experimental conditions that involve not only well-defined metathesis catalysts but also classical systems (Brzezinska 1996, Nel 1989, Nubel 1994). In a similar fashion, all of the attempts to polymerize 1,5-hexadiene were unsuccessful, and no conversion to oligomeric product was evidenced in any case. In the majority of cases, unreacted starting material could be isolated from the mixtures by vacuum transfer. This can be attributed to an incomplete activation of the W species because of the intramolecular coordination of the hexadiene. This phenomenon has been proposed as the justification of differences in the polymerization kinetics of

1,9-decadiene and 1,5-hexadiene) and indirectly evidenced by Snapper and co-workers through the isolation of a ruthenium alkylidene exhibiting intramolecular olefin complexation (Tallarico 1997).

Investigations with Oxygen Functionalized Dienes

Feldman and coworkers' successful cyclization of dienes containing a variety of functionalities using complex **32** activated by Et_4Pb appeared promising for the synthesis of functionalized ADMET polymers using classical systems (Nugent 1995). Based on these results, the ADMET polymerization of two oxygen containing α,ω-dienes, 3-butenyl 4-pentenoate (**36**) and 9-decenyl 10-undecenoate (**37**) was investigated.

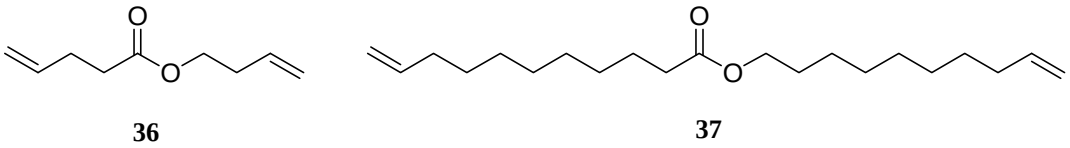

36 **37**

Figure 2-12. Structures of the two ester dienes **36** and **37**.

Our studies of the ADMET polymerization of the esters **36** and **37** reinforce the concept of negative neighboring group effect, introduced in Chapter 1 (Wagener 1993, O'Gara 1993). While the ^{1}H-NMR in the case of ester **36** shows no conversion to internal olefin after being subjected to the general polymerization conditions, the ester **37** can be efficiently converted to a polymer with a M_n of ca. 10,800 g/mol (determined by end-group analysis from the integration of the signals corresponding to the terminal vs. internal olefin in the ^{1}H-NMR). GPC of the same sample in THF vs. polystyrene

standards yields a M_n of 22,000 g/mol) and this marked difference in reactivity can be explained by the deactivation of the catalytic entity via intramolecular coordination of one of the oxygens in the ester moiety in the case of ester **36** forming stable 5- or 6-membered rings with the metal. Such deactivation has been previously observed in the case of well-defined alkylidenes after productive metathesis with an acrylate ester (Feldman 1989) and has been suggested for complex **32** with other esters (Nugent 1995). However, when we exposed the ester **37** to the general polymerization conditions described elsewhere in this paper, polymerization takes place suggesting that chelation (and deactivation derived therefrom) does not occur when enough methylene spacers are placed between the basic functionality and the reactive double bond. The ^{1}H-NMR of the polymer produced in the ADMET polymerization of ester **37** is shown in Figure 2-13.

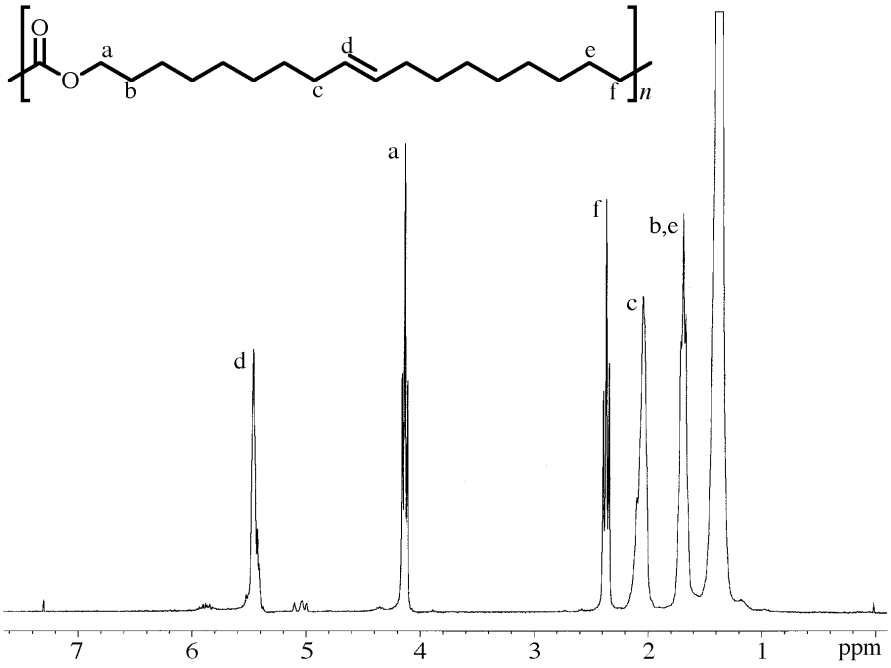

Figure 2-13. ^{1}H-NMR of poly(carbonyloxy-9-octadecene) (**38**) synthesized using complex **32** and Bu_4Sn.

Conclusions

The scope of the ADMET methodology for the synthesis of unsaturated polymers has been expanded by the exploration of aryloxy tungsten-based classical catalytic systems. *The most important feature of these systems is their ability to produce linear, soluble polymers in a clean metathesis process under bulk conditions*, in comparison to the classical systems previously studied (Lindmark-Hamberg 1987, Wagener 1990). Three complexes were successfully used as the precatalytic entities while tetrabutyltin, tetramethyltin and tri-*n*-butyltin hydride were used as activators. Tetrabutyltin was the most efficient activator to complexes **32-34** but no significant difference in activity was found among these three tungsten complexes. The experimental conditions explored in this study not only allow high conversion to polymer, but make this methodology a very promising alternative for the polymerization of novel monomer structures.

In fact, this polymerization scheme has already been suggested as the method of choice in the synthesis of poly(*p*-phenylenebutylene), a semicrystalline polymer which requires high polymerization temperatures (Steiger 1999).

CHAPTER 3
NOVEL METATHESIS CLASSICAL CATALYSTS THROUGH MODIFICATION OF THE ARYLOXIDE LIGAND

A conscious analysis of the mechanism by which transition metal halides (and derivatives) are activated by main group metal alkyls described in Chapter 2 suggests that strong alkylating agents are required to activate the precatalytic species to a significant extent. In fact, early homogeneous bicomponent systems included lithium, magnesium, and aluminum organyls as cocatalysts, and their presence motivated research in more practical cocatalysts at the expense of a lower extent of activation (Ivin 1997). The introduction of tin and lead-based activators constituted a significant advance in terms of portability and applicability of the olefin metathesis reaction to environments in which very stringent conditions are undesired.

It is also reasonable to assume that an increase in the extent of the transmetallation reaction depicted in Figure 2-4 may also be consequence of an increase in the electrophilicity of the transition metal complex. This modification would result in higher concentrations of the alkyl complexes that may in turn yield higher “true catalyst” concentrations.

This chapter describes the efforts to modify the electronic properties of a series of tungsten phenoxides through a rational approach. It also describes the search for useful

descriptors of the correlation between key ligand properties and the effect on the transition metal complexes synthesized therefrom.

Aryloxide Tungsten Complexes: The Ligand Electronic Effect

As described in Chapter 2, several “new classical catalytic systems” have been devised and synthesized through the replacement of a halide atom with a phenoxide (or in a more general way, an aryloxide) ligand, particularly from WCl_6 and $WOCl_4$. As mentioned before, this replacement brings about a series of advantages which include an increased compatibility with organic substrates and solvents, higher solubility than the parent halides, and an increased chemical stability mainly arising from the bulkiness of the ligand.

Without a doubt, the most significant effects are those observed in the electronics of the complex. When comparing the two ligands as anions (e.g., Cl^- vs. a generic ArO^-), the first evident difference is their basicity and nucleophilicity. Not only are the halide anions much less basic than the phenoxides but also less nucleophilic, two clear features derived from the negative charge stabilization by the two species.

These characteristics are also expressed in their reactivity in organometallic chemistry: halides are precursors to alkoxide and aryloxide complexes since they are easily substituted not only by the anions as nucleophiles, but also by the parent alcohol or phenol. Once substituted and when alkoxides and halides are compared, it is easy to observe that the electron withdrawing ability of these oxygenated ligands is often lower

than the parent halide. In some cases the participation of the oxygen p-electrons has significant effects on bonding and reactivity. Because of their decreased electron withdrawing abilities, the metal becomes less electrophilic when the substitution takes place, this –arguably– being the most important electronic effect.

Ligand Substituent Effects and Catalytic Activity

The development of aryloxide tungsten complexes as precatalysts for olefin (and alkyne) metathesis occurred parallel to understanding the effect that ligand substitution has on the complex properties. The pioneering work of Quignard and co-workers set the guidelines for further exploration of such effect (Quignard 1986). In their study, a series of bis(aryloxide) derivatives of WCl_6 synthesized as shown in Figure 3-1 (Quignard 1987)

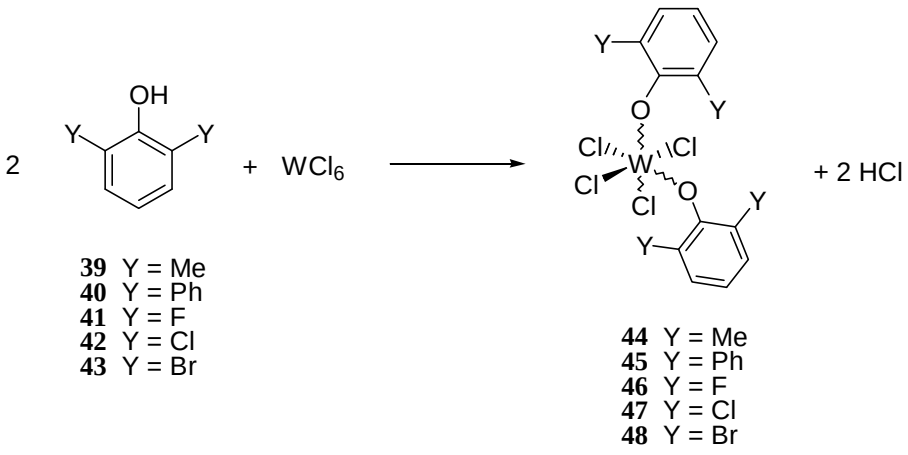

Figure 3-1. Synthesis of a series of bis(aryloxide) tungsten complexes (**44**-**48**) from WCl_6 and the parent phenols (**39**-**43**).

The catalytic properties of complexes **44**-**48** in the metathesis of linear, acyclic olefins were studied as a function of the substituent identity, the activator used, and the activation time. These experiments revealed interesting details of aryloxy tungsten-based catalysts and provided further mechanistic evidence in support of the existing proposal.

One of the reactions used by Quignard and coworkers is the equilibration metathesis of cis-2-pentene in chlorobenzene, as shown in Figure 3-2.

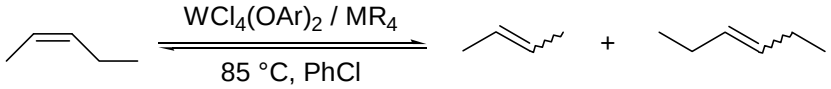

Figure 3-2. Metathesis of *cis*-2-pentene as studied by Quignard (1986). Bu_4Pb, Bu_4Sn and Me_4Sn constitute the group of activators studied.

Several features of the catalytic systems based on complexes **44**-**48** should be highlighted. First, for any given precatalyst (**44**-**48**) the activity of the system based on the activator employed decreased in the order $Bu_4Pb > Bu_4Sn > Me_4Sn$, and this trend can be correlated with an increase in the M-R bond dissociation energy.

Second, there is a rough correlation between the pK_a of the parent phenol and the catalytic activity of the corresponding catalysts, which *increases* parallel to the acidity of the phenol. This observation can be explained using the electron withdrawing effect that the substituent Y exerts on the complex, and opens a number of possibilities for ligand modification. Table 3-A summarizes some of Quignard's experimental data observed for the reaction shown in Figure 3-2.

Table 3-A. Activities of the two component systems **44**-**48** / MR_4 in the metathesis of *cis*-2-pentene expressed as equilibration times under standardized conditions.[a]

Complex	Activator		
	Me_4Sn	Bu_4Sn	Bu_4Pb
44	> 48 h	> 48 h	5 h
45	> 48 h	5 h	3 h
46	> 48 h	5 h	75 min
47	24 h	3 h	45 min
48	2 h	15 min	15 min

a) Reactions carried out in chlorobenzene at 85 °C. Substrate/precatalysts/activator = 50:1:2.

Similar conclusions were arrived at by Bell (1992) while studying the bulk polymerization of dicyclopentadiene using tungsten oxychloride derivatives activated by Bu_3SnH, synthesized as shown in Figure 3-3.

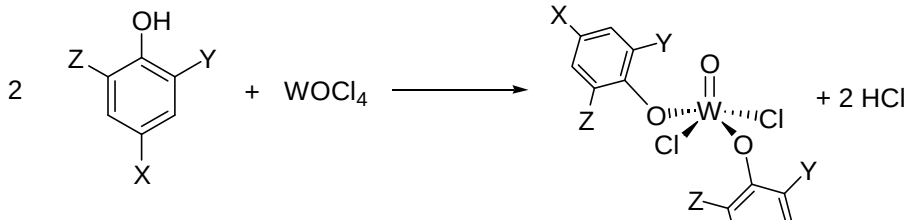

39 Z,Y = Me
40 Z,Y = Ph
42 Z,Y = Cl
43 Z,Y = Br
49 Z,Y = ^{i}Pr
50 Z,Y = OMe
51 X,Y = Cl, Z=Me

52 Z,Y = Me
53 Z,Y = Ph
54 Z,Y = Cl
32 Z,Y = Br
55 Z,Y = ^{i}Pr
56 Z,Y = OMe
57 X,Y = Cl, Z=Me

Figure 3-3. Synthesis of a series of bis(aryloxide) tungsten complexes (**32**,**52**-**57**) from $WOCl_4$ and the parent phenols.

Although the mechanism by which tungsten aryloxides are activated by tin hydrides is still unclear (for a recent discussion, see Kelsey 1997), Bell's contribution demonstrated that the mechanistic implications of the ligand substitution discussed above also apply to this type of catalytic systems. Furthermore, Bell demonstrated that two parameters, namely the AM1-calculated charge density on the phenoxide oxygen and the experimental reduction potential of the complex correlated effectively and could be used as quantitative indicators of the catalytic activity of the catalysts synthesized therefrom.

Two significant advantages were introduced in this study. First, instead of using a metathesis transformation as an amplification of the catalytic system properties, the experimental measurement of the reduction potential was chosen as an indication of the electropositive character of the metal, and correlated with the expected trend. Second, the semiempirical calculation of the charge on the oxygen atom of the corresponding phenoxide anion correlated well for the series, making of this property an attractive guide for further development of olefin metathesis catalysts. Among the explored set and in agreement with Quignard's observations, derivatives synthesized from 2,6-dibromophenol (the most acidic phenol in the series) exhibited the highest activities.

Novel Aryloxy-Tungsten Structures

During our initial experiments with classical systems as catalysts for ADMET polymerization, we explored aryloxide derivatives of tungsten (VI) oxychloride and tungsten (VI) chloride **32-34**. Based on our early observations we started a study on the

former group, following the pioneering approaches of Basset and Bell, through the modeling of a complementary series of phenoxides which can be used in the synthesis of systems of the type $WOCl_2(OAr)_2$. The appended results are shown in Figure 3-4.

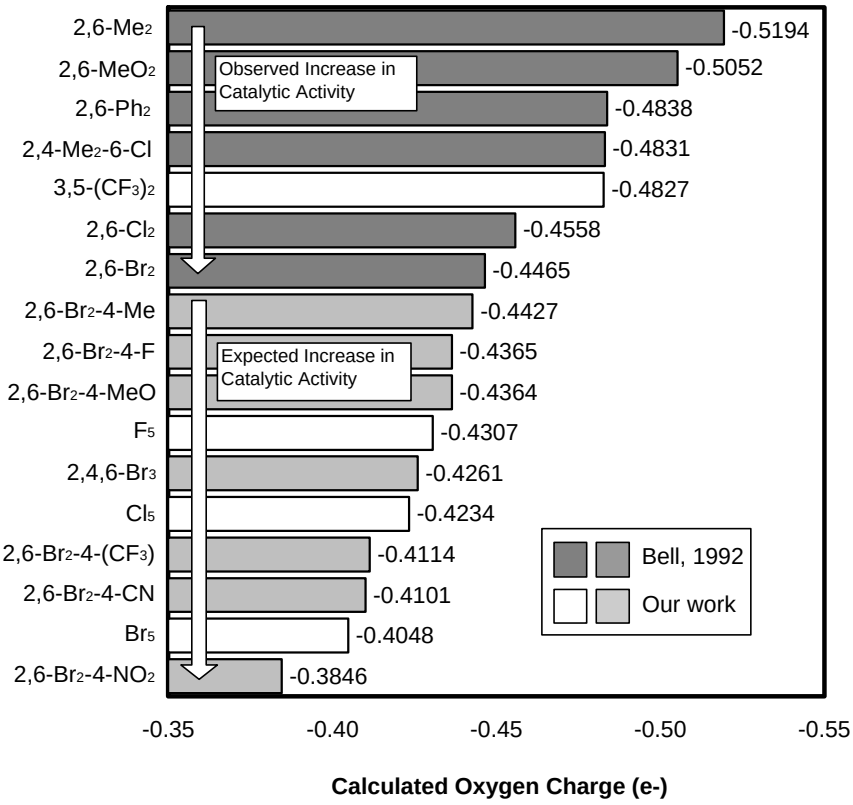

Figure 3-4. AM1-calculated charge on the oxygen atom for a series of phenoxides.

Within the modeled set the patterned columns represent the derivatives of 2,6-dibromophenoxide bearing a substituent on the *para* position. These potential ligands were chosen in light of the possibility of further correlation of the complexes properties with the substituent Hammett constant, σ. Thus it is reasonable to state that complexes derived from more electron withdrawing phenoxides should exhibit high activity as

metathesis catalysts as well. This observation encouraged us to synthesize complexes **63-67**, and study their behavior as precatalysts in olefin metathesis classical systems.

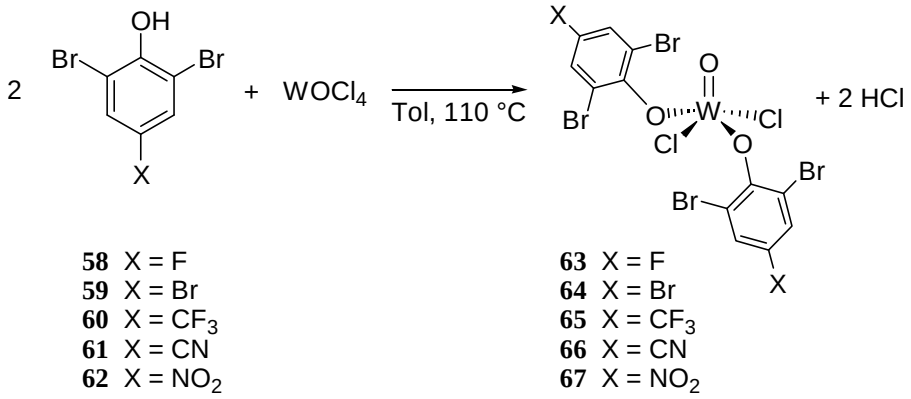

Figure 3-5. Synthesis of a new series of bis(aryloxide) tungsten complexes (**63-67**) from $WOCl_4$ and the parent 2,6-dibromophenol derivatives.

Complexes **63-67** were synthesized in a straightforward manner following the general procedure reported by Nugent (1995) which consists of refluxing $WOCl_4$ with the corresponding phenol in toluene (see Chapter 6). Essentially quantitative yields of crude material can be isolated following the removal of the solvent *in vacuo*, and this crude complex is usually of adequate purity to be used in metathesis chemistry. Complexes **63-66** can be purified through recrystallization, whereas complex **67** cannot. It is a black, insoluble powder, which has not been included in our comparative experiments.

Structural Characterization

A detailed structural analysis of the parent 2,6-dibromophenoxide complex by Nugent, Feldman and Calabrese revealed the asymmetry of complex (**32**). A non-bonding

interaction between one of the bromine atoms and the metal renders the two aryloxide ligands inequivalent (Nugent 1995).

Single crystal X-ray analysis shows similar features among complexes **63, 64** and **32**. Inequivalent phenoxide ligands are present due to a presumably weak interaction between Br1 and the tungsten atom, and such geometry distortion is (in both cases) also reflected in the inequivalent W-O-C bond angles. (Figure 3-6, Figure 3-7). The possibility of exploring its extent (through comparison of interatomic lengths and angles) as a quantitative parameter for predicting activity in the series was envisioned.

A detailed observation of structure **63** (see Table 3-C) reveals that the incorporation of the fluorine substituent in the *para* position causes an increase of the W-Br1 distance (3.205 Å in **63** vs. 3.120 Å in **32**). The same decreased interaction is also evidenced by the wider bond angle on O2 (139.28 in **32** to 142.18 in **63**). These observations can be justified by appealing to a larger extent of p donation from the oxygen orbitals of the aryloxy ligand to the empty metal orbitals, a phenomenon well documented elsewhere (Kershner 1989a,b)

At the same time, a comparison of complexes **64** and **63** suggests a tighter non-bonding W-Br interaction revealed in a shorter interatomic distance (3.149 in **64** vs. 3.205 Å in **63**). This feature as well as the angle about O2, (140.5 vs. 142.1° in **63**) again implied a correlation between the electronics on the ligand and the solid state structure. No significant differences were found when comparing the phenoxide W-O bond distances. A summary of structural data for complex **64** is shown in Table 3-E.

Table 3-B. Crystal data and structure refinement for complex **63**.

Empirical formula	$C_{12}H_4Br_4Cl_2F_2O_3W$
Formula weight	808.54
Temperature	173(2) K
Wavelength	0.71073 Å
Crystal system	Monoclinic
Space group	$P2_1/c$
Unit cell dimensions	a = 15.1172(2) Å α = 90° b = 7.9837(1) Å β =112.7430(10)° c = 16.6186(1) Å γ = 90°
Volume	1849.77(4) $Å^3$
Z	4
Density (calculated)	2.903 Mg/m^3
Absorption coefficient	15.201 mm^{-1}
F(000)	1464
Crystal size	$0.26 \times 0.22 \times 0.17$ mm^3
Theta range for data collection	2.49 to 27.49°
Index ranges	$-18 \le h \le 19$, $-8 \le k \le 10$, $-21 \le l \le 14$
Reflections collected	11725
Independent reflections	4230 [R_{int} = 0.0280]
Absorption correction	None
Refinement method	Full-matrix least-squares on F^2
Data / restraints / parameters	4230 / 0 / 218
Goodness-of-fit on F^2	1.094
Final R indices [$I>2s(I)$]	R_1 = 0.0240, wR_2 = 0.0598 [3878]
R indices (all data)	R_1 = 0.0283, wR_2 = 0.0625
Extinction coefficient	0.00138(9)
Largest diff. peak and hole	1.343 and -1.452 e. $Å^{-3}$

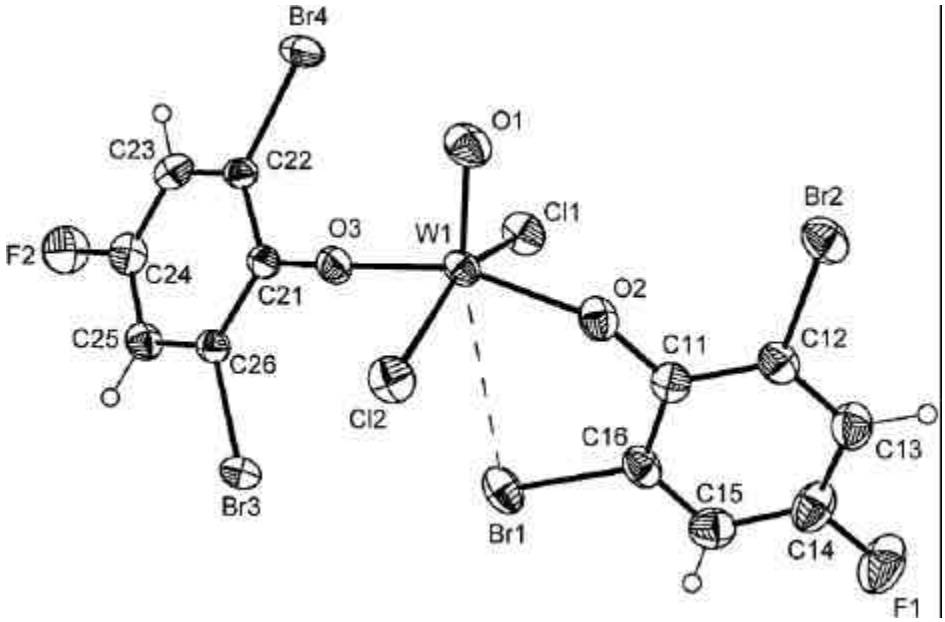

Figure 3-6. Molecular structure of **63**, with 50% probability ellipsoids, showing the atom numbering scheme.

Table 3-C. Selected bond lengths (Å) and angles (°) for complex **63**.

Bond lengths (Å)		**Bond angles (°)**	
W-O1	1.689(3)	C11-O2-W	142.1(3)
W-O2	1.879(3)	C21-O3-W	162.5(3)
W-O3	1.856(3)	O1-W-O3	102.4(2)
W-Cl1	2.3370(10)	O1-W-O2	99.6(2)
W-Cl2	2.3395(10)	O2-W-O3	157.64(13)
W-Br1	3.205(7)	O1-W-Cl1	101.99(11)
O2-C11	1.337(5)	Cl1-W-Cl2	155.9(4)
O3-C21	1.352(5)		

Table 3-D. Crystal data and structure refinement for complex **64**.

Empirical formula	$C_{12}H_4Br_6Cl_2O_3W$
Formula weight	930.36
Temperature	173(2) K
Wavelength	0.71073 Å
Crystal system	Triclinic
Space group	P_1
Unit cell dimensions	a = 7.8459(5) Å α = 94.100(1)° b = 8.8504(5) Å β = 92.687(1)° c = 14.2994(9) Å γ = 95.359(1)°
Volume	984.64(10) Å^3
Z	2
Density (calculated)	3.138 Mg/m^3
Absorption coefficient	18.320 mm^{-1}
F(000)	836
Crystal size	$0.16 \times 0.19 \times 0.23$ mm^3
Theta range for data collection	1.43 to 27.50°.
Index ranges	$-10 \le h \le 9$, $-10 \le k \le 11$, $-17 \le l \le 18$
Reflections collected	6813
Independent reflections	4417 [R_{int} = 0.0181]
Absorption correction	Integration
Refinement method	Full-matrix least-squares on F^2
Data / restraints / parameters	4417 / 0 / 218
Goodness-of-fit on F^2	0.996
Final R indices [$I>2s(I)$]	R_1 = 0.0258, wR_2 = 0.0628 [3826]
R indices (all data)	R_1 = 0.0323, wR_2 = 0.0647
Extinction coefficient	0.00135(17)
Largest diff. peak and hole	1.537 and -1.000 e. Å^{-3}

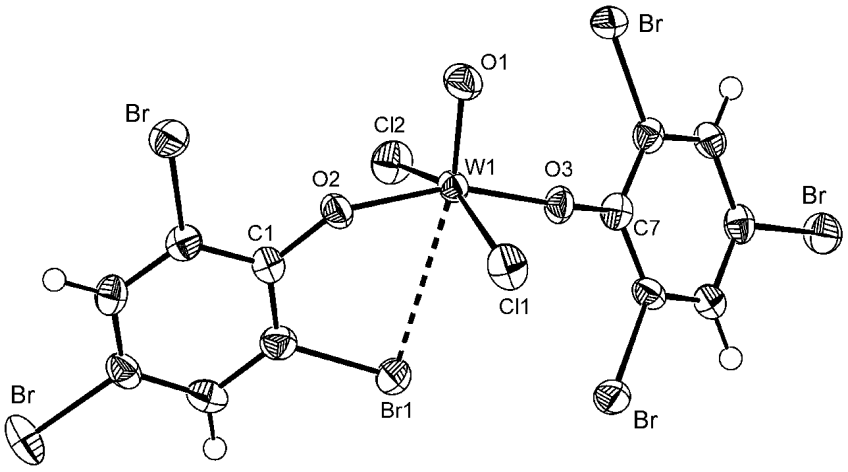

Figure 3-7. Molecular structure of **64**, with 50% probability ellipsoids, showing partial atom numbering scheme.

Table 3-E. Selected bond lengths (Å) and angles (°) for complex **64**.

Bond lengths (Å)		**Bond angles (°)**	
W-O1	1.684(4)	C1-O2-W	140.5(3)
W-O2	1.888(3)	C7-O3-W	159.2(3)
W-O3	1.859(3)	O1-W-O3	102.9(3)
W-Cl1	2.3104(13)	O1-W-O2	99.4(8)
W-Cl2	2.3302(13)	O2-W-O3	157.3(6)
W-Br1	3.149(3)	O1-W-Cl1	101.5(0)
O2-C1	1.349(6)	Cl1-W-Cl2	157.2(6)
O3-C7	1.345(6)	O2-W-Br1	75.3(3)

In contrast, crystallization of complex **65** turned out very difficult due to the high solubility of the complex in non-protic, non-coordinating solvents. A single crystal of low quality was grown from a mixture of CH_2Cl_2/toluene at -30 °C, and although the amount of disorder found in the structure refinement was very high, X-ray diffraction data reveals interesting structural information. In contrast with complexes **32**, **63** and **64**, the ligand arrangement appears to be symmetrical in complex **65**, and no W-Br interaction can be observed. A view along a Cl-W bond shows the symmetrical arrangement of the ligand set, as well as the square-based pyramidal geometry. Apparently, the effect of the trifluoromethyl group on the complex electronics is not the only significant variant influencing its conformation in the crystal.

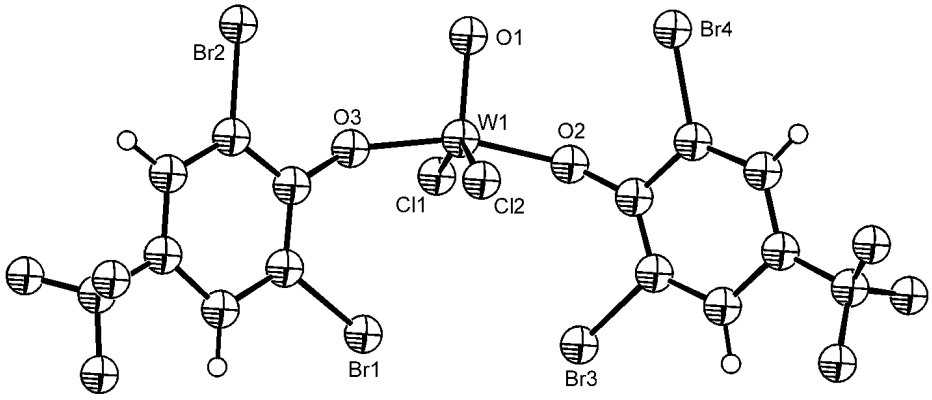

Figure 3-8. Platon view of complex **65**.

These collected observations suggest that the properties of the complexes in the solid state (e.g., bond angles, lengths) cannot be used as an inference parameter for the catalytic activity of the alkylidenes generated therefrom. No trend could be observed within the structural data.

ADMET Chemistry

The bulk polymerization of 1,9-decadiene was studied in order to explore the polymerizing ability of complexes **63**-**67** and in search of a useful probe for the comparison of their catalytic properties. It was found that complexes **63-66** efficiently catalyze the condensation polymerization of this and other hydrocarbon dienes such as 1,8-nonadiene, complementing the range of aryloxide tungsten-based classical catalysts for ADMET polymerization. Linear metathesis polymer can be obtained following the general methodology described in Chapter 2, and the combined results are shown in Table 3-F.

Table 3-F. Acyclic diene metathesis polymerization of 1,9-decadiene

Complex	**[W] mol %**[a]	**M_n (NMR)**[b]	**M_n (GPC)**[c]	**PDI**[c]
63	0.2	1300-1800	3000	1.94
64	0.2	2300	6400	2.71
65	0.2	*neg*	11,300	2.11
66	0.4	1500	-	-

a) Concentration with respect to monomer. Bulk polymerization at 85 °C, [Bu_4Sn]=2.5×[W].
b) Calculated via end-group analysis from ^{1}H-NMR data, by integrating the signals corresponding to the terminal vinyl groups vs. internal olefin. *neg* = no end groups were observable.
c) Determined by gel permeation chromatography in chloroform (see experimental) using polystyrene standards.

In concert with the previously described experiments (Chapter 2), Bu_4Sn proved again to be a better activator when compared to Bu_3SnH. In fact, the use of Bu_3SnH did not lead to an active catalyst when used with complexes **65** and **66**, which consistently decomposed upon exposure to the standard polymerization conditions. Different results were found among the studied complexes, and lower molecular weights were found in the reactions catalyzed by complexes **63** and **66**, both by NMR end-group analysis and by gel permeation chromatography (Table 3-F). The ^{1}H-NMR spectrum of a sample of polyoctenylene synthesized using complex **63** and Bu_4Sn is shown in Figure 3-9, and shows vinyl resonances attributed to terminal groups (4.9-5.0 and 5.8 ppm.)

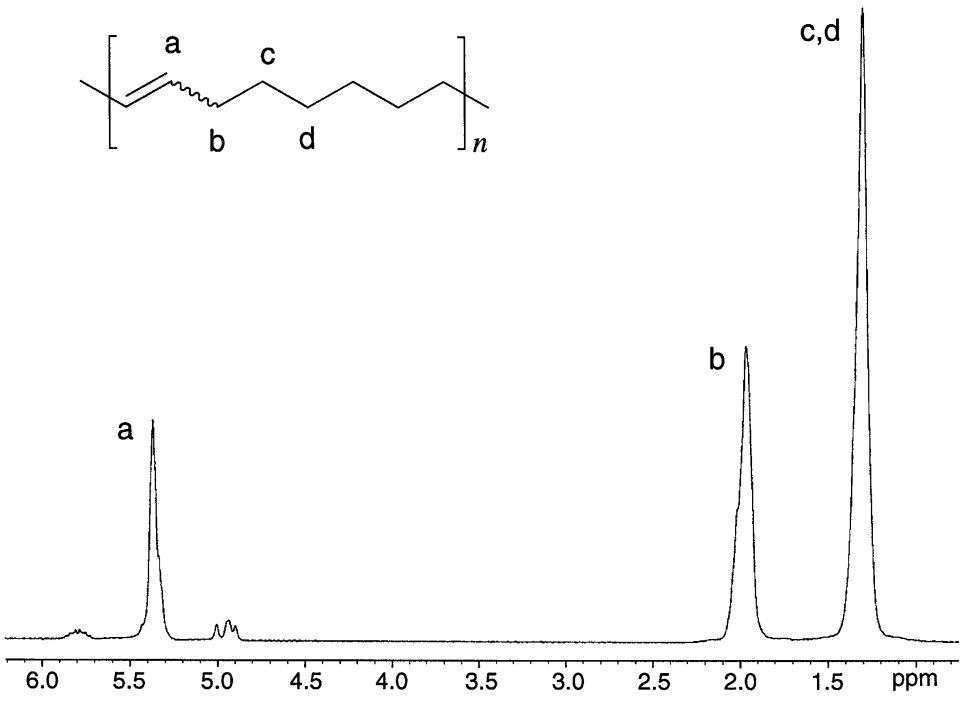

Figure 3-9. ^{1}H-NMR of a sample of polyoctenylene obtained using complex **63** and Bu_4Sn.

In contrast to the behavior shown by complexes **63** and **66**, complex **65** appears to yield the highest molecular yield polymer in good yields, probably as a consequence of the influence of its particular substituent, the trifluoromethyl group. The ^{1}H and ^{13}C-NMR spectra of a sample of polyoctenylene synthesized using complex **65** and Bu_4Sn are shown in Figure 3-10 and Figure 3-11 respectively. As demonstrated before for complexes **32**-**34**, high molecular weight polymer is obtained from this polycondensation reaction, and this fact is evidenced in the absence of resonances attributed to vinyl end groups. Furthermore, analysis of the NMR data reveals that no isomerization of the olefin groups has taken place, a competing reaction observed in other metathesis applications of analogous complexes (e.g., **5**) (Vosloo 1997, van Schalkwyk 1998).

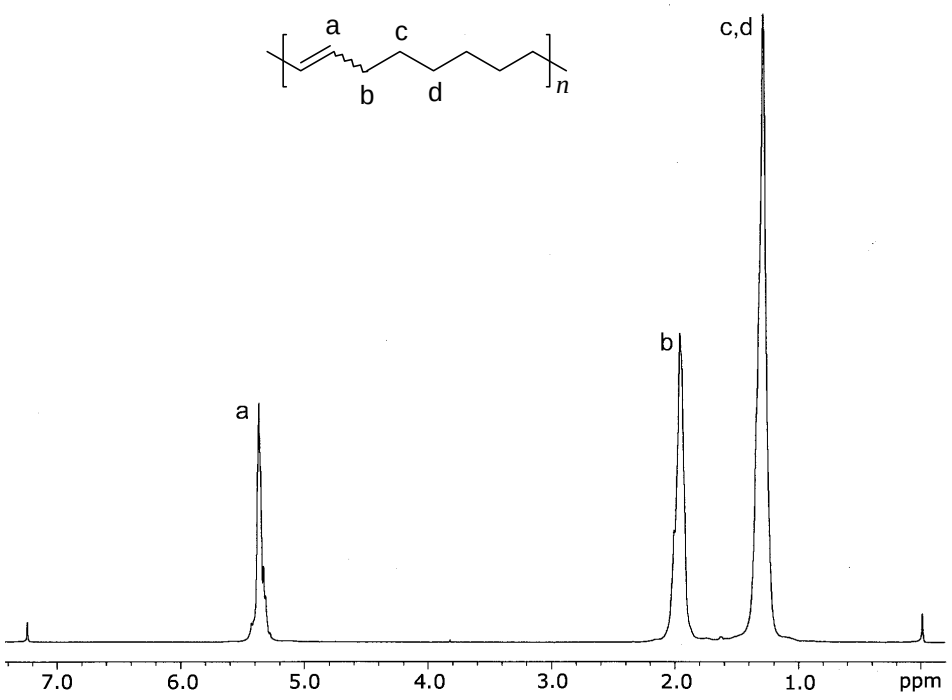

Figure 3-10. ^{1}H-NMR of a sample of polyoctenylene obtained using complex **65** and Bu_4Sn.

Although no quantitative kinetic measurements were made on the metathesis reactions catalyzed by systems based on complexes **63-66**, qualitative observations reveal two interesting features of the studied systems. The first characteristic is the apparent activity increase in agreement with the expected behavior for complexes (**32-**)**64-65** as ADMET catalysts, which seems to be especially evident for complex **65**. This is observed in a shorter induction period prior to ethylene release from the reaction mixture which can be attributed to the activation step as proposed by Quignard and co-workers (1986). In addition, the identity of the substituent X in the series affects not only the activity, but also seems to have a dramatic effect on the solubility properties of these complexes. While complex **65** is very soluble in conventional solvents, complex **67** is virtually insoluble, limiting its usability not only in ADMET but also in other metathesis applications. Although limited solubility has also been observed for complex **66** at room temperature, the complex is useful at the experimental polymerization conditions. The solubility behavior of the complexes described may also account for a low % conversion in the case of complexes **64** and **66**, for which faster decomposition kinetics with respect to complex **65** prevents the formation of high molecular weight polymer.

Also noteworthy, especially while considering the application of this methodology to other metathesis processes, is the fact that along with an increased activity in olefin metathesis, a parallel effect on the reactivity towards polar functionalities is also apparent. This is evidenced in a poor air and moisture-resistance shown in all the complexes studied, a phenomenon that is remarkably evident in complexes **66** and **67**.

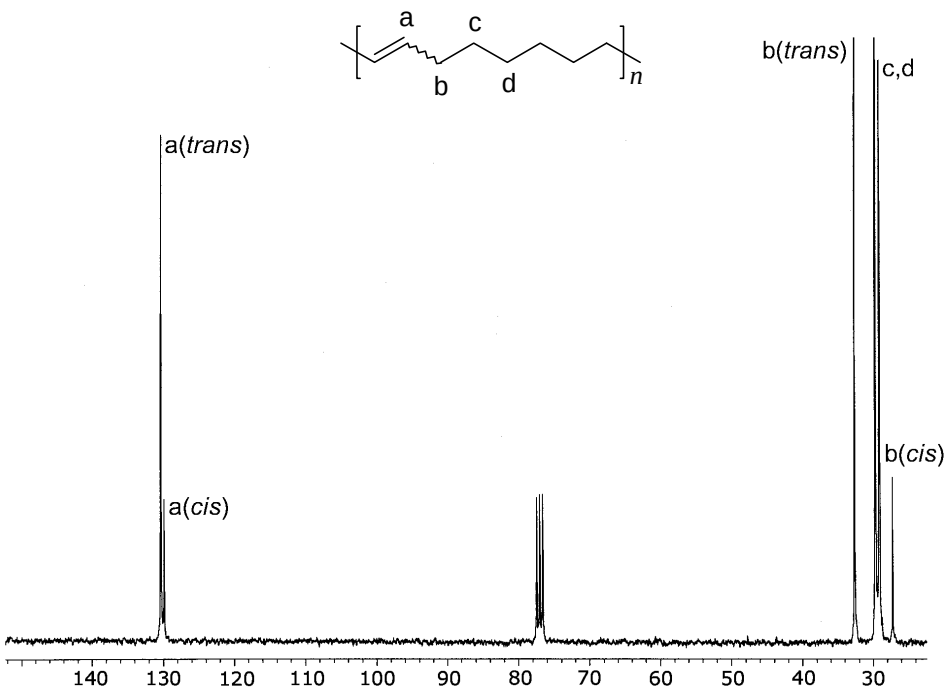

Figure 3-11. ^{13}C-NMR of a sample of polyoctenylene obtained using complex **65** and Bu_4Sn.

ROMP Chemistry

Complementary to the study of complexes **63**-**66** in ADMET polymerization, the possibility of using complexes **63**-**66** as precatalysts for ring opening metathesis polymerization (ROMP) was also explored. Processes as important as the industrial production of polydicyclopentadiene thermosets are grounded on the use of classical systems (Kelsey 1997). Heating bulk dicyclopentadiene (DCPD) in the presence of complexes **63**-**66** and Bu_4Sn yields crosslinked PDCPD after a short induction time. Although no efforts were made to determine the amount of residual monomer or the magnitude of the polymerization exotherm, the exploration of the effect of monomer to

tungsten complex (M/W) molar ratio reveals that fast polymerization occurs at ratios as high as 5000:1 M/W both under solvent and bulk conditions.

At the same time, linear polynorbornene is obtained upon exposure of a 1 M toluene solution of freshly sublimed norbornene to a mixture of complexes **63-66** and Bu_4Sn in toluene at 85 °C. The features of other aryloxide systems in the polymerization of norbornene have been previously reported (Barnes 1994, Diets 1993).

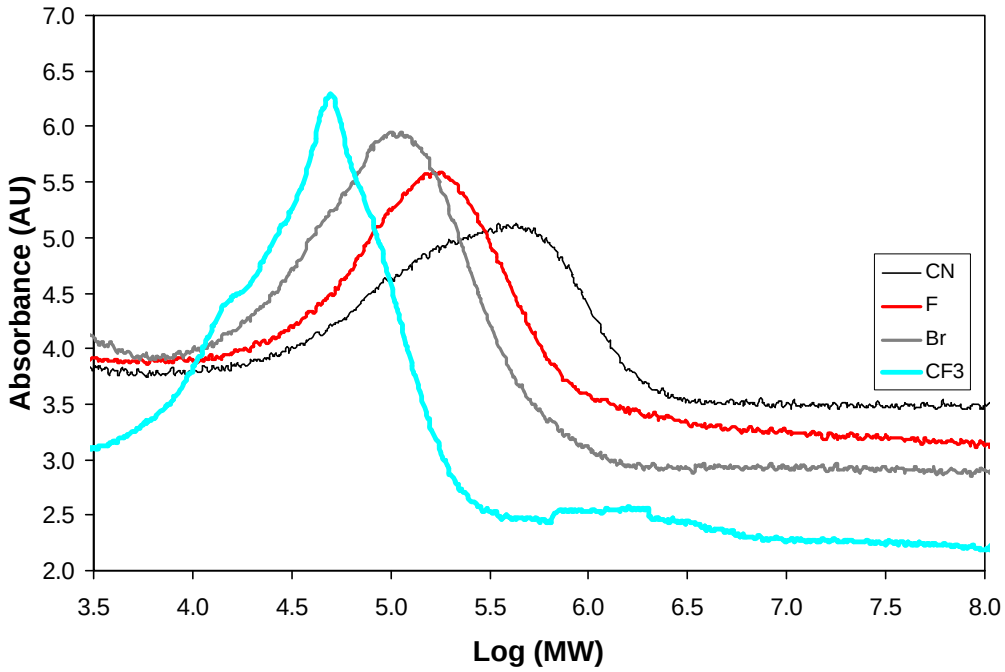

Figure 3-12. GPC traces of four polynorbornene samples synthesized using complexes **63-66**. The traces are named based on the ligand substituent

Quantitative conversion of norbornene is required in order to use its ring opening metathesis polymerization as a probe for comparative catalytic activity among the systems studied. In the case of solution polymerizations run for extended times (at W/M

ratios of 100:1), catalyst decomposition occurs before the monomer is totally consumed, and lower yields of polymer can be obtained (71-84% purified polymer). Although it is safe to overlook this fact while studying ROMP chemistry, the difference in molecular weights (M_p) can be attributed to differences in either the propagation rates or the extent of activation, and the designed experiments do not allow the determination of which factor is more significant for the studied series. While stronger alkylating agents such as aluminum or lead alkyls are needed for the conversion of analogous systems bearing less electron withdrawing phenoxide ligands, milder cocatalysts (e.g., Bu_4Sn) can be used to activate systems in which the metal is made more electropositive (Nugent 1995, Quignard 1986, Kelsey 1997). The same was anticipated (*vide infra*) for systems **63**-**66** which, having a similar affinity for norbornene differ in the amount of actual catalyst formed, not in their propagation kinetics. This would determine the number of growing chains and have a clear effect on the molecular weights observed among the series. In order to test this assumption, the formation of polynorbornene at short polymerization times should reveal features of the initiation (or activation in our case) and propagation.

The GPC traces shown in Figure 3-12 belong to the solution polymerization of norbornene stopped after 15 minutes, i.e. before catalyst decomposition becomes apparent and before any secondary processes take place. Monomodal molecular weight distributions were found in all cases, and the polydispersities found ranged from 1.8 to 3.3. An increasing PDI value in the series **65**-**64**-**63** suggests that the availability (concentration and rate of formation) of initiating species varies based on the ligand substituent, affecting the properties of the polymers obtained. The largest PDI value was found in the case of complex **66**; this observation can be attributed to an inefficient

initiation step, an observation in agreement with other metathesis processes. It is noteworthy that if a constant extent of activation and similar initiation kinetics were to be assumed for all four complexes, then the overall propagation constants extrapolated from differences in the molecular weights would still fall within the same order of magnitude. The effect of substitution on the conversion kinetics has been subject to further exploration using a more sensitive probe based on ring closing metathesis chemistry.

Ring Closing Metathesis

The behavior and applicability of the complexes reported herein as precatalysts for ring closing metathesis (RCM) was also explored.

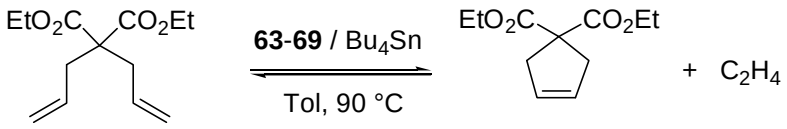

Figure 3-13. Ring closing metathesis of diethyl diallylmalonate.

The results obtained indicate that while complexes **63**-**65** effectively catalyze the RCM of diethyl diallylmalonate, complex **66** decomposes before any significant conversion of the starting material occurs (Table 3-G). The applied experimental methodology consists in the introduction of the olefin after 5 minutes of interaction of the W complex with Bu_4Sn at the activation temperature (90 °C), and monitoring the reaction by GC and NMR spectroscopy.

Table 3-G. Ring closing metathesis of diethyl diallylmalonate.

Complex	Conditions[a]	%C 90 min[b]	%C Final[b]
63	[S]=1 M, [S]/[W]=25	51 (46)	86 (88)
64	[S]=1 M, [S]/[W]=25	37 (-)	54 (49)
65	[S]=1 M, [S]/[W]=25	57 (50)	89 (90)
65	[S]=0.25 M, [S]/[W]=12.5	74 (71)	94 (92)
66	[S]=1M, S/W=25	<10 (-)	29 (19)

a) Toluene, 85 °C, [Bu_4Sn]=2.5×[W], 5 min activation time.
b) Determined by gas chromatography (see experimental) using α-ionone as internal standard. Values in parenthesis were extracted from ^{1}H-NMR data by integrating the signals corresponding to the allylic methylene group of product and diene.

The results shown in Table 3-G are in concert with the observed behavior of complexes **63**-**66** in both ADMET and ROMP chemistry, for they suggest that the identity of substituent X seems to affect not only the electronics of the complex (both in activity and chemical stability) but also its solubility. At the same time, the increased chemical sensitivity of complexes **63**-**66** with respect to their parent, non substituted complex **32**, can be observed in the substrate to precatalyst ratio (S/W) required to drive the reaction to excellent yields. While complex **32** has been reported to yield the cyclic diester in 86 % after 1 h at 90 °C (Nugent 1995), the use of complex **65** only afforded the product in similar yields (89 %) when reacted for longer periods of time (ca. 4 h). Carrying out the reaction at lower S/W ratio and lower concentration (0.25 M) resulted in very high percent conversion (Table 3-G, entry 4). Attempts to carry out the reaction using the same

conditions reported for **32** and Et_4Pb (Nugent 1995) derived in a 47 % conversion (NMR) after 60 min, and 50 % (NMR) after 90 min. Although this decreased conversion could be attributable to a faster decomposition of the alkylidene formed upon activation, it is more likely to reflect the lower extent of activation achieved with Bu_4Sn when compared to Et_4Pb.

Conclusions

A series of tungsten aryloxide complexes were designed, synthesized, and their properties investigated in the catalysis of various olefin metathesis processes. Complexes **63**-**66** catalyze the ADMET polymerization of hydrocarbon dienes, the ring opening polymerization of norbornene and dicyclopentadiene, and –to some extent– the ring closing metathesis of diethyl diallylmalonate. An exploration of catalysis conditions in the above mentioned processes reveals that substitution of the aryloxide ligand causes a modification of the electronics of the complexes, evidenced not only in qualitative differences in catalytic activity, but also in the chemical stability and the solubility behavior exhibited by the studied complexes. Although initially considered as a possible tool in the prediction of the physicochemical behavior of complexes **32**,**63**-**67**, structural analysis show that the observation of properties in the solid state cannot be associated with features such as catalytic activity.

CHAPTER 4
TOWARDS HIGH METAL CONTENT ADMET POLYCARBOSTANNANES USING CLASSICAL AND WELL-DEFINED METATHESIS CATALYSTS

As described in Chapter 1, the rules governing the relationship among monomer structure, reactivity and catalytic systems in ADMET polymerization have been the focus of active research efforts. Complementing the research described in the previous chapters which was mainly concentrated on novel synthetic methodology and catalytic systems, investigations on new routes towards tin containing polymers using ADMET chemistry are herein described.

Metal-Containing Polymers

Although relatively new, the synthesis of organometallic polymers has become an extensively investigated and fruitful new discipline and has emerged as a possible route towards materials exhibiting unique properties arising from both the metallic and the organic components (Manners 1996, Rehahn 1998). Interest in metallopolymers has grown constantly not only because of the possible applications predicted for some of these systems, but also because of the variety of synthetic tools and obtainable structures that a number of organometallic reactions and substrates offer to the polymer chemist.

The four general groups in which organometallic polymers have been classified are shown in Figure 4-1.

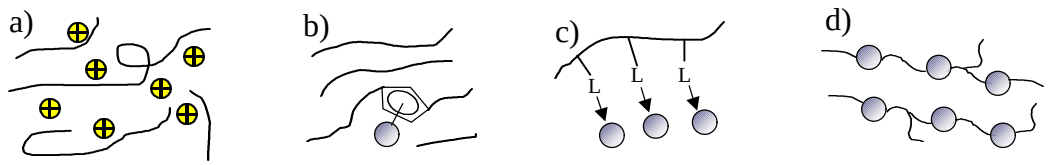

Figure 4-1. General representation of a) ionic, b) π-complex, c) coordination and d) covalent type metal containing polymers.

Among the numerous combinations of structures and properties available today, metallopolymers obtained through the polymerization of monomers containing a covalent metal-carbon bond still represent a relatively small portion (Pomogailo 1994). This is a clear representation of the marked stability of chelate and –in general– coordination complexes with respect to covalent structures, as well as the many possibilities offered by coordination chemistry in terms of oxidation states, ligand combinations, and metal incorporation. Such advantages have been creatively explored in strategies where the propagation reaction involves coordination phenomena (Pomogailo 1994).

Tin-Containing Polymers

The polymerization of monomers containing tin as a substituent yields in most cases polymers with tin-containing side chains, and several examples of organometallic polymers of tin belong to this category. The polymerization of olefins such as tin

acrylates is the most common route to tin-containing polymers, and this specific example has become a widely use approach towards polymeric biocides.

As demonstrated by Cummins (1991), ring opening metathesis polymerization can also be a route towards organometallic polymers. Microphase-separated block copolymers possessing the structure shown in Figure 4-2 could be synthesized from norbornene and norbornene-type metal chelates.

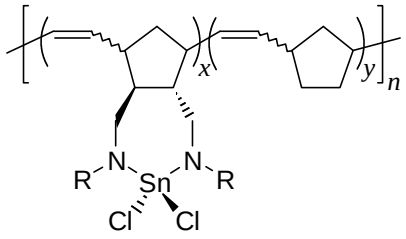

Figure 4-2. Microphase-separated block copolymers containing Sn(VI) moieties synthesized via ROMP.

Polystannanes

Polymetallanes is the name given to the family of organometallic polymers containing backbones exclusively made of metals connected by σ bonds. The vast majority of the research on polymetallane structures has been concentrated on the development of polysilanes, due to their optical and electrical properties (Miller 1989, West 1986, Reichl 1996). Along with their silicon and germanium analogues, polystannanes have attracted a great deal of attention in recent times, and synthetic routes towards this type of materials are in constant development. One of the earliest approaches to polystannanes consists in the coupling of dialkyltin dihalides, and a variety of

experimental procedures have been reported since as early as 1964. Representative examples of reaction conditions are shown in Table 4-A.

Table 4-A. Experimental conditions used in the synthesis of polystannanes from dialkyltin dichlorides.

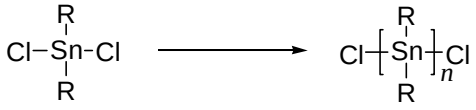

68 **69**

Conditions	Product	Reference
Na, Toluene reflux	R = Bu, M_n = 2100	Neumann 1964a
Na, 15-Crown-5, Toluene reflux	R = Bu, M_n = 13,800	Zou 1992
Na, 15-Crown-5, Toluene reflux, light exclusion / sonication, 1-5 h	R = Bu, $M_n = 1 \times 10^6$	Devylder 1996
SmI_2, THF/HMPA, 23 °C, 24 h	R = Et, 74 % M_n = 3980 PDI = 1.21	Yokoyama 1995, Mochida 1998a
SmI_2, THF, 65 °, 5 h	R = Et, 76 % M_n = 3570 PDI = 1.15	
Electrochemical, Cu electrode, DME	R = Bu, Oct M_n = 6000 - 11,000 PDI = 1.3 - 2.6	Okano 1998

A serious disadvantage found in the procedures listed above (except for the electrochemical method developed by Okano) is the use of large amounts of alkali metals or SmI_2, and alternative methodologies are desired in view of the predicted applications of these materials.

Another elegant approach towards polystannanes consists in the transition metal-catalyzed dehydropolymerization of dialkyl (or diaryl) tin dihydrides, an extension

of a synthetic methodology employed in the synthesis of polysilanes from silicon dihydrides (Tilley 1993, Imori 1994). This reaction has been shown to proceed in the presence of organometallic complexes of a variety of transition metals, summarized in Table 4-B. Among the different experimental conditions reported, the activity, product yields and high molecular weights found by Imori (1995) are remarkable.

Table 4-B. Experimental conditions used in the synthesis of polystannanes from dialkyltin dihydrides.

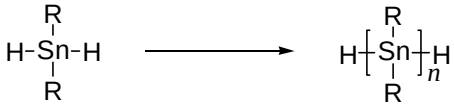

70 **71**

Conditions[a]	**Reference**
A variety of Zr and Hf complexes, mainly metallocenes.	Imori 1995, Lu 1996
Zr and Hf metallocene dichlorides or W, Mo, Cr hexacarbonyls in the presence of Al hydrides	Woo 1997
Pd/Fe dinuclear complexes	Braunstein 1998

During the last decade, the interest on the properties of macrostructures built with group 14 metals led Sita and coworkers (1994) to the exploration of a controlled route to linear polystannanes (Sita 1992, Shibata 1998). In this approach, the oligostannane chains are built one atom at a time, which although considered a limitation for the extension of this methodology to higher macromolecules, has given valuable insight into the fundamentals of polymetallane structures (Figure 4-3).

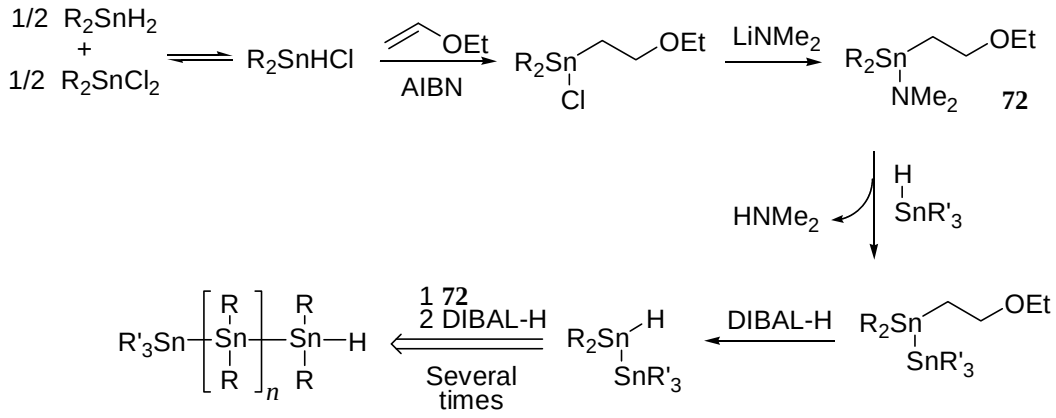

Figure 4-3. Sita's strategy towards pure, linear polystannane oligomers.

The extensive research on linear polystannanes can be easily justified when their physical properties are considered. Polydialkylstannanes display a σ-σ^* transition at 390-400 nm which represents a red shift of ca. 70 nm with respect to their silicon analogues, while polydiarystannanes seem to exhibit σ,π-conjugation and even lower bandgaps (430-440 nm) have been observed (Lu 1996). In addition, Imori and coworkers (1995) observed thermochromic behavior in some polydialkylstannanes as well as fast, irreversible photobleaching initiated by UV or visible light. These properties are very promising in terms of possible applications in sensor devices and in semiconductor technology. In fact, although only at a very preliminary stage, conductivities in the order of 0.3 S cm^{-1} were found in polydialkylstannanes doped with SbF_5 (Imori 1995).

Polycarbostannanes

Polymers that contain covalently bound carbon and tin atoms along the backbone are known as polycarbostannanes. The first examples of polycarbostannane polymers

were synthesized via step polymerization of diolefins (or diacetylenes) and tin dihydrides, as shown in Figure 4-4 (Leusink 1964, Noltes 1961, 1962).

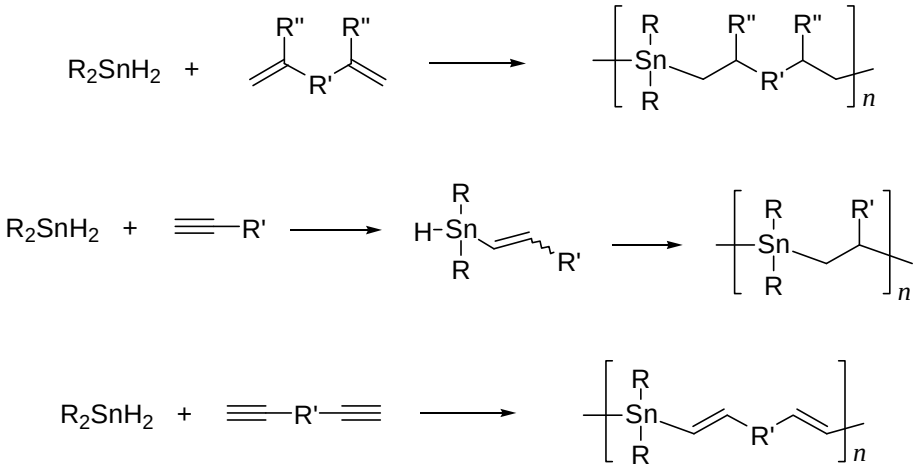

Figure 4-4. General scheme for the synthesis of step addition polymers between dialkyltin dihydrides and diolefins or acetylenic compounds.

Another interesting example of polymers containing tin atoms incorporated along the backbone is the family of structures shown in Figure 4-5. In this case, the polymers are synthesized from tin-containing α,ω-diynes and metal or aryl dihalides leading to materials in which the effect of σ,π-conjugation on the optical properties of the polymers was investigated (Hagihara 1994).

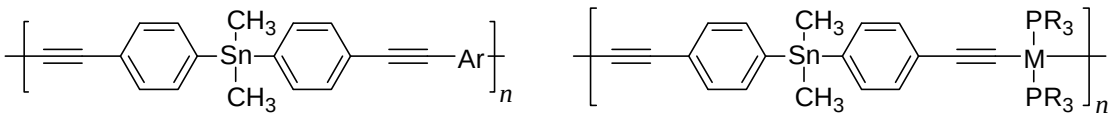

Figure 4-5. Structures of tin-containing σ,π-conjugated structures (Hagihara 1994). M = Pt, Pd.

Polycarbostannanes via ADMET Polymerization

As presented in Chapter 1, ADMET polymerization is a valuable tool for the synthesis of unsaturated polymers containing a variety of functional groups (Figure 1-7). In 1997, Wolfe demonstrated that Schrock's molybdenum catalyst **26** could be used in the polymerization of the stannadienes **73** and **74** to yield high molecular weight poly[bis(4-pentenyl)di-*n*-butylstannane] (**75**) as well as linear (**76**) and cyclic (**77**) oligomers of poly[bis(3-butenyl)di-*n*-butylstannane]. The studies performed by Wolfe demonstrated the feasibility of synthesizing tin-containing polymers via ADMET polymerization, as well as the compatibility between the metathesis catalyst **26** and the alkyltin moiety.

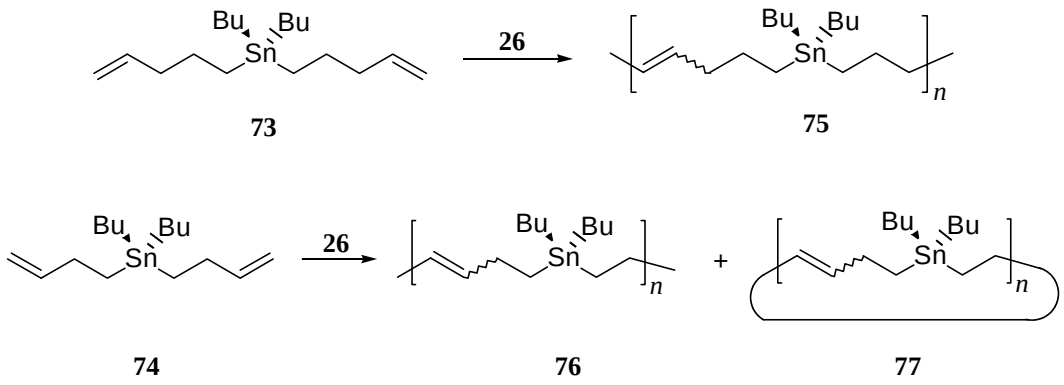

Figure 4-6. ADMET polymerization of bis(alkenyl)di-*n*-butylstannanes by Wolfe (1997).

Monomer-Activated Metathesis Polymerization

By 1997 ADMET polymerization had become a new route towards tin-containing polymers, as demonstrated by Wolfe (1997). At the same time, the availability of a new

methodology for ADMET polymerization using soluble aryloxide tungsten-based catalysts (Chapter 2) and the fact that tetraalkyltin complexes were used as activators of these and other classical catalytic systems (Nubel 1994, Ivin 1997) allowed the consideration of bis(alkenyl)dialkyltin compounds as both monomers and activators for ADMET polymerization. The same stannadienes studied by Wolfe (1997) were considered as possible monomers, namely bis(3-butenyl)di-*n*-butylstannane (**74**) and bis(4-pentenyl)di-*n*-butylstannane (**73**).

Poly[bis(4-pentenyl)di-*n*-butylstannane]

Similar to the behavior observed in the bulk polymerization of hydrocarbon monomers (Chapter 2) by systems composed of a tungsten aryloxide complex and a tetraalkyltin activator, the polymerization of diene **73** proceeds with ease. When a mixture of 100 equivalents of diene **73** and 1 equivalent of complex **32** was heated to the activation temperature (85-90 °C) under an argon atmosphere, a slight color change was accompanied by gas evolution. During the first three hours of reaction the viscosity increased significantly and ethylene evolution was observed. Exposure of this mixture to vacuum accelerates the bubbling, and the reaction is completed after ca. 7 h under reduced pressure. The observed polymerization carried out without the use of an external activator suggests that the activation takes place through the mechanism discussed in Chapter 2 and represents *the first case in which a reagent serves as both the monomer and the activator in a metathesis polymerization* (see below).

Contrary to the observed results in the case of hydrocarbon monomers, purification of the title polymer under normal conditions did not proceed as expected.

After the first precipitation of the polymer from warm chloroform into methanol an insoluble gel was obtained suggesting partial crosslinking of the product. In order to present an explanation to this phenomenon, the mechanism of catalyst activation for this particular polymerization needs to be analyzed in detail.

Proposed activation mechanism

In agreement with the mechanism detailed in Chapter 2, the active catalyst is formed in a two-step sequence. The first step (shown in Figure 4-7) consists of the alkylation of 1 equivalent of complex **32** by 2 equivalents of diene **73** yielding a dialkyl complex (**78**) and the tin halide **79**.

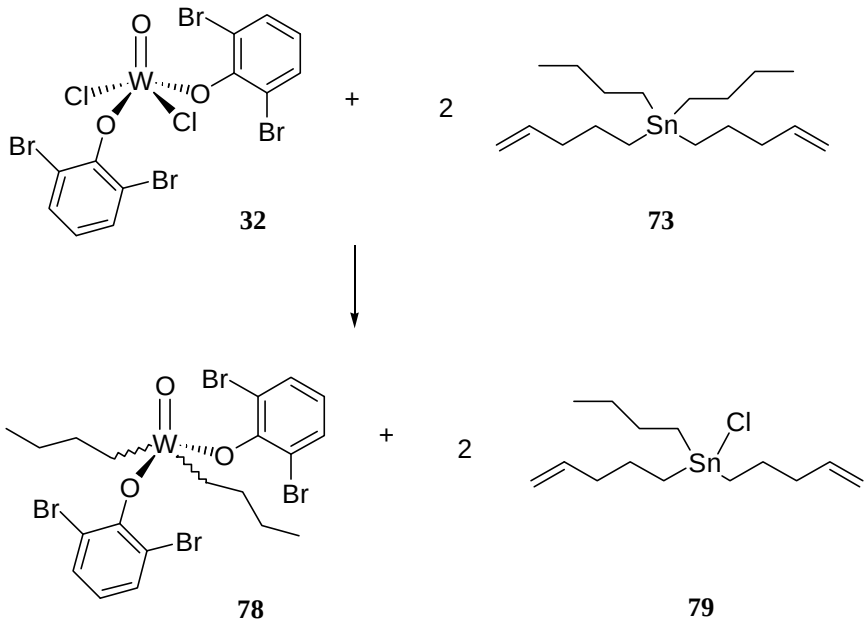

Figure 4-7. First step in the proposed mechanism for the formation of an active catalyst from complex **32** and the stannadiene **73**: alkylation.

The second step is the thermally induced α-abstraction reaction shown in Figure 4-8, which leads to the formation of the oxocarbene **80** and a molecule of *n*-alkane (butane in the example).

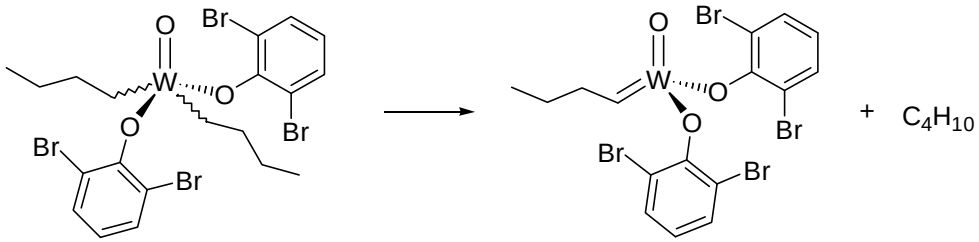

78 **80**

Figure 4-8. Second step in the proposed mechanism for the formation of an active catalyst from complex **32** and the stannadiene **73**: α-abstraction.

The properties of the product obtained can be explained by the incorporation of tin chloride moieties in the polymer. As depicted in Figure 4-7, two equivalents of the stannane chloride **79** are formed in the transmetallation reaction and this is a difunctional monomer that can be incorporated in the polymer chain. Isolation and purification of the polymer using wet solvents and exposure of the polymer sample to the atmosphere may cause partial hydrolysis of the Sn-Cl bonds and lead to the formation of tin hydroxides, which can in turn crosslink the polymer. A general scheme for this phenomenon is shown in Figure 4-9. Although no direct evidence exists for this reaction, modification of the purification conditions to eliminate the moisture sources affords linear, soluble polymer. In turn, when the polymerization is performed at higher monomer to precatalyst ratio (250:1) no gelation is observed upon precipitation of the polymer under normal conditions, which can be attributed to a lower concentration of Sn-Cl bonds in the

polymer chains. Furthermore, samples of the same polymer synthesized using the molybdenum complex **26** by Wolfe (1997) do not crosslink upon exposure to moisture, an observation that supports the proposed crosslinking route.

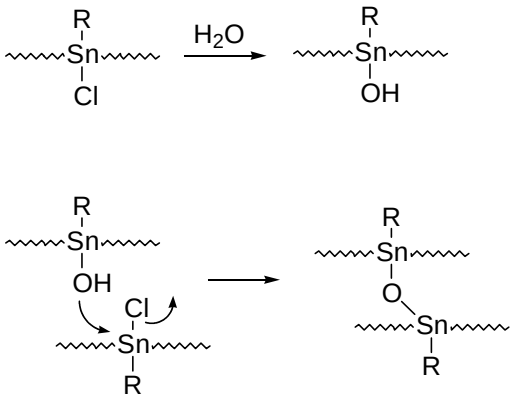

Figure 4-9. Proposed mechanism for chemical crosslinking of the polymer obtained from the ADMET polymerization of diene **73** using complex **32** (100:1).

Optimization of the experimental conditions led to the isolation of polymer **75** through the clean polymerization of diene **73** using the tungsten complexes **32** or **33**.

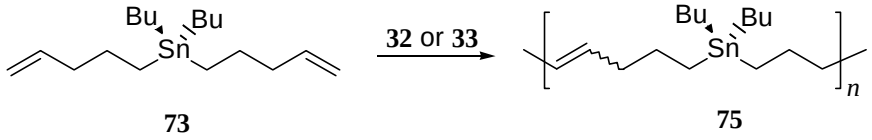

73 **75**

Figure 4-10. ADMET polymerization of bis(4-pentenyl)di-*n*-butylstannane using complexes **32** or **33** and no external activator (250:1).

Polymer **75** has the same physical properties described by Wolfe (1997). It is a viscous liquid, soluble in halogenated and aromatic solvents, but insoluble in polar solvents such as methanol from which it can be precipitated. High molecular weight was

observed in all cases (GPC and ^{13}C-NMR end-group analysis). The summarized characterization data is presented in Table 4-C.

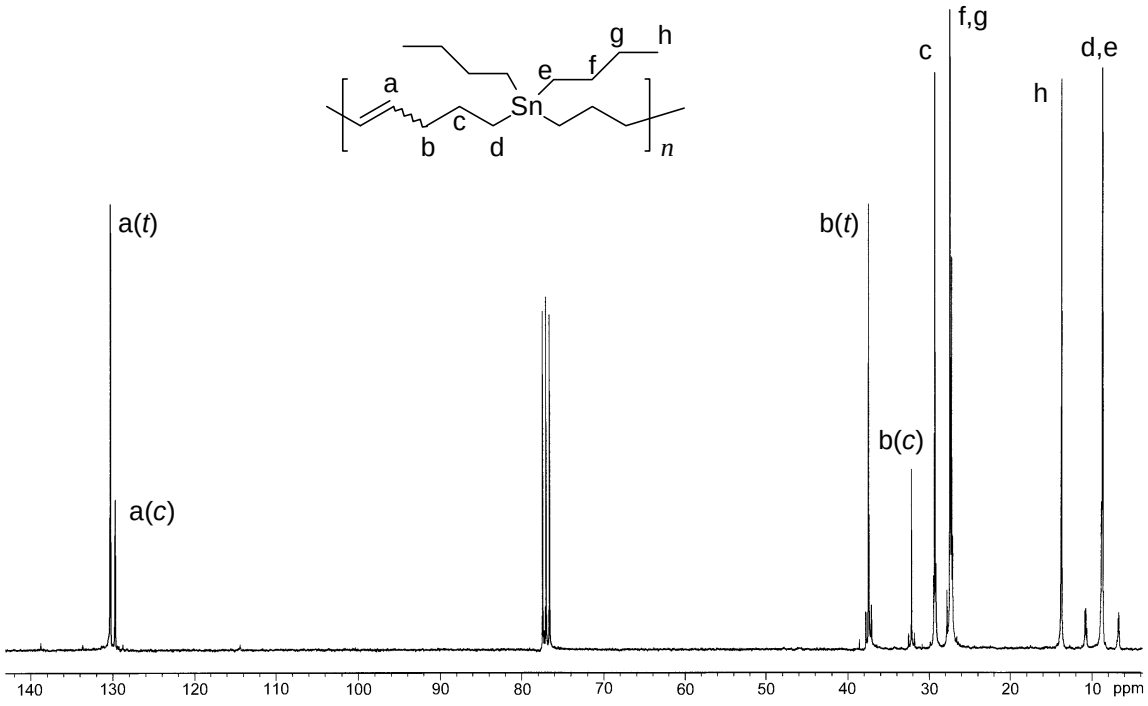

Figure 4-11. ^{13}C-NMR of polymer **75** synthesized using complex **33** and no external activator (250:1).

Several interesting features can be observed in the NMR spectral characteristics of polymer **75**. First, the polymer contains mainly *trans* linkages (80% from quantitative ^{13}C-NMR data), a figure in agreement with other ADMET polymers. Second, three distinct signals can be observed in the ^{119}Sn-NMR of the polymer samples analyzed (Figure 4-12) and their relative intensities correspond to the calculated statistical distribution of tin atoms between olefins with different stereochemical arrangements (Table 4-C).

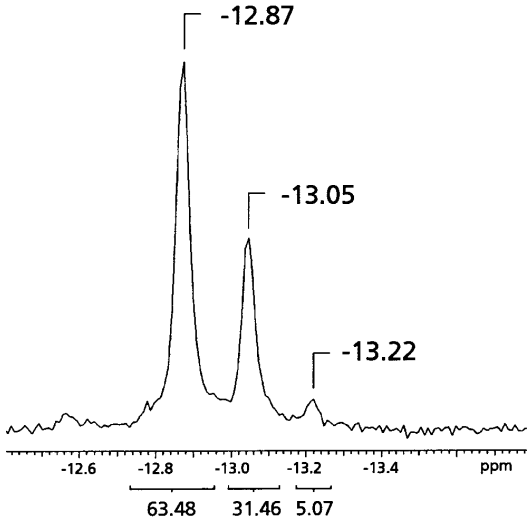

Figure 4-12. ^{119}Sn-NMR of polymer **75** synthesized using complex **32** and no external activator (250:1). The signals correspond to Sn atoms between *trans-trans*, *trans-cis* and *cis-cis* double bonds.

One of the most important characteristics of polymer **75** is its thermal behavior. When heated under a nitrogen atmosphere above the onset decomposition temperature elimination of the organic components takes place, and the weight of the residual material accounts for the theoretical amount of metal introduced in the polymer. Similarly, decomposition under an air atmosphere shows a slightly higher ceramic yield, attributable to partial oxidation to tin oxide. This behavior had not only been observed in the samples synthesized using the well-defined molybdenum catalyst **26** (Wolfe 1997) but also in other tin-containing polymers (Imori 1995). This suggests that possible applications of these materials could be based on this behavior, making of ADMET polycarbostannanes precursors to ceramic materials and metallic thin films. However, the physical state of the polymers synthesized to date impedes the casting of free-standing films, which limits their applicability. Efforts to overcome this difficulty are discussed in a later section.

Table 4-C. Polymerization of stannadiene **73** using a well-defined catalyst (**26**) (Wolfe 1997) and tungsten precatalysts **32** and **33**.

Catal.	Experimental Conditions	M_n		*trans*:*cis* ratio	^{119}Sn-NMR Intensities	
		GPC	^{13}C-NMR	(^{13}C-NMR)	Calcd.	Obs.
26[a]	RT-60 °C, 48 h	36 000	17 000	79:21	64:32:4	65:30:5
32	85-100 °C, 36 h	17 000	9300	79:21	64:32:4	64:31:5
33	90-100 °C, 48 h	30 000	16 000	80:20	64:32:4	63:32:5

a) Wolfe (1997), appended for comparison.

Poly[bis(3-butenyl)di-*n*-butylstannane]

The second stannadiene studied was bis(3-butenyl)di-*n*-butylstannane, which yielded both cyclic and linear oligomers with the well-defined molybdenum complex **26** (Wolfe 1997). Because of the removal of a methylene group between the olefin and the tin atom, the metal content of the polymer increases (ca. 38 vs. 35 % Sn in polymer **75**).

Complexes **32** and **33** are also activated when heated to 85-90 °C in the presence of diene **74** and form carbene species able to catalyze ADMET polymerization. However, even if the same experimental observations described for polymer **75** (ethylene evolution and increase in the mixture viscosity) are present, complexes **32** and **33** are unable to drive the conversion yield above 75 %. Less than 20 % functional group conversion is observed in the case of complex **32**, whereas after 36 h of reaction complex **33** yields low molecular weight oligomer, as well as ring closing metathesis product. The significant

decrease in activity observed upon reduction of the spacing length between the olefin and the tin moiety with both well-defined (Wolfe 1997) and classical catalysts is still an unexplained phenomenon. The ring closing metathesis product present in the described reaction mixture, can be isolated as the main product when the reaction is carried out in the presence of solvent ([diene] = 0.1 M in toluene, 100:1 substrate/precatalyst) (Figure 4-13).

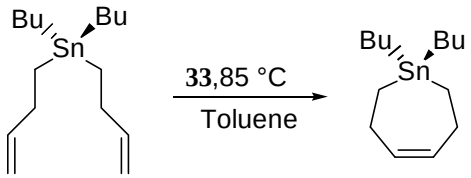

74 **81**

Figure 4-13. Self-activated ring closing metathesis of bis(3-butenyl)di-*n*-butylstannane (**74**) yielding the 7-membered ring **81**.

Spectroscopic analysis of the resulting product (after catalyst and solvent removal reveals the formation of the cyclic product. In turn, mass spectrometry reveals a difference of 28 units with respect to the base peak in the CI-MS of the starting material, which accounts for the molecule of ethylene released in the reaction. The yield based on ^{1}H-NMR is ca. 83 %, and the incomplete conversion is evidenced by the starting material signals present in both ^{1}H- and ^{13}C-NMR. This conversion constitutes the *first example of a substrate-activated ring closing metathesis*. The ^{13}C-NMR of the reaction product is shown in Figure 4-14

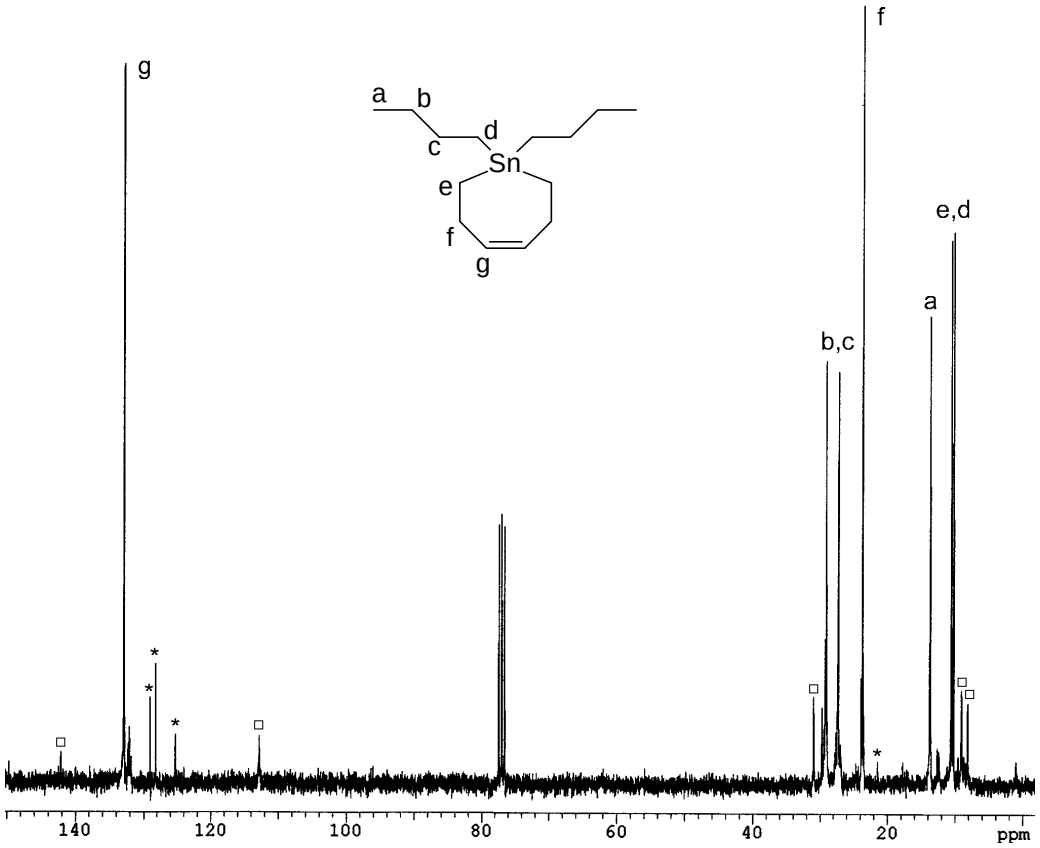

Figure 4-14. ^{13}C-NMR of compound **81**. The following impurities were present in the crude preparation (after solvent removal) * = Residual toluene, □ = starting material.

New Polycarbostannanes

The synthesis of dibutyl derivatives by Wolfe and reported herein motivated the search for new polycarbostannane structures. An extrapolation of the thermal behavior observed for polymers **75** and **76** (Wolfe 1997) suggests that polymers designed with higher metal content should lead to higher % of metal deposition (higher ceramic yields).

Furthermore, new polycarbostannane structures containing side chains different than *n*-butyl groups should not only have an effect on the amount of metal incorporation but also on the physical properties and chemical reactivity of the obtained polymers. For example, it is reasonable to hypothesize that a reduction of the size of the side chains (with respect to e.g., polymer **75**) should increase the observed glass transition temperature.

With this in mind, two new monomer structures were conceived both containing different metal weight % and structural properties which may lead to differences in the macroscopic physical properties of the polymers synthesized therefrom.

Monomer Synthesis

The synthesis of bis(4-pentenyl)dimethylstannane (**82**) and bis(4-pentenyl)diphenylstanane (**83**) was performed through the Grignard alkenylation of the corresponding tin dihalides as reported by Wolfe (1997).

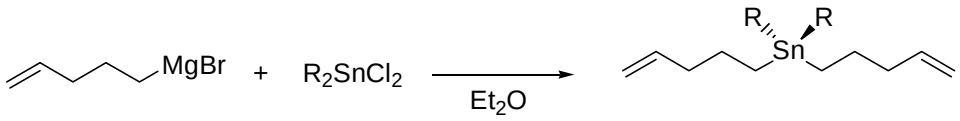

82 R = Me, 67 %
83 R = Ph, 55 %

Figure 4-15. Synthesis of stannadiene **82** and **83** from the commercially available tin dihalides.

The monomers were purified by distillation at reduced pressure followed by vacuum transfer from CaH_2 and several freeze-pump-thaw cycles.

Poly(dimethyldi-*n*-butylstannane)

Mixing an equivalent of Schrock's molybdenum catalyst **26** with 250 equivalents of the stannadiene **82** at room temperature under an argon atmosphere results in vigorous ethylene evolution, evidencing ADMET polymerization. Exposure of the mixture to vacuum for ca.48 h at room temperature followed by heating to 60 °C for an extra 2 days, results in the formation of high molecular weight polymer, which is isolated in essentially quantitative yield after precipitation from a chloroform solution into methanol. Polymer 84 is a viscous liquid at room temperature, soluble in halogenated solvents. The ^{1}H- and ^{13}C-NMR spectra are shown in Figure 4-17 and Figure 4-19 respectively.

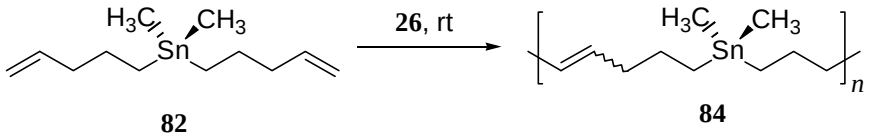

82 **84**

Figure 4-16. ADMET polymerization of bis(4-pentenyl)dimethylstannane (**82**) yielding high molecular weight polymer **84**.

Gel permeation chromatography ($CHCl_3$, polystyrene standards) and ^{1}H-NMR end group analysis confirm the formation of high molecular weight polymer, yielding M_n values of 20,100 and 21,800 g/mol respectively. A recalculation of the relaxation times employed in the acquisition of quantitative ^{13}C-NMR spectra for polymer **84** was performed (Figure 4-18), but no improvement on the quantitative data was found.

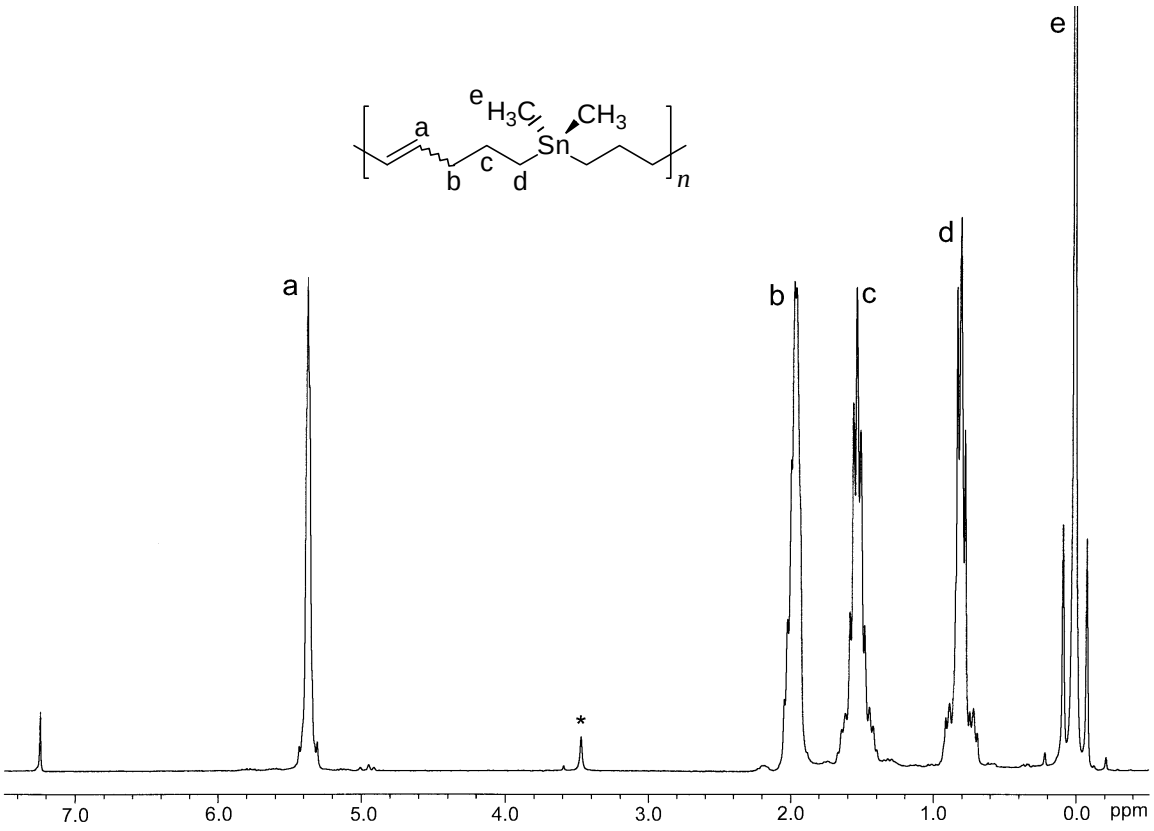

Figure 4-17. ^{1}H-NMR spectrum of polymer **84** synthesized using Schrock's molybdenum catalyst **26**. * = residual methanol from precipitation.

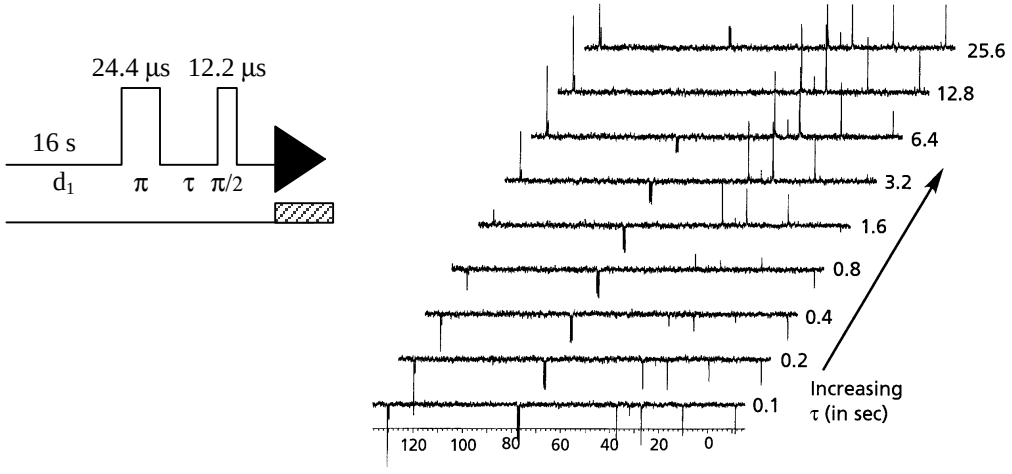

Figure 4-18. Inversion recovery experiment: determination of the longest ^{13}C relaxation time in a sample of polymer **84** for accurate quantification using ^{13}C-NMR.

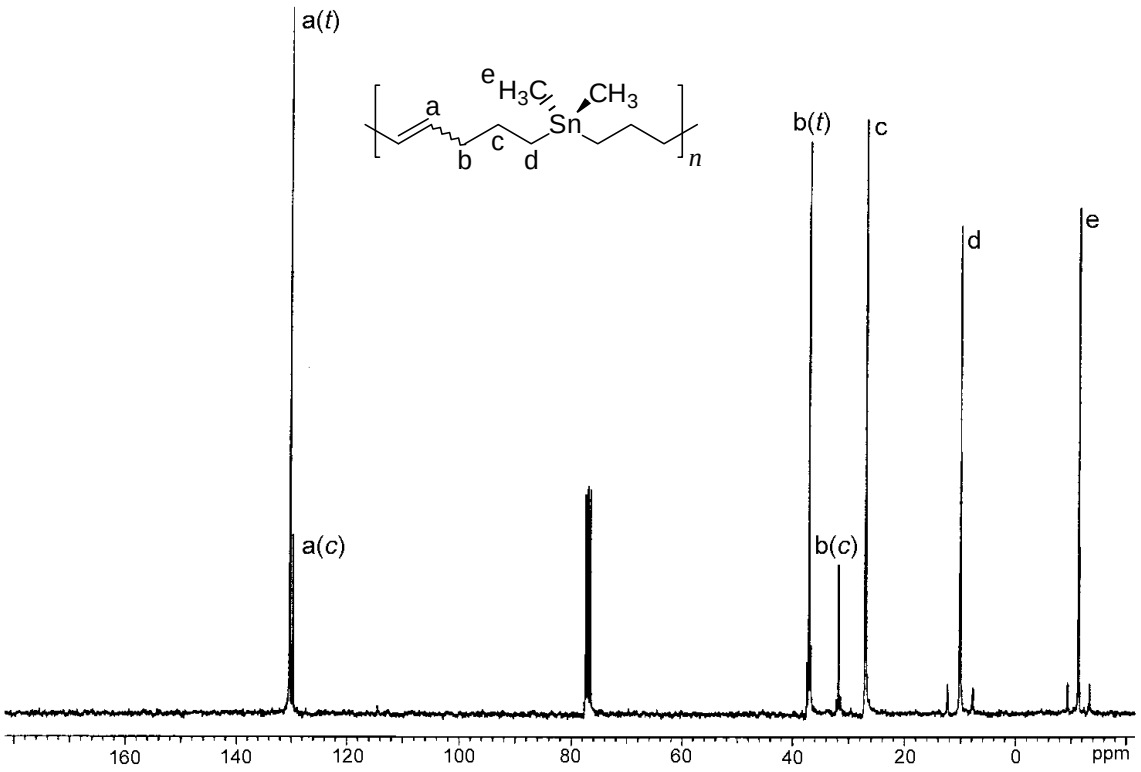

Figure 4-19. ^{13}C-NMR spectrum of polymer **84** synthesized using Schrock's molybdenum catalyst **26**.

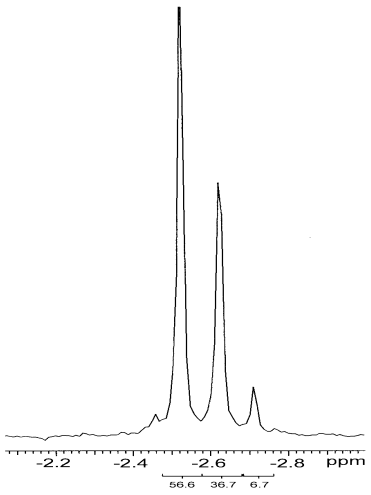

Figure 4-20. ^{119}Sn-NMR spectrum of polymer **84** synthesized using Schrock's molybdenum catalyst **26**. The signals correspond to Sn atoms between *trans-trans*, *trans-cis* and *cis-cis* double bonds.

^{119}Sn-NMR analysis of the polymer shows, resembling its di-*n*-butyl analogue, three distinct resonances that correspond to the three types of tin atoms generated from their placement between *trans-trans*, *cis-trans* and *cis-cis* olefin linkages, and the intensities found for these signals correspond to the calculated values from quantitative ^{13}C-NMR data.

Differential scanning calorimetry (DSC) reveals that although polymer **84** displays a higher T_g than its di-*n*-butyl analogue (**75**), this thermal transition occurs at a very low temperature (ca. -89 °C). This observation suggests that the effect of the reduction of the side-chain size is not significant enough to bring the T_g above room temperature and make of this amorphous polymer a solid at room temperature.

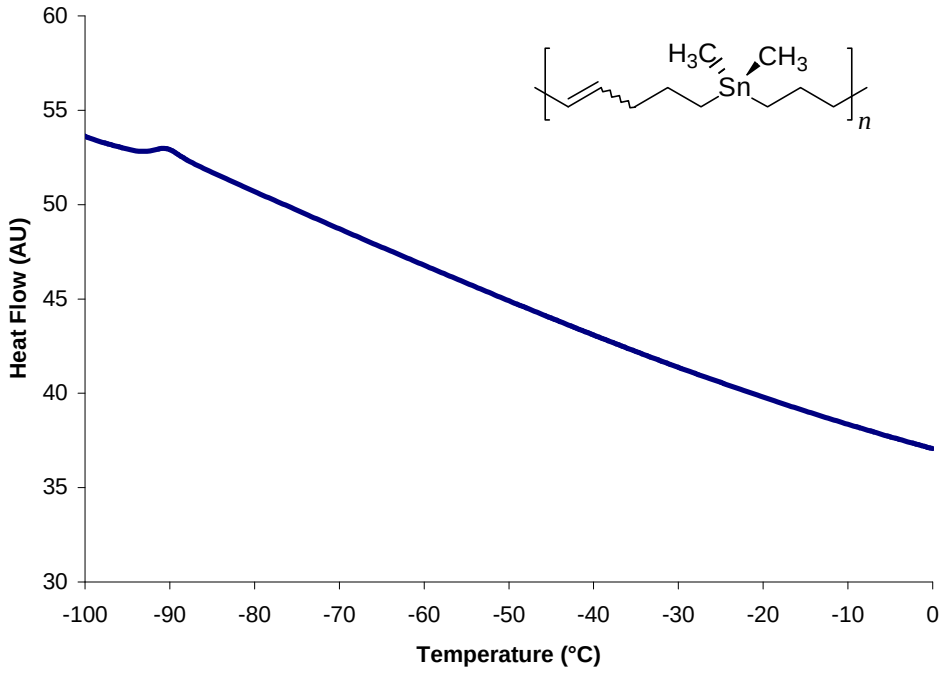

Figure 4-21. Second heating DSC trace for polymer **84**, at a rate of 2 °C/min.

In turn, thermogravimetric analysis of polymer **84** displays one of the most significant differences with respect to polymer **75**, for which the residual weight % after decomposition corresponds to the expected metal weight %. Furthermore, the ceramic yield and weight loss rate shown in the TGA of polymer **84** seem to be dependent on the heating rate, as shown in Figure 4-22 (e.g., the 10% weight loss temperatures found at 20 and 40 °C/min are 354 and 331 °C respectively.

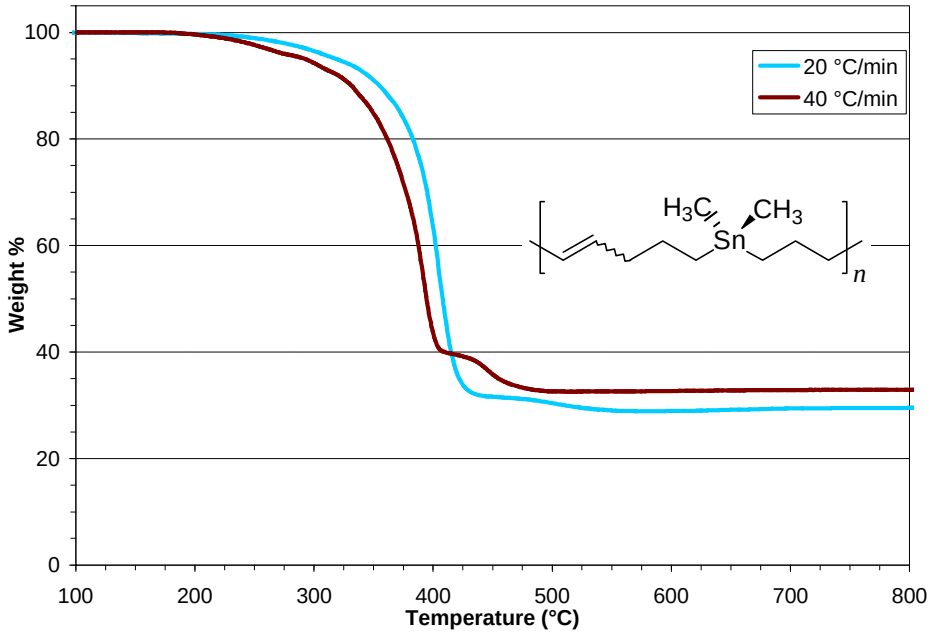

Figure 4-22. Thermogravimetric analysis of polymer **84** at two different heating rates.

Ceramic yields of ca. 29 and 33 % were obtained from the TGA analyses at 20 and 40 °C/min, which could be an indication of different decomposition pathways generating different amounts of volatile materials.

Poly(diphenyldi-*n*-butylstannane)

The work of Lu and Tilley (1996) demonstrated that diarylstannanes exhibit σ,π-conjugation and low bandgaps (430-440 nm). The derivatization possibilities inherent to aromatic substituents in polycarbostannanes motivated an evaluation of the reactivity and a synthetic methodology involving diarylstannanes.

The polymerization of bis(4-pentenyl)diphenylstannane proceeds smoothly in the presence of Schrock's molybdenum complex **26** at room temperature, and a viscosity increase is accompanied by constant ethylene evolution. However, this polymerization seemed to proceed slower than for the di-*n*-butyl or dimethyl analogous structures and bubbling could still be observed after ca. 14 days of reaction.

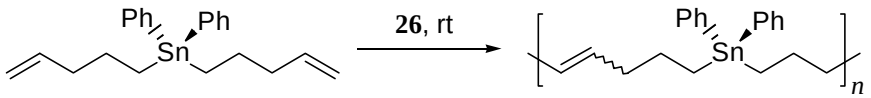

83 **85**

Figure 4-23. ADMET polymerization of bis(4-pentenyl)diphenylstannane (**85**) yielding high molecular weight polymer **85**.

^{1}H- and ^{13}C-NMR reveal that the product (isolated as a viscous liquid at room temperature) is indeed the expected ADMET polymer. The presence of signals due to end groups indicates that high molecular weight was not obtained. Proton and carbon NMR end-group analysis allow the calculation of the number average molecular weight for the title polymer yielding 7400 and 8200 g/mol respectively, in agreement with the value of 9100 determined by gel permeation chromatography.

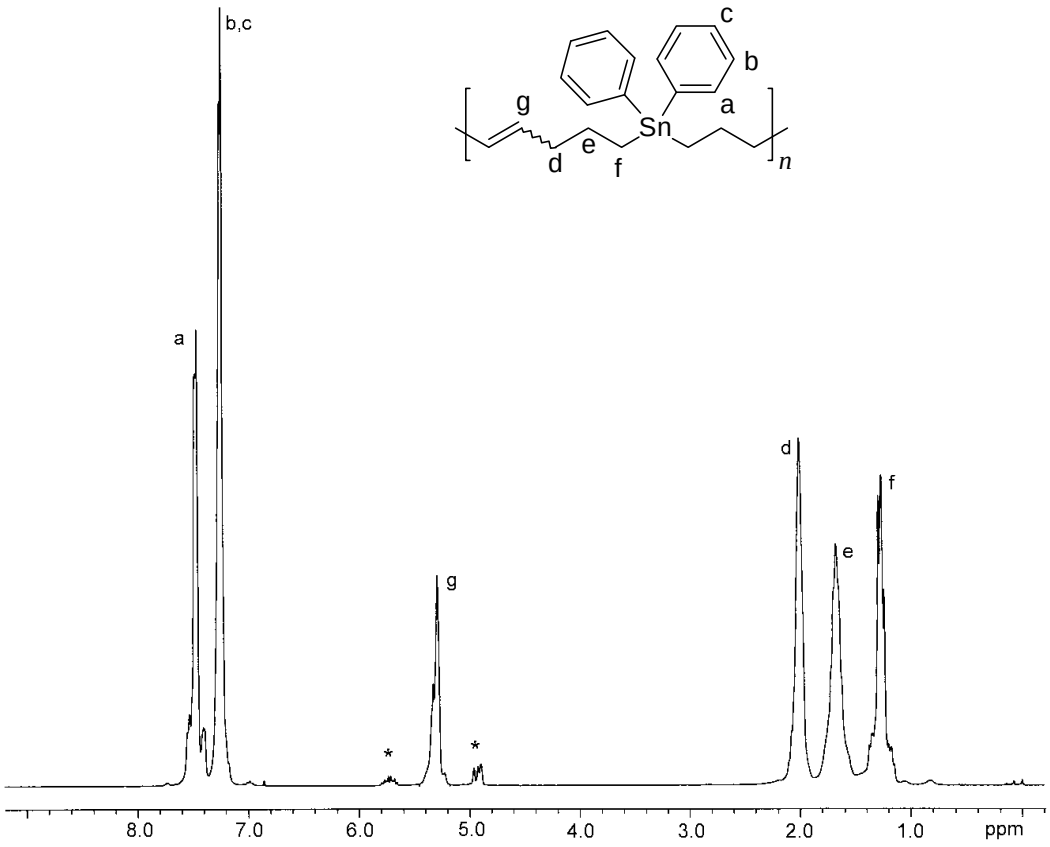

Figure 4-24. ^{1}H-NMR spectrum of polymer **85** synthesized using Schrock's molybdenum catalyst **26**. * = signals due to vinyl end groups.

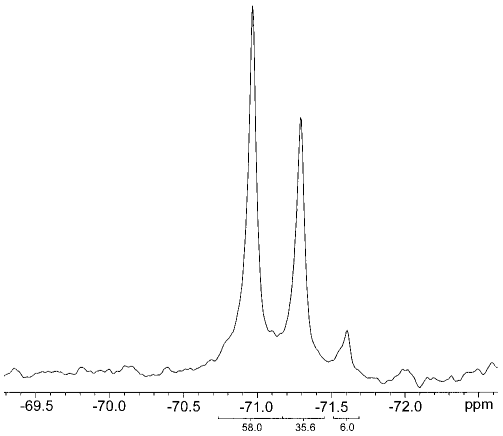

Figure 4-25. ^{119}Sn-NMR spectrum of polymer **85** synthesized using Schrock's molybdenum catalyst **26**. The signals correspond to Sn atoms between *trans-trans*, *trans-cis* and *cis-cis* double bonds.

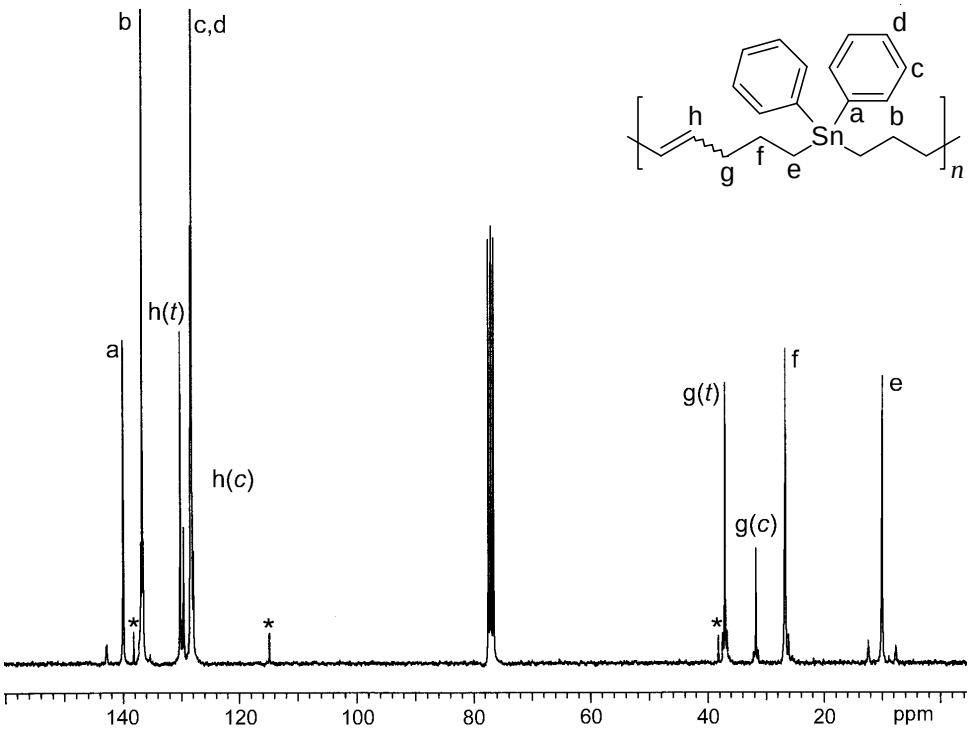

Figure 4-26. ^{13}C-NMR spectrum of polymer **85** synthesized using Schrock's molybdenum catalyst **26**. * = signals due to vinyl and allyl end groups.

The thermal behavior of polymer **85** reveals interesting characteristics imparted by the substitution by an aromatic moiety. Differential scanning calorimetry shows a dramatic increase in the glass transition temperature of polymer **85** (T_g = -29 °C) with respect to its di-*n*-butyl and dimethyl analogues (< -110 °C and -89 °C respectively). This observation suggests that the identity of the side chains is a determinant factor in the glassification of the polymer, apparently of greater importance than the backbone, which could be expected to be constant in polymers **75**, **83** and **85**.

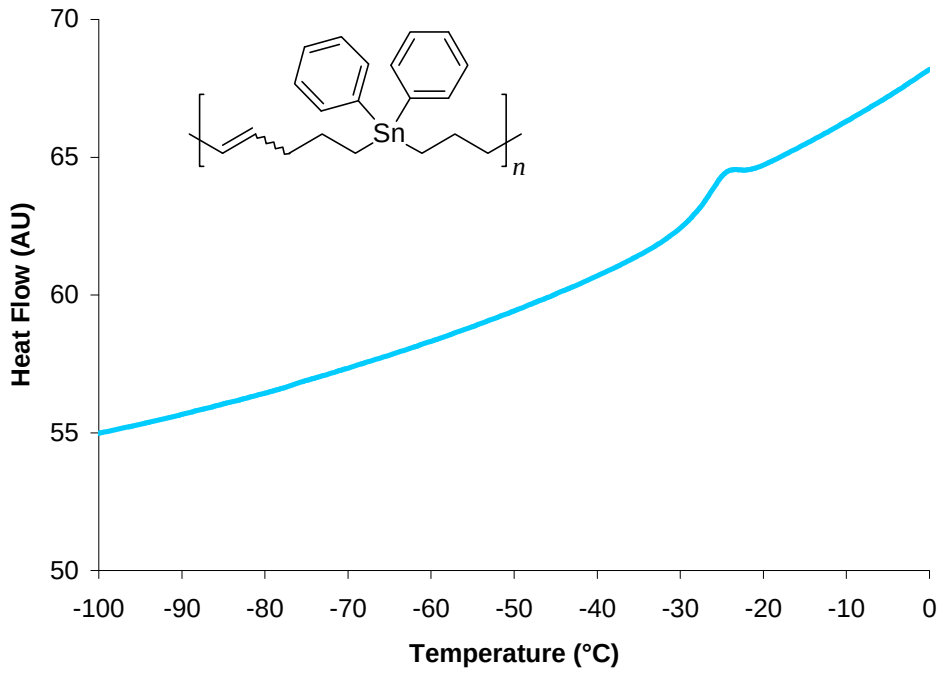

Figure 4-27. Second heating DSC trace for polymer **85**, at a rate of 2 °C/min.

Complementing the results provided by DSC, thermogravimetric analysis (20 °C/min) shows that polymer **85** can also be a precursor to elemental tin upon heating above the decomposition temperature (which onset was calculated to be 304 °C). The polymer displays thermal stability up to ca. 250 °C, and 10% weight loss occurs at 345 °C. No substantial differences were found in the TGA traces at two different heating rates (20 and 40 °C). Furthermore, the ceramic yield obtained experimentally for polymer 85 (30.06%) corresponds to the calculated value based on metal weight percent (30.98 %). This agreement suggests that the decomposition pathway followed by the title polymer does not involve the formation of tin-containing volatile species, and implies a dependence on the size of the side chain.

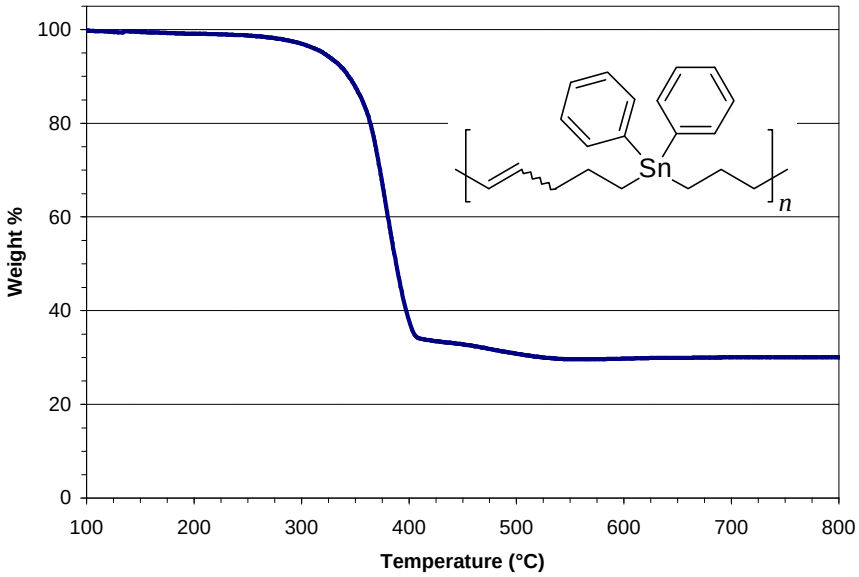

Figure 4-28. Thermogravimetric analysis of polymer **85**.

Oligostannane Segments in ADMET Polymers

The synthesis of ADMET polymers that contain a polymetallane segment was studied in the search for the basic rules that govern the compatibility between polymetallanes and hydrocarbon structures. The synthesis of polymers containing both functionalities may be a useful route towards materials combining the interesting physicochemical properties observed in polystannanes with the advantages inherent to both aliphatic and hydrocarbon segments, and ADMET polymerization appeared as a promising synthetic alternative.

Monomer Synthesis

The recently reported advances in the synthesis of segmented copolymers using ADMET polymerization appeared as attractive guidelines for the synthesis of telechelic oligostannadienes, which could be not only homopolymerized to yield high metal content metallopolymers but also reacted with other functionalized dienes to yield copolymer structures with attractive physical properties and promising applications.

The first step towards ADMET polymers containing polymetallane segments consisted of the design and synthesis of suitable diene monomers containing at least one metal-metal σ bond. In order to determine the compatibility between this functionality and the metathesis catalysts employed in the polymerization, the efforts were concentrated on the preparation of di- and tristannane dienes. Among the different methodologies available for the synthesis of oligostannanes, the alkenylation of a tri- or distannane dichloride appeared as an interesting attractive since a variety of carbonated segments can be introduced by the choice of the alkenylating group.

The synthetic route towards the distannane diene **90** involving the alkenylation of tetrabutyldistannane dichloride (**89**) is shown in Figure 4-29. A one-pot synthesis scheme was devised based on the difficulties often associated with the purification of tin halides. This scheme comprises the *in situ* generation of Bu_2SnHCl (**88**), its dehydrogenative coupling to the distannane dichloride **89**, and the subsequent reaction of this dichloride with a nucleophilic alkenyl group,

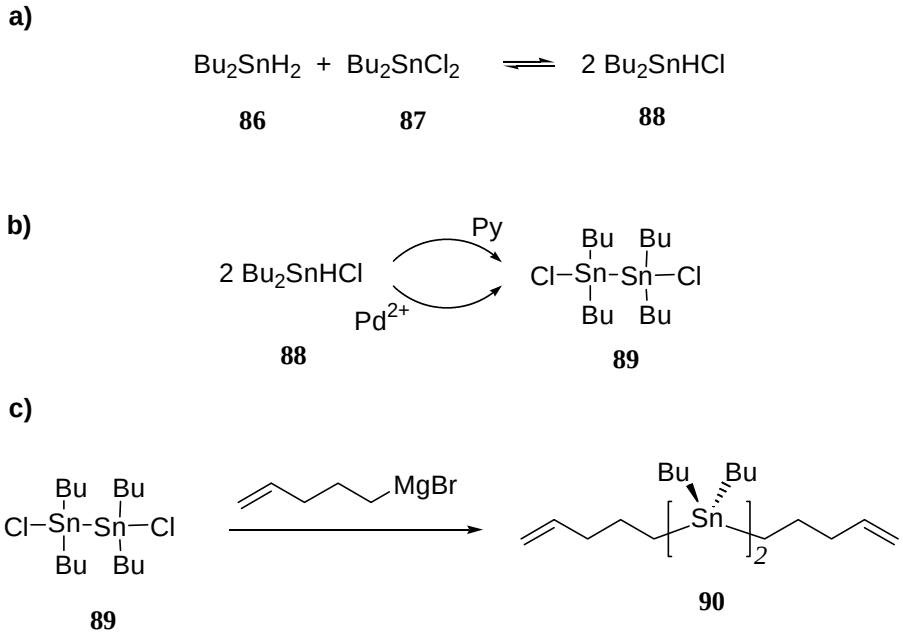

Figure 4-29. Synthetic scheme devised for the synthesis of the distannane diene **90**.

The room temperature disproportionation of equimolar amounts of Bu_2SnCl_2 (**86**) and Bu_2SnH_2 (**87**) leading to Bu_2SnHCl (**88**) has been previously reported (Neumann 1964b, Sita 1992, Kawakami 1995). Although not a quantitative reaction, the equilibrium concentrations are reached in ca. 10 min at 25 ºC (Figure 4-30).

Addition of a catalytic amount of dry pyridine to this mixture has also been reported to cause the quantitative decomposition of Bu_2SnHCl to the distannane dichloride **89** (Neumann 1964b, Kawakami 1995). This as well as other previously reported methodologies mediated by transition metals (Braunstein 1998, Jousseaume 1987) were explored for the coupling step in order to ensure a high yield reaction. Among the experimental routes explored, the palladium catalyzed coupling appears to be the most efficient, and $Bu_4Sn_2Cl_2$ solutions are obtained after – often vigorous – hydrogen evolution from the precursor Bu_2SnHCl solutions. The disappearance of the signal

centered at 44.6 ppm (Figure 4-30, c) and the simultaneous appearance of a new sharp singlet at 109.0 ppm ($^{1}J_{^{119}Sn-^{117}Sn}$ = 2420 Hz) in the (proton decoupled) ^{119}Sn-NMR (Figure 4-30, d), have proven to be very useful in the monitoring of this reaction. This methodology can be extended to other polystannane dichlorides, which can be used as precursors for diene monomers.

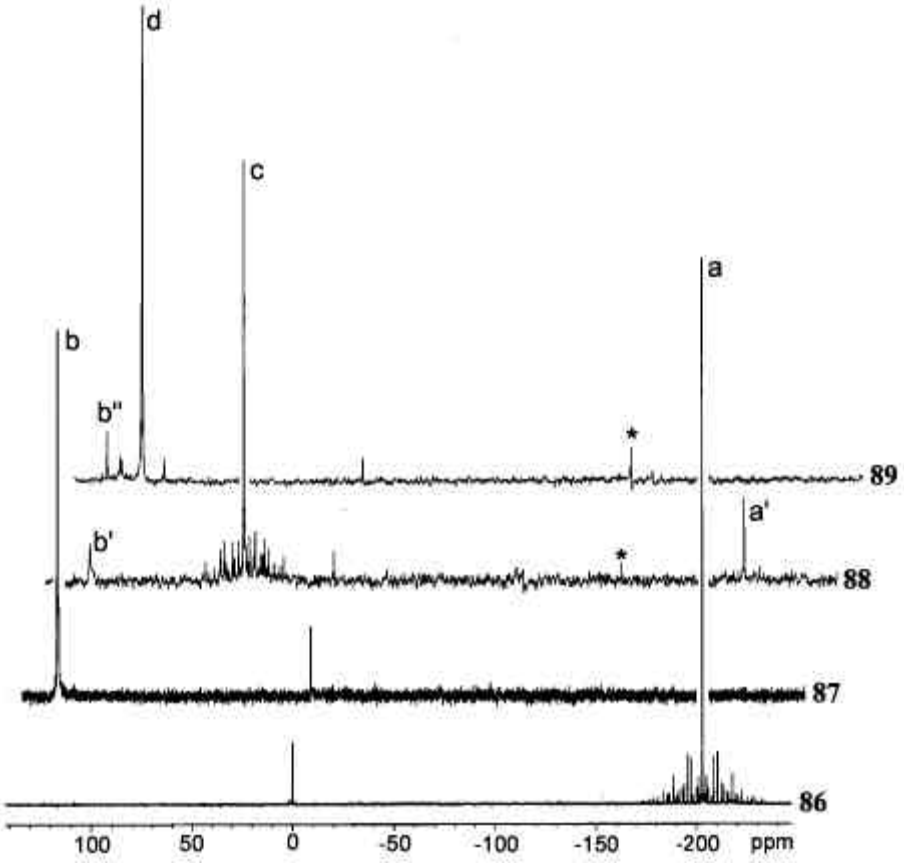

Figure 4-30. ^{119}Sn-NMR study of the disproportionation of Bu_2SnH_2 (**86**) and Bu_2SnCl_2 (**87**) into Bu_2SnHCl (**88**) and its subsequent conversion to $Bu_2ClSn\text{-}SnClBu_2$ (**89**) by action of a catalytic amount of $PdCl_2(PPh_3)_2$. * = unassigned signals.

The alkenylation of the distannane dichloride is also a facile reaction. Gentle reflux of the dichloride with the Grignard reagent generated from 5-bromo-1-pentene

affords after standard workup a mixture containing dienes **90**, **73**, and **91** as main components (identified by their distinct resonances in the ^{119}Sn-NMR, Figure 4-31). However, the experimental conditions studied did not afford the distannadiene **90** free of other dienes, and attempts to separate these dienes have also proven unsuccessful. Figure 4-32 shows the analytical HPLC trace of the mixture of stannadienes obtained in the reaction.

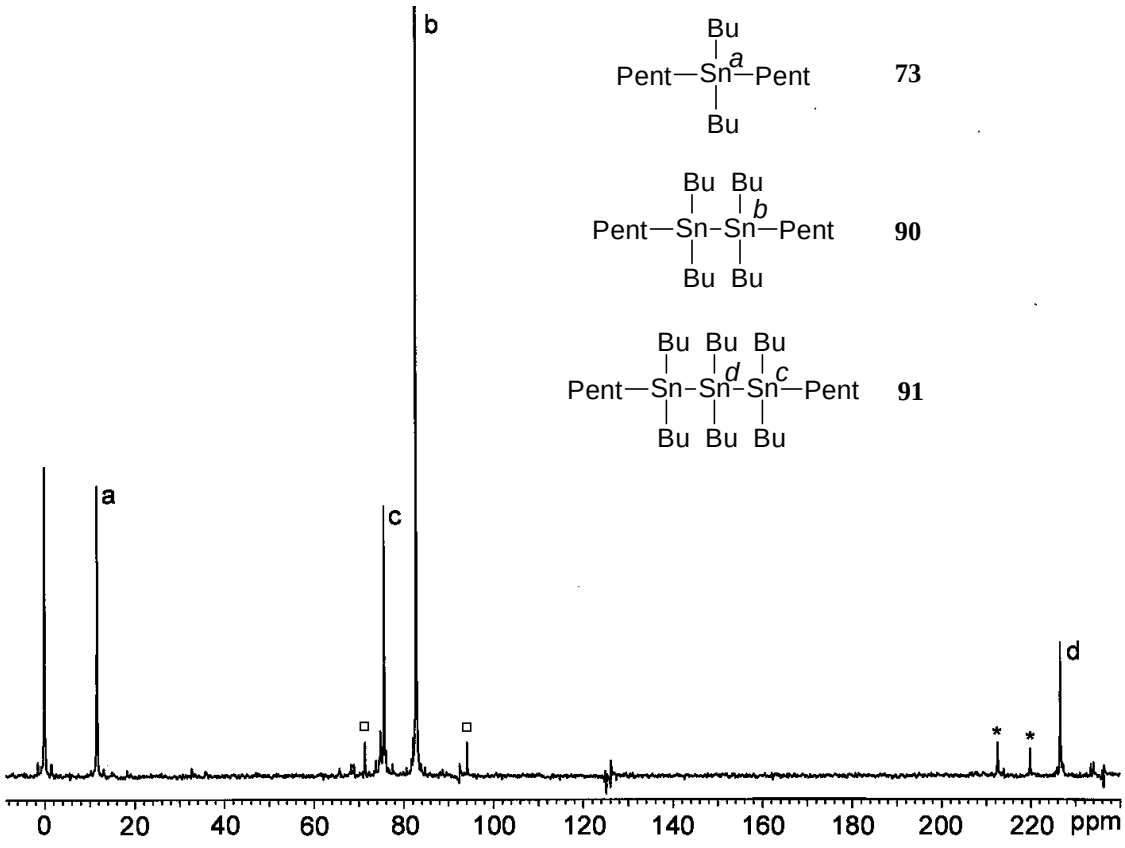

Figure 4-31. ^{119}Sn-NMR of the monomer mixture obtained in the one-pot synthesis of distannane diene **90**. * = higher oligostannane dienes. □ = ^{119}Sn-^{119}Sn satellites.

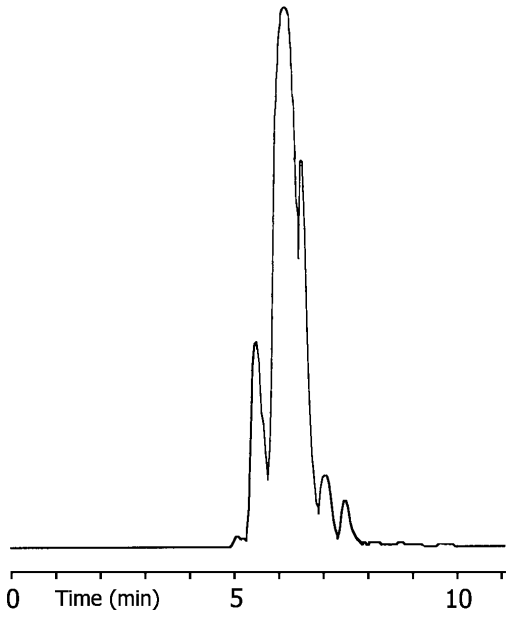

Figure 4-32. Reverse phase analytical HPLC trace of the mixture of dienes **92** showing three major components. No resolution optimization was performed. Conditions: isocratic elution at 1 % ethyl acetate, detection at 254 nm.

Bu_2SnCl_2 remaining from the incomplete disproportionation reaction (Figure 4-29**b**) accounts for the presence of **73**, while the coupling of more than one equivalent of Bu_2SnH_2 with Bu_2SnHCl explains the presence of diene **91** and other higher oligostannane dienes. Surprisingly, these compounds are quite stable not only to aqueous workup of the Grignard reaction but also to adsorbents such as silica gel, which allows isolation of the mixture in adequate purity for ADMET polymerization.

ADMET Polymerization

Upon exposure to the molybdenum catalyst **32,** this purified diene mixture (**92**) produced the ADMET polymer **93** in almost quantitative yield. (Figure 4-33) Ethylene evolution in very vigorous during the first 4 h of the reaction, and the viscosity of the

reaction mixture increases steadily suggesting polymerization. After this time, the ethylene bubbling rate decreases but continues throughout the reaction until viscosity prevents magnetic stirring.

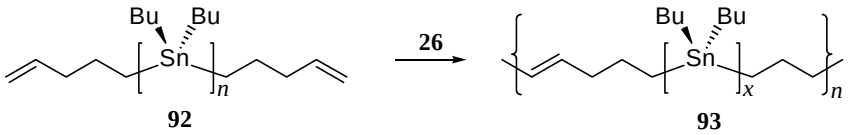

92 **93**

Figure 4-33. ADMET polymerization of the oligostannane dienes mixture **92** yielding polymer **93**.

Characterization of the crude polymer sample reveals that polymerization has indeed taken place, along with the incorporation of all the stannadienes present in **92**. Both ^{13}C and ^{1}H-NMR of the polymer show the conversion from terminal dienes to internal olefins. New signals at 5.5-5.6 ppm (^{1}H), and at 131.2 and 130.6 ppm (^{13}C) account for the new olefin linkages, in both *cis* and *trans* isomeric forms. Polymerization is also evident by the splitting of the ^{119}Sn signals originally present in the monomer mixture, due to the slightly different magnetic environments caused by the olefin linkages.

Precipitation of the polymers from $CDCl_3$ or C_6D_6 solutions into dry methanol yields the polymers as viscous liquid samples. In a typical experiment, the determination of molecular weight by end group analysis based on ^{1}H-NMR spectroscopy suggests an average degree of polymerization of 20 (Calculated M_n = 11,000 g/mol). However, at very long reaction times (24-48 h), high molecular weight polymer is isolated and no signals

due to end groups can be observed. Figure 4-34 shows the ^{1}H-NMR of a high molecular weight oligostannane-containing ADMET polymer (**93**).

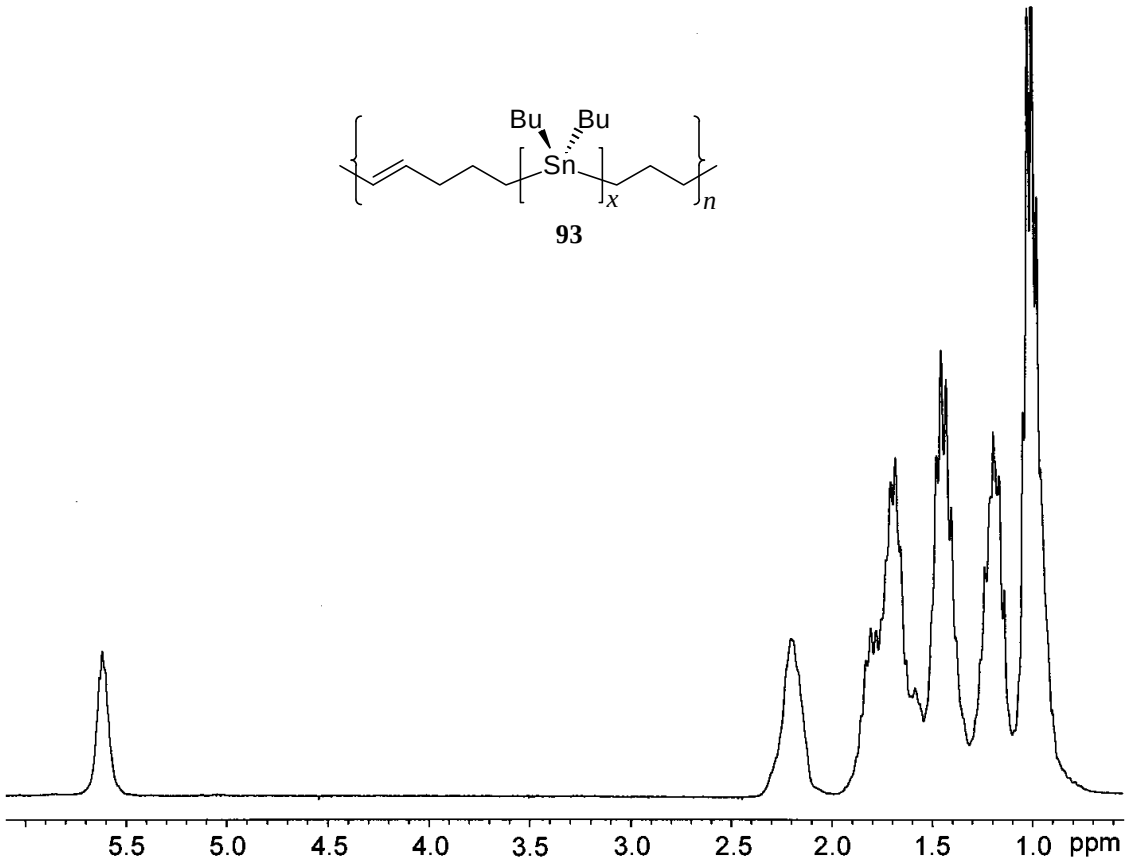

Figure 4-34. ^{1}H-NMR of polymer **93**. Absence of end groups signals suggest high molecular weight.

Polymer **93** is a viscous liquid which exhibits a thermal behavior similar to that observed in other polycarbostannanes. Thermogravimetric analysis reveals a decomposition onset of ca. 300 °C which suggests high thermal resistance under a nitrogen atmosphere. In addition, the metal % found after total volatilization of the organics corresponds to a ceramic yield of 37 %, a 91 % metal recovery with respect to the theoretical 40% metal weight.

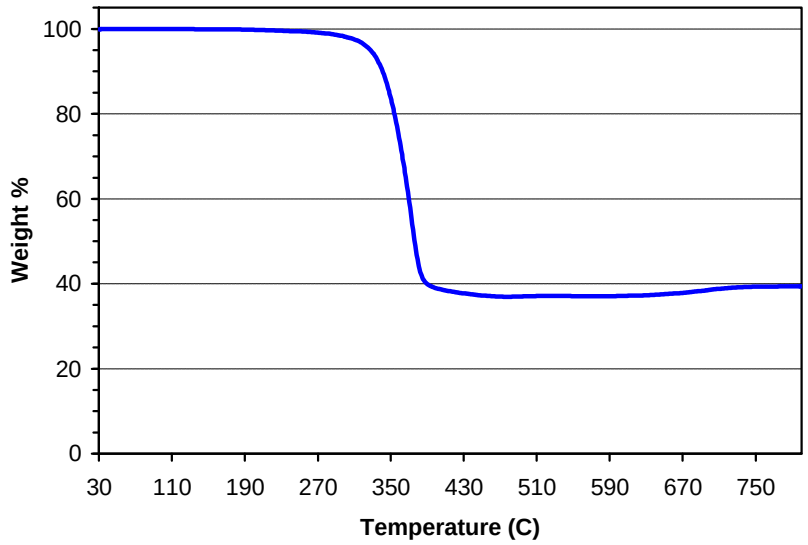

Figure 4-35. Thermogravimetric analysis of polymer **93**.

Conclusions

Acyclic diene metathesis polymerization has been established as a useful synthetic route to polymers containing tin along the backbone. An exploration of the physical and especially thermal properties of the organometallic polymers synthesized suggests that they are not only determined by the primary structure of the polymer, but also of significant interest in the search for possible applications of well defined metallopolymers.

The polymerization of bis(4-pentenyl)di-*n*-butylstannane using the aryloxy tungsten complex **32** and no external cocatalysts reported herein constitutes *the first*

example of a monomer-activated metathesis polymerization catalyzed by a classical system, and its mechanistic implications on the polymeric product were extended to a methodology for the ring closing metathesis of diene **74**.

Two new polycarbostannane structures containing ca. 46 and 30 % metal weight were synthesized in a facile process which involved the design of the stannandienes used as monomers and their subsequent polymerization using Schrock's molybdenum system **26**. The investigations on a synthetic methodology for the preparation of ADMET polymers containing short oligostannane segments was also demonstrated, and constitutes the first step towards polymers containing polymetallane segments.

CHAPTER 5
POLYCARBOGERMANES VIA ADMET POLYMERIZATION

The thermal and optical behavior of organometallic polymers of group 14 elements have been attracted a significant interest in recent years (Miller 1989, Birot 1995). Among these, germanium-based polymers have demonstrated potential utility in microlithography (Mochida 1996) and in the preparation of ceramic materials (Brefort 1994). The availability of novel well defined polymeric structures involving polycarbogermanes is of utmost importance for the development of precise applications of this type of materials. This chapter describes the synthesis of main chain germanium-containing polymers via the ADMET polymerization of germanadienes.

Main Chain Germanium Containing Polymers

Polygermanes

Contrary to polysilanes and polystannanes, polygermanes have received limited attention, although efforts concentrated on their synthesis are being actively investigated.

The most common synthetic approach to polygermanes is the self coupling of germanium dihalides in a Wurtz-type reaction. Despite the high molecular weights obtained in the reaction, low yields (<30 %) are often observed which has limited their applicability (Trefonas 1985, Miller 1987, Hayashi 1992, Mochida 1994). Alternative

coupling methods have resulted in higher yields at the expense of the polymer molecular weight (Mochida 1992). The only documented transition metal-mediated synthesis leads to the formation of high molecular weight polymer, but a high degree of branching was found as the result of a poorly controllable procedure (Reichl 1996). The synthesis of network polymers by copolymerization with polyfunctional chlorosilanes reported by Huang (1996), as well as the investigation on the effect of reticulation on the micropatterning behavior of crosslinked polygermanes (Mochida 1996) are also of notable interest.

Polycarbogermanes

Examples of polymeric materials incorporating germanium have been in the literature since the 1960s. In the area of polycarbogermanes, special attention has been dedicated to polymers that containing a conjugated segments between the germanium atoms in order to explore not only their pyrolysis behavior but also the extent and consequences of σ,π-conjugation such as electrical conduction and various optical properties.

Wurtz-type condensation reactions are the most common building blocks of current synthetic schemes towards saturated and unsaturated polycarbogermanes. Hayashi and coworkers (1992) reported an interesting approach from digermane dichlorides as shown in Figure 5-1.

Polymer **96** and **97** (and other analogous structures) contain both an organic (carbon based) conjugated segment and a digermane bond, which was shown to extend the conjugation length. The electronic conductivities of polymers of this type can be

increased from 10^{-9} to 10^{-4} S cm^{-1} by exposure to SbF_5 vapor in the vacuum making them conductors. In addition, the rapid decomposition of the polymer films was investigated using UV-Vis spectroscopy, which revealed that although Ge-Ge bond scission occurred the molecular weight of the polymer remained essentially the same. It was found that oxygen insertion between the dimetallane bond was the operating mechanism, which disrupts conjugation causing photobleaching of the polymer film and making these materials suitable for incorporation in light sensing devices (Mochida 1998b).

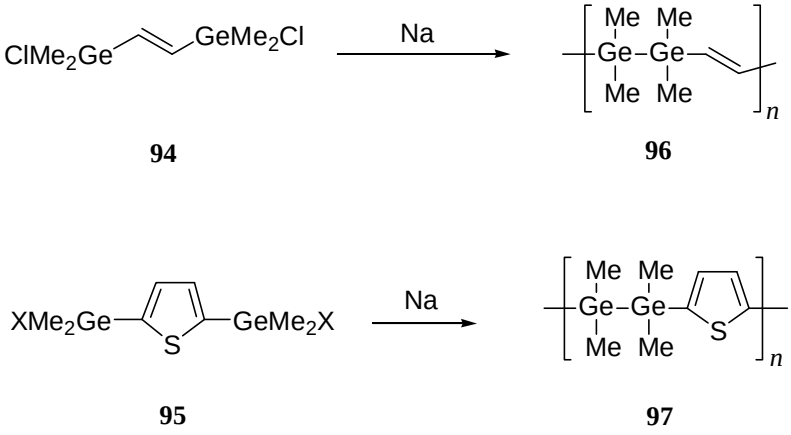

Figure 5-1. Structures of σ,π-conjugated polycarbogermanes synthesized by Wurtz-type Ge-Ge coupling.

Analogously, polycarbogermanes containing diacetylene segments exhibit σ,π-conjugation, and a number of such systems have been reported by Henner and coworkers as precursors to germanium-based ceramics (Brefort 1994). Such contribution has been pivotal in the establishment of reticulated organometallic polymers as preceramic materials. The synthesis (Figure 5-2) involves the generation of organolithium

reagents from diacetylenes and its subsequent coupling with germanium (and other) dihalides.

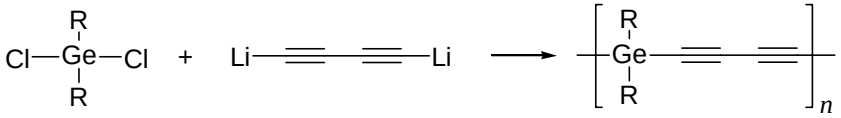

98

Figure 5-2. Synthesis of acetylenic polycarbogermanes.

Redox active polymers containing ferrocenyl units have been prepared through the ring opening polymerization of germa- (Foucher 1994, Reddy 1995, Peckham 1996) and digermaferrocenophanes (Mochida 1998c) by thermal and transition metal-mediated processes (Figure 5-3).

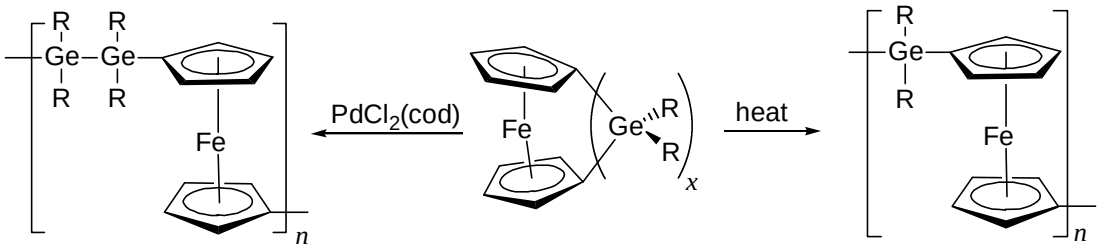

103 R = Me

99 *x* = 1, R = Me
100 *x* = 1, R = Et
101 *x* = 1, R = Ph
102 *x* = 2, R = Me

103 R = Me
104 R = Et
105 R = Ph

Figure 5-3. Synthesis of polycarbogermanes containing ferrocenyl units.

Another interesting example of germanium incorporation in polycarbogermanes is the synthesis of poly(germanium thiolate) **106** which contains a covalent

sulfur-germanium bond along the main chain of the polymer through the reaction of germylenes with thiethane (Figure 5-4).

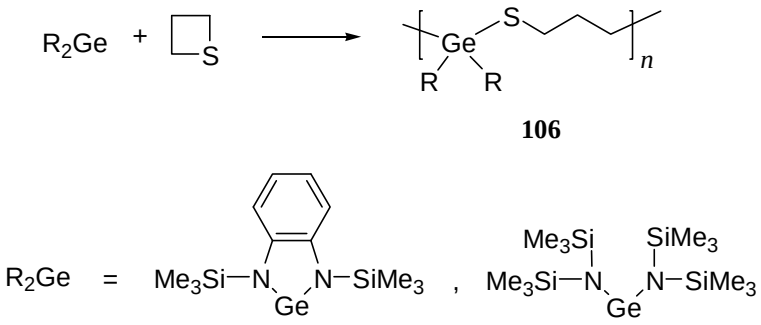

Figure 5-4. Shoda's synthesis of poly(germanium thiolates) in a redox process (Shoda 1996).

Germanium-Containing Polymers via Metathesis

The first synthetic scheme towards germanium containing polymers to involve the metathesis reaction was reported by Cho (1990). In this case, alkyne metathesis was employed in the cyclopolymerization of dipropargylgermanes, as shown in Figure 5-5.

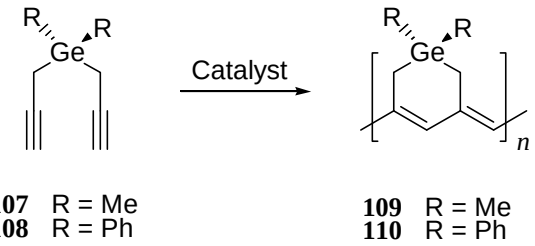

Figure 5-5. Alkyne metathesis cyclopolymerization of dipropargylgermanes.

Cho and coworkers utilized Mo and W halides activated by aluminum or tin alkyls as the catalytic systems, and investigated the thermal and electrical properties of polymers **109** and **110**. Although the cyclopolymers **109** and **110** possess a conjugated backbone, low electronic conductivities were reported (ca. 10^{-11} S cm^{-1}) and no efforts to increase this value were reported.

Years later, Finkelshtein (1997) demonstrated that high molecular weight polymers containing trialkylgermyl groups as side chains could be synthesized through the polymerization of germanium-substituted norbornenes, in a reaction catalyzed by a series of ill-defined ruthenium-based complexes (Figure 5-6). High molecular weights were found in all polymerizations.

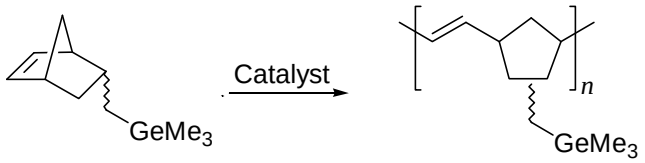

111 **112**

Figure 5-6. Synthesis of a germanium containing ROMP polymer by Finkelshtein (1997).

Polymer 112 exhibits good film forming properties and an increased permeability to a series of gases with respect to polynorbornene.

In brief, the field of main chain germanium-containing polymers has been underexplored, although promising applications have already been postulated for this family of organometallic polymers.

ADMET Polycarbogermanes

The incorporation of different functional groups in ADMET polymers is the outcome of an appropriate monomer design, a process which often comprises a study not only in functionality-catalyst compatibility, but also in the prediction of the polymer properties based on the structure of the parent diene. The interesting physical and chemical properties exhibited by a polycarbostannanes made via ADMET (Chapter 4) have motivated the investigations on organometallic polymers containing germanium described herein.

Monomer Synthesis

The synthesis of germanadiene monomers can be achieved with relative ease. The parent dialkylgermanium dichloride is used as the starting material and moderate to good yields are obtained in a straightforward Grignard reaction. (Figure 5-7) Careful purification of monomers **113**-**115** (> 99.5% purity by glc) involves fractional distillation, drying over CaH_2 and vacuum transfer followed by several freeze-pump-thaw cycles. Monomers **113**-**115** were characterized by ^{1}H-NMR, ^{13}C-NMR, and MS, and gave satisfactory elemental composition data.

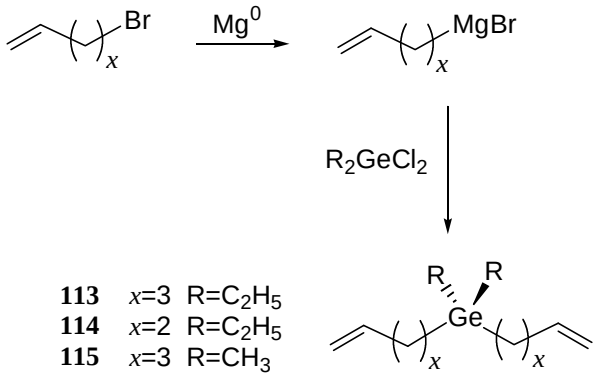

Figure 5-7. Synthesis scheme for the germanadienes **113-115**.

ADMET Polymerization

When exposed to catalysts **26** or **28** (0.4 mol %, see Table 5-A), monomers **113-115** condense to high molecular weight polymers in a clean olefin metathesis process. (Figure 5-8) Ethylene evolution is indicated by a constant bubbling throughout the polymerization, while a steady increase in viscosity suggests an increase in degree of polymerization in good agreement with a step polymerization scheme (Odian 1991). After 24-36 hours of reaction, magnetic stirring of the reaction mixture becomes impossible and an increase in the reaction temperature (up to 60 °C) usually contributes to achieving higher molecular weight. After 48-72 hours, no apparent evolution of ethylene is observed and exposing the contents of the reaction mixture to the atmosphere terminates the polymerization.

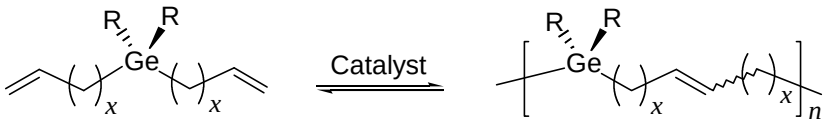

113 *x*=3 R=C_2H_5
114 *x*=2 R=C_2H_5
115 *x*=3 R=CH_3

116 *x*=3 R=C_2H_5
117 *x*=2 R=C_2H_5
118 *x*=3 R=CH_3

Figure 5-8. Synthesis of unsaturated polycarbogermanes **116-118** via ADMET polymerization.

Polymers **116-118** are viscous liquids, readily soluble in toluene, $CHCl_3$, and CH_2Cl_2, but virtually insoluble in other conventional organic solvents. The chemical structure of polymers **116-118** is confirmed by examining the ^1H and ^{13}C-NMR spectra, which reveal the expected structure of linear unsaturated polycarbogermanes. Integration of the two olefin signals in the quantitative ^{13}C-NMR (e.g. 130.4 and 129.8 ppm for **116**), shows that the polymers contain mainly *trans* linkages (ca. 71-84 %, see Table 5-A) between repeat units, an observation consistent with many other ADMET polymers which agrees with the relative stability of the *trans* and *cis* isomers formed in an equilibrium process. The ^{13}C-NMR of polymer **116** is shown in Figure 5-9. Both ^1H and ^{13}C-NMR suggest a high degree of polymerization for **116** and **117** since the signals corresponding to terminal olefin (due to end-groups) are either not observable or of very low intensities. Low signal-to-noise ratio for such signals prevents an estimation of the number average molecular weight of the polymers by end-group analysis. However, in the case of polymer **118**, although high molecular weight is suggested by both ^1H and ^{13}C-NMR, the presence of other unassigned, low intensity signals in the olefin region of the ^{13}C-NMR may be an indication of either the formation of cyclic oligomers or to partial isomerization of the

terminal double bonds. This behavior is also supported by the larger polydispersity as well as the difference with the calculated M_n obtained from chromatographic analysis. Molecular weight determination by gel permeation chromatography in $CHCl_3$ (polystyrene standards) shows that high molecular weight (M_n = 18 000 and 14 000 g/mol respectively) can be achieved for polymers **116** and **117**, while a lower molecular weight is found for **118** (ca. 5300). An apparent decreased reactivity of monomer **115** towards the metathesis catalysts employed in our study was observed.

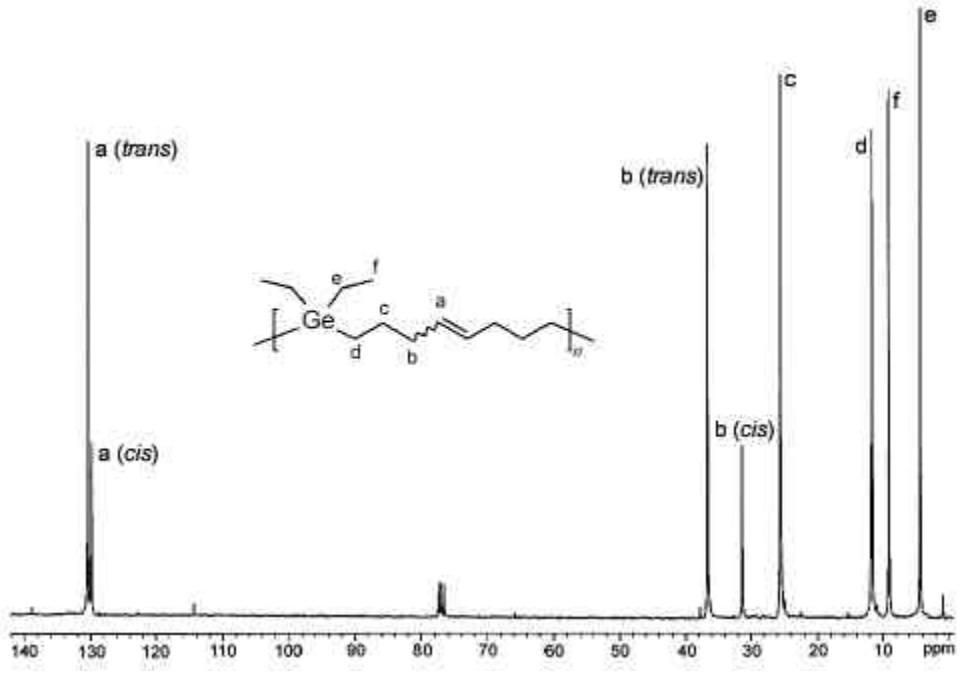

Figure 5-9. ^{13}C-NMR of poly[bis(4-pentenyl)diethylgermane] (**116**) polymerized using Schrock's molybdenum complex **26**.

Thermal analysis reveals some of the most interesting features of the germanium-containing polymers described herein. Thermogravimetric analysis (TGA) shows that polymers **116**-**118** are stable up to 250 °C, the temperature at which thermal

decomposition begins (Table 5-A lists the 10% weight reduction temperatures, $T_{10\%}$). TGA also shows 17 % weight recovery after heating a sample of polymer **116** to 800 °C under a N_2 atmosphere, while the residual material in the case of polymers **117** and **118** is 8% and 3% respectively. These residues may be attributed to elemental germanium by analogy to the behavior exhibited by ADMET polycarbostannanes, but no definitive determination of the chemical identity of this product was made. Although the metal recovery is not quantitative (e.g. the expected metal content in **118** is ca. 29 %), potential applications of these materials could be based in this behavior. The TGA traces for the three polymers are shown in Figure 5-10.

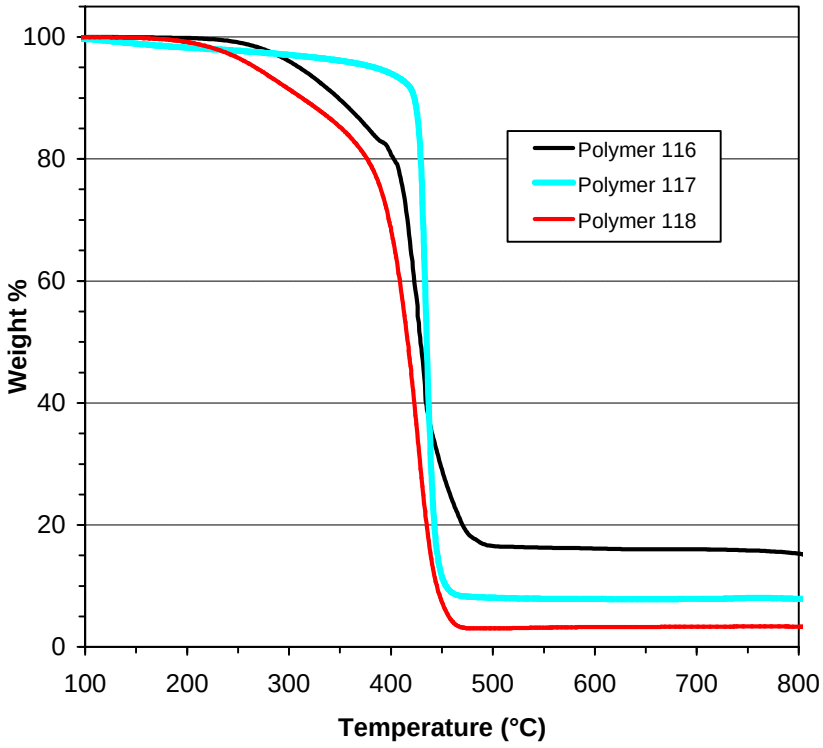

Figure 5-10. TGA traces of polymer **116-118** under a N_2 atmosphere obtained at 20 °C/min.

Differential scanning calorimetry (DSC) in turn shows that polymers **116-118** are completely amorphous. No melting temperatures could be observed in the range –110 to 0 °C, while a glass transition could be found at -89 and -98°C for polymers **116** and **117** respectively (Figure 5-11). The combined characterization data is summarized in Table 5-A.

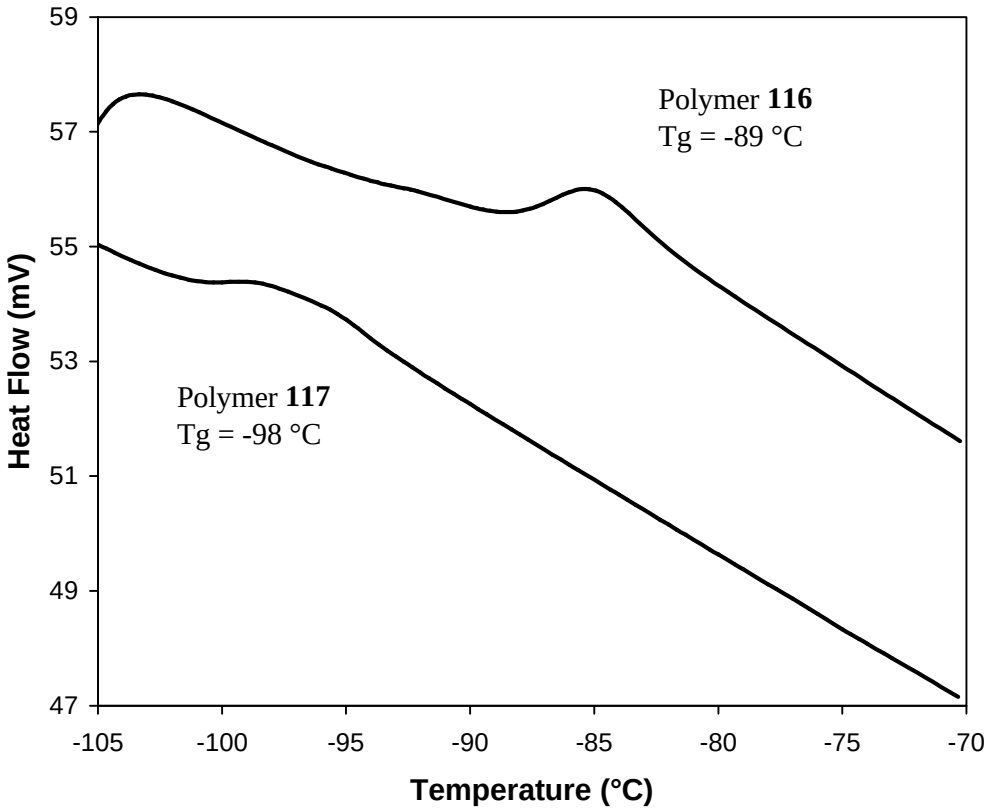

Figure 5-11. Second heating DSC traces for polymers **116** and **117** obtained at 2 °C/min.

Extrapolation of the observed behavior of monomer **115** to the structure-reactivity rules that govern the ADMET polycondensation of germanium-containing dienes may indicate that the gem-dimethyl substitution has a detrimental effect on the propagation

reaction. For example, attempts to synthesize polymer **118** using Schrock's molybdenum alkylidene **1** turned futile. However, this observation may not reflect a true chemical behavior but an improper choice of experimental conditions or an inadequate monomer purification. Although the monomer and polymer analysis (e.g., compositional data) are in good agreement with the expected values making the latter assumption unlikely to be the explanation for the observed behavior, the properties of monomer **118** with respect to its diethyl analogues should not be different enough to prevent a high degree of polymerization to be achieved.

Table 5-A. Summarized characterization data on polymers **116-118** obtained via ADMET polymerization.

Polymer	**Catalyst** [a]	M_n [b]	**PDI** [b]	$T_{10\%}$ [c] (°C)	**Residual Wt %** [c]	T_g [d] (°C)	**% *trans*** [e]
116	**26**	14 800	1.79	353	17 %	-89	71 %
117	**26**	18 000	1.42	428	8 %	-98	84 %
118	**28**	5300	1.82	290	3 %	---	73 %

[a] All polymerizations run at 0.4 % mol catalyst in neat monomer.
[b] Determined by GPC in $CHCl_3$ using polystyrene standards.
[c] Determined by TGA.
[d] Determined by DSC.
[e] Determined by integrating the *trans* and *cis* olefin signals in the quantitative ^{13}C-NMR.

In comparison to other ADMET metallopolymers, polymers **116-118** exhibit a similar pyrolysis behavior than the observed for the tin-containing analogues, although the % weight recovered in TGA analysis does not correspond to the theoretical

weight-metal content, as is the case for analogous tin-containing polymers (Chapter 4). Such an observation can be rationalized by appealing to the formation of more volatile species in the case of germanium, or to the presence of different decomposition pathways for the two types of polymers. The former explanation has literature precedent, and similar behavior was observed when comparing the thermal behavior of linear and network polygermanes for which the ceramic yield was significantly higher.

Analogously, DSC analyses of the polycarbostannanes reveal very low glass transition temperatures (ca. –90 °C and lower), as well as amorphous character. This observation implies that the conformation of the polymers (due to the identity of the side chains and the geometry of the heteroatom) is not only likely to be similar, but also the determining factor of the thermal properties of these two families of polymers. A comparison to the analogous ADMET polycarbosilanes is more difficult because of the structural differences between the two groups of polymers studied. In a fashion that resembles their Sn and Ge analogues, all homopolymers synthesized from aliphatic siladienes seem to be amorphous (DSC), and crystallinity is only introduced either by copolymerization with hydrocarbon monomers such as 1,9-decadiene (Smith 1991), or by the incorporation of aromatic moieties in the backbone (Cummings 1996). However, a marked difference is observed in their pyrolysis behavior since no silicon residue is found when the materials are decomposed under a nitrogen atmosphere (Smith 1991). This feature suggests that derivatization procedures may be necessary to improve the ceramic yield of the Si- and Ge-based materials. ADMET copolymerization of organometallic dienes should provide access to ceramic precursors in which the elemental composition is determined by the stoichiometric ratio of the comonomer units.

Conclusions

A methodology for the synthesis of organometallic polymers containing germanium along the polymer main chain has been devised. The application of this synthetic scheme yielded three new metallopolymer structures. Polymers **106**-**108** are viscous liquids which contain up to 34% metal weight, with number average molecular weights ranging from 5000 to 18 000 g/mol and were obtained in a clean metathesis polycondensation process.

CHAPTER 6
EXPERIMENTAL

Instrumentation and Analysis

^{1}H (300 MHz) and ^{13}C-NMR (75 MHz) spectra were run in either a Varian VXR-300 or a Varian Gemini-300 superconducting spectrometer system in $CDCl_3$ or C_6D_6 and are referenced to internal tetramethylsilane (0.05% v/v). A pulse sequence with gated decoupling (decoupler off during preparation and pulse, on during acquisition) and 20 seconds preparation delay was employed for quantitative ^{13}C-NMR analysis. ^{19}F-NMR (282 MHz) spectra were run in a Varian VXR-300 superconducting spectrometer system in $CDCl_3$ and are referenced to internal $CFCl_3$ (0.05% v/v). ^{1}H-decoupled ^{119}Sn-NMR (112 MHz) spectra were run in a Varian VXR-300 superconducting spectrometer system in C_6D_6 and are referenced to internal tetramethyltin (1% w/w).

Gel permeation chromatography analysis were performed in a Waters Associates model 590 chromatograph using either THF or chloroform as the eluent (1.0 mL/min). Refractive index (Perkin Elmer LC-25) and UV (Spectroflow 757) detectors were used, and all molecular weight data are reported based on calibration with polystyrene standards (M_p = 580, 1900, 7700, 12000, 30000, 48900, 59000, 79000, 139400, 650000). 10 μL of a 1% w/v filtered sample solution were used in all cases.

Thermogravimetric analysis was performed in a Perkin Elmer TGA7 instrument in the range 100-800 °C at a heating rate of 20 °C/min under N_2 atmosphere. Differential scanning calorimetry was performed in a Perkin Elmer DSC7 instrument at a heating/cooling rate of 20 °C/min in the range of

Low resolution mass spectrometry analysis were performed in a Finnigan GCQ Ion Trap mass spectrometer using either electron impact (EI) or chemical ionization (CI). High resolution EI, CI and LSIMS analysis were performed in a Finnigan MAT95Q hybrid sector mass spectrometer. Elemental analysis were performed by Atlantic Microlab Inc. (Norcross, GA).

Materials and Techniques

All manipulations were performed under dry argon using standard Schlenk or drybox techniques unless specified. The purification of solvents was as follows. Toluene and pentane were deolefinated using concentrated sulfuric acid, dried over CaH_2 and distilled. The distillate was refluxed over a sodium/potassium amalgam, distilled, and stored over 4Å molecular sieves under argon. Diethyl ether and tetrahydrofuran were distilled from sodium/benzophenone ketyl and stored over 4Å molecular sieves under argon. Carbon tetrachloride was refluxed over $CaCl_2$, distilled and stored over 4Å molecular sieves under argon.

1,5-hexadiene, 2-methyl-1,5-hexadiene, 1,7-octadiene, 1,8-nonadiene, and 1,9-decadiene (Aldrich Chemical Co.) were distilled, dried over CaH_2, degassed by

several freeze-pump-thaw cycles, stirred overnight on a potassium mirror and vacuum transferred to a flask containing 4 Å molecular sieves. 4-bromo-1-butene and 5-bromo-1-pentene were purified by fractional distillation at reduced pressure from CaH_2. Norbornylene was purified by sublimation and stored in a Kontes™ flask protected from light and heat. Commercial grade dicyclopentadiene (DCPD) was purified by sublimation of the low boiling impurities under constant reduced pressure (9-10 cm Hg) for ca. 45 min, followed by addition of 4Å molecular sieves under an argon atmosphere (Klosiewicz 1987). Schrock's molybdenum complex **26** and Grubbs' ruthenium benzylidene **28** were synthesized following published procedures (Schrock 1990b, Nguyen 1993).

Tri-*n*-butyltin hydride was purified by vacuum distillation followed by vacuum transfer and stored under an argon atmosphere. BHT (2,6-di-tert-butyl-4-methylphenol), α-ionone, tetrabutyltin, tetramethyltin, di-*n*-butyltin dichloride, dimethyltin dichloride, diphenyltin dichloride, diethylgermanium dichloride, dimethylgermanium dichloride, 2,6-dibromophenol, 2,4,6-tribromophenol, 2,6-dibromo-4-fluorophenol, pentafluorophenol, 2,6-dibromo-4-nitrophenol, 3,5-dibromo-4-hydroxybenzonitrile, tungsten (VI) chloride, and tungsten (VI) oxychloride were purchased from either Acros Organics or Aldrich Chemical Co. and used without further purification.

Synthesis and Characterization

Experimental for Chapter 2

Polymerization of 1,9-decadiene with $WOCl_2(O\text{-}2,6\text{-}C_6H_3Br_2)_2$ and tri-*n*-butyltin hydride

1,9-decadiene (1.00 g, 500 equiv.) was charged to a 50 mL round bottom flask equipped with a Kontes™ valve and a magnetic stir bar in an argon-purged drybox. The pre-catalyst, $WOCl_2(O\text{-}2,6\text{-}C_6H_3Br_2)_2$ (1 equiv.), was then added to the reaction flask and the mixture was stirred for 10 minutes under an argon atmosphere. The flask was sealed and taken from the drybox to a high vacuum Schlenk line where it was heated to 65 °C under a slow argon stream. Tri-*n*-butyltin hydride (2.5 equiv.), was then added *via* syringe to the mixture, and heating continued until a distinct color change (from dark red to black/dark orange) was observed. At this point, the flask was closed and the pressure was slightly reduced by a short evacuation. The mixture was heated in a closed system for ca. 2 h, or until a significant increase in viscosity was appreciable. Exposure of the mixture to constant vacuum was then provided, and the polymerization continued for 48-72 h or until no further ethylene evolution was observed. The crude polymer was dissolved in chloroform or toluene, filtered through a short pad of celite and added dropwise into stirring, cold acetone or methanol. Collection of the polymer by filtration, ad drying under vacuum for 12 h, afforded pure polyoctenylene in high yields (75-95 %)

Polymerization of 1,9-decadiene with $WOCl_2(O\text{-}2,6\text{-}C_6H_3Br_2)_2$ and tetrabutyltin (general polymerization procedure)

1,9-decadiene (1.00 g, 500 equiv.) was charged to a 50 mL round bottom flask equipped with a Teflon Rotoflo valve and a magnetic stir bar in an argon-purged drybox. The pre-catalyst, $WOCl_2(O\text{-}2,6\text{-}C_6H_3Br_2)_2$ (1 equiv.), was then added to the reaction flask and the mixture was stirred for 10 minutes under an argon atmosphere. Tetrabutyltin (2.5 equiv.), was then added *via* syringe to the mixture. The flask was sealed and taken from the drybox to a high vacuum Schlenk line where it was heated to 85 °C under a slow argon stream. Vigorous evolution of ethylene was observed during the first six hours of reaction. After this time, the reaction mixture was exposed to continuous vacuum and stirred for 48 hours or until magnetic stirring became impossible due to the viscosity of the mixture. The heat was removed and the solid residue was dissolved in hot toluene prior to its precipitation into stirring cold acetone or methanol. High yields were observed in all polymerization reactions (75-97 %).

ADMET polymerization of 1,8-nonadiene

In an argon-purged atmosphere, dry 1,8-nonadiene (1.00 g, 8.1 mmol, 500 equiv.), $WOCl_2(O\text{-}2,6\text{-}C_6H_3Br_2)_2$ (12.5 mg, 16 μmol, 1 equiv.), and tetrabutyltin (11 μL, 32 μmol, 2 equiv.) were charged to a 50 mL flask equipped with a Kontes™ valve and a magnetic stirbar. The flask was sealed, taken to a Schlenk line, and subsequently heated to 85 °C under a slow argon stream. After ca. 1 h, ethylene evolution was evident, and the mixture viscosity increased steadily therefrom. Polymerization was completed by leaving the system under vacuum at 85 °C for 24 h. After this time, the reaction was stopped by

exposing the mixture to the atmosphere. Chloroform was added to the crude mixture, and the resulting solution was added dropwise to cold, stirring acetone, affording pure polyheptenylene. The purified polymer was filtered and dried under vacuum at room temperature for 14 h. Yield: 84 %. ^{1}H-NMR ($CDCl_3$) δ (ppm) = 5.36 (2H); 1.98 (4H); 1.27 (6H). ^{13}C-NMR ($CDCl_3$) δ (ppm) = 130.3 (*trans* *C*H=*C*H-CH_2-); 129.8 (*cis* *C*H=*C*H-CH_2-); 32.6; 29.6; 29.5; 28.8; 28.7; 27.2 (allylic, *cis* CH=CH-*C*H_2-).

ADMET polymerization of 9-decenyl 10-undecenoate (**37**)

In an argon-purged drybox, monomer **37** (500 mg, 1.6 mmol, 100 equiv.), $WOCl_2$(O-2,6-$C_6H_3Br_2$)$_2$ (12 mg, 16 μmol, 1 equiv.) and tetrabutyltin (11 μL, 32 μmol, 2 equiv.) were charged to a 50 mL flask adapted with a Kontes™ valve and a magnetic stirbar. The resulting mixture was stirred at room temperature for 10 minutes and the flask was taken to a Schlenk line, where its contents were heated to 80 °C under argon. The pressure of the system was reduced by a short evacuation to the line, and bubbling was observed after ca. 30 min. Short evacuations were performed every 20 minutes thereafter. Ethylene evolution and a viscosity increase suggested the formation of polymer. The mixture was stirred for 20 hours, and the reaction was stopped by opening the valve to the atmosphere. The polymer was purified by dissolving the crude mixture in $CHCl_3$ and adding dropwise the resulting solution into cold, stirring acetone. The purified polymer was isolated by filtration, and dried under vacuum at room temperature. Yield: 355 mg (71 %). ^{1}H-NMR ($CDCl_3$) δ (ppm) = 5.4 (2H); 4.0 (t, 2H); 2.4 (t, 2H); 1.9 (4H); 1.6 (4H); 1.2-1.4 (20H). ^{13}C-NMR ($CDCl_3$) δ (ppm) = 173.9 (C=O); 130.3 (*trans* *C*H=*C*H-CH_2); 129.8 (*cis* *C*H=*C*H-CH_2-); 64.4 (-COO-*C*H_2-); 34.4 (-*C*H_2-COO-); 32.6

(allylic, *trans* CH=CH-*C*H_2-); 29.7; 29.6; 29.4; 29.3; 29.2; 29.2; 29.1; 28.6; 27.2 (allylic, *cis* CH=CH-*C*H_2-); 25.9; 25.0.

Experimental for Chapter 3

Semiempirical calculations

All calculations were performed using Hyperchem Pro release 5.1 for Windows (Hyperchem Professional Release 5.1 for Windows. Hypercube Inc., Gainesville, FL, USA, 1997). Charge data were extracted from AM1 calculations on the phenoxide anion (singlet multiplicity declared in all cases) following an initial geometry optimization routine of the parent phenol using the MM+ force field module.

Synthesis of *trans*-bis(2,6-dibromo-4-fluorophenoxy)tungsten (VI) oxychloride

In a flame-dried 125 mL Schlenk flask equipped with a reflux condenser and a magnetic stirbar, a solution of 2,6-dibromo-4-fluorophenol (1.48 g, 5.5 mmol, 2.2 equiv.) in 10 mL toluene was added via cannula to a solution of tungsten (VI) oxychloride (0.86 g, 2.5 mmol, 1 equiv.) in 15 mL of anhydrous toluene. The resulting dark purple solution was refluxed under an argon stream for 6 h. After this time, the solvent was removed in vacuo, and a dark red solid was obtained. Recrystallization from CH_2Cl_2/*n*-pentane yielded complex **46** as a dark red microcrystalline solid in 66 % yield (1.21 g). ^{1}H-NMR ($CDCl_3$) δ (ppm) = 7.39 (d, $^3J_{H\text{-}F}$ = 8.0 Hz). ^{19}F-NMR ($CDCl_3$) δ (ppm) = -110.2 (t, $^3J_{H\text{-}F}$ = 7.3 Hz). Elemental Anal. Calcd for $C_{12}H_4Br_4Cl_2F_2O_3W$: C, 17.83; H, 0.50. Found: C, 17.91; H, 0.40.

Single crystal X-ray diffraction data were collected at 173 K on a Siemens SMART PLATFORM equipped with a CCD area detector and a graphite monochromator utilizing MoK_α radiation (λ = 0.71073 Å). Cell parameters were refined using 8192 reflections. A hemisphere of data (1381 frames) was collected using the ω-scan method (0.3 frame width). The first 50 frames were remeasured at the end of data collection to monitor instrument and crystal stability (maximum correction on *I* was < 1 %). Psi scan absorption corrections were applied based on the entire data set. The structure was solved by the Direct Methods in *SHELX97,* and refined using full-matrix least squares. The non-H atoms were treated anisotropically, whereas the hydrogen atoms were calculated in ideal positions and were riding on their respective carbon atoms. A total of 218 parameters were refined in the final cycle of refinement using 3878 reflections with $I > 2s(I)$ to yield R_1 and wR_2 of 2.40 % and 5.98 % respectively. Refinement was done using F^2.

Synthesis of *trans*-bis(2,4,6-tribromophenoxy)tungsten (VI) oxychloride

A solution of 2,4,6-tribromophenol (3.82 g, 11.55 mmol, 1.96 equiv.) in 40 mL of anhydrous toluene was added to a solution of tungsten (VI) oxychloride (2.01 g, 5.88 mmol, 1.00 equiv.) in 40 mL of anhydrous toluene placed in a 250 mL Schlenk flask, and the resulting dark purple solution was refluxed under argon for 14 h. Removal of the solvent in vacuo yielded a dark purple/black solid. Dry CH_2Cl_2 (40 mL) was used to dissolve the solid, but only partial dissolution was observed after filtration. The filtered solid (3.89 g, 71%) was characterized as the product. Addition of a layer of *n*-pentane to

the filtrate, and storage at –30 °C for 40 days afforded X-ray quality single crystals. ^{1}H-NMR ($CDCl_3$) δ (ppm) = 7.60 (s). Elemental Anal. Calcd for $C_{12}H_4Br_6Cl_2O_3W$: C, 15.49; H, 0.43. Found: C, 15.24; H, 0.38.

Single crystal X-ray diffraction data were collected at 173 K on a Siemens SMART PLATFORM equipped with a CCD area detector and a graphite monochromator utilizing MoK_α radiation (λ = 0.71073 Å). Cell parameters were refined using 6813 reflections. A hemisphere of data (836 frames) was collected using the ω-scan method (0.3° frame width). The first 50 frames were remeasured at the end of data collection to monitor instrument and crystal stability (maximum correction on *I* was < 1 %). Psi scan absorption corrections were applied based on the entire data set. The structure was solved by the Direct Methods in *SHELX97,* and refined using full-matrix least squares. The non-H atoms were treated anisotropically, whereas the hydrogen atoms were calculated in ideal positions and were riding on their respective carbon atoms. A total of 218 parameters were refined in the final cycle of refinement using 3826 reflections with $I > 2s(I)$ to yield R_1 and wR_2 of 2.58 % and 6.28 % respectively. Refinement was done using F^2.

Synthesis of 2,6-dibromo-4-(trifluoromethyl)-phenol

In a 125 mL erlenmeyer flask, a solution of 4-(trifluoromethyl)phenol (á,á,á-trifluoro-*p*-cresol) (5.00 g, 30.9 mmol) in ca. 70 mL deionized water was stirred at room temperature, while bromine was added dropwise until the product precipitated as a white thick oil. The product was kept in the liquid state by heating the flask with a heat gun (ca. 80 °C), and bromine was added until no further decoloration was observed and a

faint yellow color was kept in the bottom phase. Cooling to room temperature afforded the crude phenol. The water was decanted and the product was dissolved in warm *n*-pentane, dried with $MgSO_4$, and filtered. The solution volume was reduced, crystallization was started at room temperature and completed by placing the product solution in the refrigerator overnight. The first batch of crystals was collected by decanting the solution and air-drying the solid product. A second batch of crystals was obtained by slow evaporation of the solvent from the decanted solution. Combined yield: 8.89 g (89 %). The product was dried overnight under vacuum. ^{1}H-NMR ($CDCl_3$) δ (ppm) = 7.72 (s, 2H); 6.16 (s, 1H). ^{19}F-NMR ($CDCl_3$) δ (ppm) = -62.4 (s).

Synthesis of *trans*-bis(2,6-dibromo-4-(trifluoromethyl)phenoxy)tungsten (VI) oxychloride

In an argon-purged drybox, tungsten (VI) oxychloride (1.02 g, 2.98 mmol, 1.0 equiv.) was charged to a 150 mL Schlenk flask, and dissolved in 10 mL of anhydrous toluene. The flask was sealed and taken to a Schlenk line, where a condenser was attached. A solution of 2,6-dibromo-4-(trifluoromethyl)phenol (1.90 g, 5.94 mmol, 1.99 equiv.) in 15 mL anhydrous toluene was then added via cannula, and the resulting mixture was refluxed for 48 h under argon. Removal of the solvent in vacuo afforded a dark red solid. Recrystallization of the title complex was performed using *n*-pentane at -30 °C. The combined yield after 3 attempted recrystallizations was 1.46 g (54 %). X-ray quality single crystals were grown from concentrated CH_2Cl_2/toluene solutions in a drybox at –30 °C. ^{1}H-NMR ($CDCl_3$) δ (ppm) = 7.89. ^{19}F-NMR ($CDCl_3$) δ (ppm) = -62.9 (s). Elemental Anal. Calcd for $C_{14}H_4Br_4Cl_2F_6O_3W$: C, 18.51; H, 0.44. Found: C, 18.99; H, 0.58.

Synthesis of *trans*-bis(2,6-dibromo-4-cyanophenoxy)tungsten (VI) oxychloride

In an argon-purged drybox, tungsten (VI) oxychloride (2.00 g, 5.85 mmol, 1.0 equiv.) was charged to a 200 mL Schlenk flask, and dissolved in 40 mL of anhydrous toluene. The flask was sealed and taken to a Schlenk line, where a condenser was attached. A solution of 3,5-dibromo-4-hydroxybenzonitrile (3.41 g, 12.3 mmol, 2.10 equiv.) in 50 mL anhydrous toluene was then added via cannula, and the resulting mixture was heated to 60 °C for 4 h under an argon stream to ensure slow evaporation of the diethyl ether. The solution was then refluxed for an additional 48 h. Removal of the toluene in vacuo afforded a red solid. A series of two recrystallizations of the title complex in CH_2Cl_2/*n*-pentane at -30 °C afforded 3.19 g (66 %) of a red microcrystalline solid. Attempts to obtain X-ray quality crystals turned futile. ^{1}H-NMR δ (ppm) = 7.92 (s). Elemental Anal. Calcd for $C_{14}H_4Br_4Cl_2N_2O_3W$: C, 20.44; H, 0.49; N, 3.41. Found: C, 18.92; H, 0.69, N, 3.02.

ROMP of dicyclopentadiene

Solution polymerization of dicyclopentadiene experiments were conducted as follows: A solution of the tungsten precatalyst and the organotin activator in anhydrous toluene was heated to 85 °C. After 5-10 minutes, a 2 M solution of DCPD was added via syringe. Immediate gelation was observed in all cases, and the polymer was purified by addition of methanol to the swollen polymer in hot toluene. The polymer was dried in a vacuum oven (50 °C) for 48 h until constant weight was obtained. Yields were almost

quantitative in all cases although gas chromatography revealed the presence of small amounts (not determined) of dicyclopentadiene in the combined extracts.

Bulk polymerization of dicyclopentadiene was conducted by warming up DCPD (35-40 °C) in glass vials, and adding the corresponding amount of precatalyst and cocatalyst directly to the liquid monomer. Heating of the resulting mixture for 6-24 h afforded solid, crosslinked polydicyclopentadiene which was not characterized.

ROMP of norbornene

A solution of precatalyst (1.0 equiv.) and activator (2.5 equiv.) in anhydrous toluene was heated to 85 °C in a Schlenk flask equipped with a rubber septum and a magnetic stirbar under an argon atmosphere. After 5-10 minutes, a 2 M solution of norbornene (100 equiv. monomer) was added to the original mixture via syringe and an immediate color change could be observed along with an increase in the mixture viscosity. The polymerizations were stopped after 15 minutes for comparison of molecular weights at less than 100% conversion by the addition of methanol containing a small amount of BHT to the reaction mixtures. The solid polymers were decanted, redissolved in $CHCl_3$, filtered through a pad of celite, precipitated into methanol-BHT and dried under vacuum at room temperature. Spectral data for all polynorbornene samples obtained in our study matched the reported literature values (Ivin 1997).

RCM of diethyl diallylmalonate

A solution of precatalyst (1.0 equiv.) and activator (2.5 equiv.) in anhydrous toluene was heated to 85 °C in a Schlenk flask equipped with a rubber septum and a

magnetic stirbar under an argon atmosphere. After 5-10 minutes, neat diethyl diallylmalonate (25 equiv. unless specified) was added via syringe and the resulting mixture (1 M in diene) was stirred for and additional 4 h or until gas chromatography suggests a constant substrate to product ratio. The mixture was then cooled to room temperature and passed through a pad of celite. Removal of the solvent in vacuo afforded crude product, and no further purification was performed. Substrate to product ratios were found by cross correlation of gas chromatography (using either α-ionone and ^{1}H NMR data (integration of allylic methylene groups in both product and staring material.)

Experimental for Chapter 4

Synthesis of bis(4-pentenyl)di-*n*-butylstannane (**73**)

A clean, dry, 250 mL three-neck reaction flask equipped with a reflux condenser, a 125 mL addition funnel, and a magnetic stir-bar was purged with argon and charged with 2.35 g (97.0 mmol, 3.6 equiv.) of freshly ground magnesium turnings and 40 mL of anhydrous diethyl ether. 5-Bromo-1-pentene (12.1 g, 81.0 mol, 3.0 equiv.) in 60 mL of dry ether was then added to the reaction mixture in small portions *via* the addition funnel until the reaction began to reflux. The remainder of the solution was then added at a rate that maintained a gentle reflux. The reaction was allowed to stir for 0.5 hours and then refluxed for 1 hr. The reaction was cooled to room temperature, and 8.19 g (26.9 mmol, 1.0 equiv.) of di-*n*-butyltin dichloride in 40 mL of ether was added dropwise *via* the addition funnel over a period of 2.5 hours. Upon completion of the addition, the reaction was stirred for 1 hour and then refluxed for 20 hours. The reaction was cooled to room temperature, and the solution was poured into 300 mL of ice cold 1 M aqueous NH_4Cl

solution. The organic layer was separated, washed with 300 mL (3 × 50 mL) of deionized H_2O, dried over $MgSO_4$, filtered, and concentrated *in vacuo*. The remaining liquid was dried over CaH_2 under Schlenk vacuum for 48 hours before being fractionally distilled under full Schlenk vacuum with collection of the fraction boiling at 148-150 °C. The collected colorless liquid was vacuum-transferred to a Kontes™ flask and subject to several freeze-pump-thaw cycles. Yield: 6.91 g (69 %). ^{1}H-NMR ($CDCl_3$): δ (ppm) = 5.8 (m, 2 H); 4.9 (m, 4 H); 2.1 (q, 4 H); 1.6 (m, 4H); 1.5 (m, 4H); 1.3 (m, 4H); 0.9(m, 14H). ^{13}C-NMR ($CDCl_3$) δ (ppm) = 138.7 (CH_2=*C*H-), 114.4 (*C*H_2=CH-), 38.6 (CH_2=CH-*C*H_2-), 29.3 (CH_2=CH-CH_2-*C*H_2-CH_2-Sn), 27.4 (CH_3-CH_2-*C*H_2-CH_2-Sn), 26.6 (CH_3-*C*H_2-CH_2-CH_2-Sn), 13.7 (*C*H_3-CH_2-CH_2-CH_2-Sn), 8.8 (CH_2=CH-CH_2-CH_2-*C*H_2-Sn), 8.6 (CH_3-CH_2-CH_2-*C*H_2-Sn). ^{119}Sn-NMR (C_6D_6) δ (ppm) = -13.0.

Synthesis of bis(4-pentenyl)dimethylstannane

Magnesium powder (2.97 g, 122 mmol, 3.6 equiv.) was charged to a flame-dried three neck flask equipped with a reflux condenser, an addition funnel and a stirbar. The metal was suspended in 40 mL anhydrous diethyl ether, and a solution of 4-bromo-1-pentene (15.2 g, 102 mmol, 3.0 equiv.) in anhydrous diethyl ether (60 mL) was added dropwise via the addition funnel at a rate that maintained a gentle reflux. The reaction was refluxed for an additional 2 h, and cooled to room temperature. A solution of dimethyltin dichloride in anhydrous THF was then added via the addition funnel over a period of 2 h, and the resulting mixture was refluxed for 20 h. The reaction was cooled to room temperature, diluted with 200 mL diethy ether, and carefully poured over ice cold 1

M NH_4Cl. The organic layer was separated, and the aqueous layer was extracted with diethyl ether (3 × 50 mL). The organics were combined, washed with deionized water (3 $_4$. Removal of the solvent in vacuo yielded ca. 11 g of a pale yellow liquid, which was dried overnight over CaH_2, fractionally distilled, and vacuum transferred to a Kontes^{TM} flask. Yield: 6.8 g (67 %). ^{1}H-NMR ($CDCl_3$): δ (ppm) = 5.77 (ddt, 2 H); 4.95 (m, 4 H); 2.02 (q, 4 H); 1.56 (m, 4H); 0.80 (t, 4H); 0.04 (s, $^2J_{H\text{-}Sn}$ = 54 Hz, 6H). ^{13}C-NMR ($CDCl_3$) δ (ppm) = 138.7 (CH_2=*C*H-), 114.4 (*C*H_2=CH-), 38.3 (CH_2=CH-*C*H_2-), 26.3 (CH_2=CH-CH_2-*C*H_2-CH_2-Sn), 9.9 (CH_2=CH-CH_2-CH_2-*C*H_2-Sn), -11.5 (*C*H_3- Sn). ^{119}Sn-NMR (C_6D_6) δ (ppm) = -2.5.

Synthesis of bis(4-pentenyl)diphenylstannane

A flame-dried 250 mL three-neck flask was adapted with a condenser and a 125 mL addition funnel under an argon atmosphere. Magnesium powder (1.11 g, 45.6 mmol, 2.8 equiv.). was charged to the flask and suspended in 25 mL anhydrous diethyl ether. A solution of 5-bromopentene (6.00 g, 40.3 mmol, 2.5 equiv.) in 30 mL anhydrous diethyl ether was then added dropwise (via the addition funnel) at a rate that maintained a gentle reflux. The reaction was kept under reflux for one hour after the addition had finished, and a solution of diphenyltin dichloride (5.58 g, 16.2 mmol, 1.0 equiv.) in ca. 40 mL dry diethyl ether was added over a period of 2 h via the addition funnel. The remaining mixture was refluxed for 72 h. The reaction was cooled to room temperature, diluted with ca. 100 mL diethyl ether and carefully poured over cold 1 M NH_4Cl. The organic layer was separated, the aqueous layer was washed with diethyl ether (3 × 25 mL) and the organics were combined and washed with deionized water (3 × 25 mL). The resulting

solution was dried with $MgSO_4$, filtered and the solvent was removed in vacuo, yielding a pale yellow liquid. The product was distilled from CaH_2 at reduced pressure (bp 142 °C at 0.1 mm Hg), vacuum transferred to a Kontes^{TM} flask in a high vacuum line, and degassed by several freeze-pump-thaw cycles. Yield: 3.62 g (55 %). ^{1}H-NMR (C_6D_6): δ (ppm) = 7.48 (d, 4H); 7.18 (m, 6H); 5.66 (m, 2 H); 4.94 (m, 4 H); 2.02 (q, 4 H); 1.66 (m, 4H); 1.22 (t, 4H). ^{13}C-NMR (C_6D_6) δ (ppm) = 140.6 (aromatic, ipso); 138.9 (CH_2=*C*H-CH_2-); 137.6 (aromatic, *ortho*); 129.3 (aromatic, *meta*, *para*); 115.6 (*C*H_2=CH-CH_2-), 39.1 (CH_2=CH-*C*H_2-); 27.0 (CH_2=CH-CH_2-*C*H_2-CH_2-Sn); 10.5 (CH_2=CH-CH_2-CH_2-*C*H_2-Sn). ^{119}Sn-NMR (C_6D_6) δ (ppm) = -70.0. CI-MS: 335 ($C_{16}H_{24}Sn$) 100 %.

Polymerization of **73** using Mo(=CHMe$_2$Ph)(N-2,6-C_6H_3-^{i}Pr$_2$)(OCMe(CF$_3$)$_2$)$_2$ (**26**)

Monomer **73**, (1.02 g, 2.75×10^{-3} mol, 500 equiv.) was charged to a 35 mL round bottom flask equipped with a Teflon Rotoflo valve and a magnetic stir-bar in an argon-purged drybox. Catalyst **26**, (5 mg, 6.5×10^{-6} mol, 1 equiv.) was then charged to the reaction vessel. The valve was sealed and the flask was taken from the drybox to a high-vacuum Schlenk line and evacuated while stirring *via* magnetic agitation. The polymerization was allowed to stir at room temperature until the viscosity of the reaction mixture hindered free mixing (approximately 12 hours). The temperature was then raised to 45 °C for 24 hours and then to 60 °C for 48 hours. The polymerization was terminated by exposure of the evacuated vessel to the atmosphere. The polymer mixture was then dissolved in $CDCl_3$ and characterized *via* proton and quantitative carbon NMR. The polymer mixture was then precipitated into vigorously stirring cold methanol from which polymer **75** was isolated in approximately quantitative yield. ^{1}H-NMR: δ (ppm) = 5.4 (m,

br, 2H); 2.0 (m, br, 4 H); 1.5 (m, 8H); 1.3 (m, 4H); 0.9 (m, 14H). ^{13}C-NMR: δ (ppm) = 29.3; 27.4; 27.3; 27.2; 13.8; 8.8; 8.7. ^{119}Sn-NMR: δ (ppm) = -12.8 (*trans-trans*); -13.0 (*trans-cis*); -13.2 (*cis-cis*).

Polymerization of **73** using $WOCl_2(O\text{-}2,6\text{-}C_6H_3\text{-}Br_2)_2$ (**32**)

Monomer **73**, (1.016 g, 2.737×10^{-3} mol, 250 equiv.) was charged in a 50 mL round bottom flask equipped with a Teflon Rotoflo valve and a magnetic stir-bar in an argon-purged drybox. Aryloxy tungsten complex **32**, (8 mg, 1.035×10^{-5} mol, 1 equiv.) was then charged to the reaction vessel and the mixture was stirred for 10 minutes under argon. The valve was then sealed and the flask was taken from the dry box to a high vacuum Schlenk line and evacuated while being stirred *via* magnetic agitation. The temperature was slowly raised to 70 °C and vigorous evolution of ethylene was observed during the first 36 hours of reaction. The system was then heated to 90 °C and kept at this temperature until the magnetic stirring was no longer possible due to the viscosity of the mixture. The reaction was then allowed to cool to room temperature and dissolved in dry $CDCl_3$. The crude polymer was characterized by tin, proton, and quantitative carbon NMR. Further purification of the polymer was performed by precipitation of the polymer from dry $CDCl_3$ into dry methanol using standard Schlenk techniques. Yield: 75%. ^{1}H-NMR: δ (ppm) = 5.4 (m, br, 2H); 1.9 (m, br, 4 H); 1.5 (m, 8H); 1.3 (m, 4H); 0.9 (m, 14H). ^{13}C-NMR: δ (ppm) = 130.3 (*trans*); 129.7 (*cis*); 37.4 (allylic, *trans*); 32.2(allylic, *cis*); 29.3; 27.4; 27.2; 13.7; 8.8; 8.7. ^{119}Sn-NMR: δ (ppm) = -12.8 (*trans-trans*); -13.0 (*trans-cis*); -13.2 (*cis-cis*).

Polymerization of bis(4-pentenyl)diphenylstannane (**83**) with $Mo(=CHMe_2Ph)(N\text{-}2,6\text{-}C_6H_3\text{-}^iPr_2)(OCMe(CF_3)_2)_2$ (**26**)

In an argon-purged drybox, the molybdenum alkylidene **26** (5 mg, 1 equiv.) was charged to a 50 mL Kontes™ flask. Neat bis(4-pentenyl)diphenylstannane (0.6 g, 250 equiv.) was then added and with stirring, and vigorous bubbling evidenced the polymerization reaction . The flask was sealed, taken to a high vacuum Schlenk line, and the reaction mixture was exposed to vacuum, continuing the polymerization at room temperature. The viscous reaction mixture was stirred until no further bubbling was observed or until the increased viscosity prevented magnetic agitation. Exposure of the reaction mixture to the atmosphere yielded the expected polymer in almost quantitative yield as a viscous liquid, which was characterized without further purification. ^{1}H-NMR: δ (ppm) = 5.4 (m, br, 2H); 1.9 (m, br, 4 H); 1.5 (m, 8H); 1.3 (m, 4H); 0.9 (m, 14H). ^{13}C-NMR: δ (ppm) = 130.3 (*trans*); 129.7 (*cis*); 37.4 (allylic, *trans*); 32.2(allylic, *cis*); 29.3; 27.4; 27.2; 13.7; 8.8; 8.7. ^{119}Sn-NMR: δ (ppm) = -12.8 (*trans*-*trans*); -13.0 (*trans*-*cis*); -13.2 (*cis*-*cis*).

Ring closing metathesis of bis(3-butenyl)di-*n*-butylstannane using $WOCl_2(O\text{-}2,6\text{-}C_6H_3\text{-}Br_2)_2$ (**32**)

A solution of complex **32** (43 mg, 56 μmol, 1 equiv.) in 30 mL anhydrous toluene was placed in a flame-dried Schlenk flask adapted with a condenser and a magnetic stirbar. Bis(3-butenyl)-di-*n*-butylstannane (1.00 g, 2.9 mmol, 52 equiv.) was then added via syringe, and the system was heated to 80-90 °C for 2 h. Decomposition of the catalyst was evident due to a blue/green color in the solution. The mixture was cooled to room

temperature and filtered through a bed of celite. Removal of the solvent in vacuo yielded 590 mg (64.3 %) of a colorless liquid. Chromatographic and NMR analysis of the liquid showed that it was essentially the expected product 1,1-di-*n*-butyl-1-stannacyclohept-4-ene, containing a small amount of starting material. ^{1}H-NMR δ (ppm) = 5.68 (t, 2H); 2.32 (q, 4H); 1.40 (m, 4H); 1.18 (m, 4H); 0.96 (t, 4H); 0.80-0.60 (m, 10H). ^{13}C-NMR: δ (ppm) = 132.8; 29.1; 27.2; 23.7; 13.7, 10.6; 10.2. ^{119}Sn-NMR: δ (ppm) = -33.2.

Synthesis of 6,6,7,7-tetrabutyl-6,7-distanna-1,11-dodecadiene

In a flame-dried Schlenk tube, a solution of 1.24 g (4.05 mmol, 1.0 equiv.) of Bu_2SnCl_2 in 6 mL of anhydrous diethyl ether was added via syringe to neat Bu_2SnH_2 (1.01 g, 4.26 mmol, 1.05 equiv.), and this mixture was stirred under an argon atmosphere for 15 minutes. Dry pyridine (33 µL, 0.40 mmol, 0.1 equiv.) was added, and the mixture was stirred for an additional 4 h. The solvent was removed *in vacuo* and the colorless liquid obtained was weighed and redissolved in 5 mL of diethyl ether (*Solution 1*).

A suspension of powdered Mg (0.294 g, 12.11 mmol, 3.0 equiv.) in diethyl ether (6 mL) was kept in a flame-dried three-neck round bottomed flask under an argon atmosphere. A solution of freshly distilled 5-bromo-1-pentene (1.67 g, 11.18 mmol, 2.75 equiv.) in diethyl ether (6 mL) was then slowly added and this mixture was refluxed for 2 h, time after which *Solution 1* was slowly dropped using an addition funnel. The resulting mixture was refluxed for 20 h, cooled to room temperature and the supernatant solution was cannula-filtered to a Schlenk tube. Addition of pentane (15 mL) and a second cannula filtration afforded a solution which was washed twice with ice-cold 1 M NH_4Cl

(2 × 15 mL), dried over $MgSO_4$ and filtered through a pad of silica gel. The solvent was removed *in vacuo* and 1.44 g (64%) of a colorless viscous liquid were obtained. This product is a mixture of the three tin containing dienes 6,6-dibutyl-6-stanna-1,10-undecadiene, 6,6,7,7-tetrabutyl-6,7-distanna-1,11-dodecadiene, and 6,6,7,7,8,8-hexabutyl-6,7,8-tristanna-1,12-tridecadiene in an undetermined ratio. ^{1}H-NMR: δ (ppm) = 5.7-5.9 (m, 2 H); 5.0-5.2 (m, 4 H); 2.0-2.2 (m, 4 H); 1.6-1.9 (m); 1.3-1.6 (m); 1.3-1.1 (m); 0.8-1.1 (m). ^{13}C-NMR: δ (ppm) = 139.2 (CH_2=*C*H-CH_2-), 115.5 (*C*H_2=CH-CH_2-), 39.5 (CH_2=CH-*C*H_2-), 33.9, 31.7, 30.2, 28.9, 28.5, 27.5, 14.5, 11.6-11.3, 10.9-10.6, 9.6-9.3. ^{119}Sn-NMR: δ (ppm) = -12.4 (**73**, C-*Sn*-C), -76.4 (**91**, C-Sn-Sn-*Sn*-C), -83.5 (**90**, C-Sn-*Sn*-C), -227.3 (**91**, C-Sn-*Sn*-Sn-C). Elemental Anal. Calcd for $C_{26}H_{54}Sn_2$: C, 51.70; H, 9.01. Found: C, 51.67; H, 8.76. HR-MS for $C_{22}H_{45}Sn_2$ ((**90**)-C_4H_9). Calcd: 547.1569 m/z. Found 547.1579 m/z (Average of two analysis).

ADMET polymerization of **92**

In an argon purged dry box, catalyst (**26**) (5 mg) was weighed and placed in a 50 mL round bottomed flask adapted with a Rotoflo valve. The monomer mixture (**92**) (400 mg) was then added to the flask which was in turn sealed and taken to a high vacuum Schlenk line. Ethylene evolution could be evidenced at room temperature during the first 12 h of reaction. After this time, the system was heated to 60 ºC and the reaction was continued for 24 h. The reaction was stopped by removal of the heat when magnetic agitation became impossible or when no further bubbling could be evidenced, and the crude viscous polymeric product (**93**) was dissolved in C_6D_6. ^{1}H-NMR: δ (ppm) =

5.5-5.6 (b); 2.0-2.4 (b); 1.6-1.9 (m); 1.3-1.6 (m); 1.3-1.1 (m); 0.8-1.1 (m). ^{13}C-NMR: δ (ppm) =131.2, 130.6, 38.7, 38.5, 33.9, 31.7, 30.3, 28.9, 28.5, 14.5, 11.6, 11.0, 9.6. ^{119}Sn-NMR: δ (ppm) = -11.5, -11.6, -11.8; -75.4, -75.5; -82.6, -82.8, -82.9, -83.0; -226.3, -226.4.

Experimental for Chapter 5

Synthesis of bis(4-pentenyl)-diethylgermanium (**113**). (6,6-diethyl-6-germana-1,10-undecadiene)

A flame-dried round bottom flask was adapted with a reflux condenser and an addition funnel. Magnesium powder (2.17 g, 89.3 mmol) was suspended in ca. 40 mL anhydrous diethyl ether. A solution of 5-bromo-1-pentene (10.7 g, 71.4 mmol) in ether (25 mL) was added to the Mg suspension at a rate at which spontaneous reflux was obtained. The Grignard reagent solution was refluxed for an additional hour and cooled to room temperature, prior to the slow addition of a solution of diethylgermanium dichloride (4.80 g, 23.8 mmol) in 25 mL ether. The resulting reaction mixture was refluxed for ca. 24-30 h, cooled to room temperature and carefully poured over ice-cold 1 M NH_4Cl. Extraction with ether, drying over $MgSO_4$ and removal of the solvent *in vacuo*, yielded a pale yellow liquid. Further purification by vacuum fractional distillation, followed by vacuum transfer from CaH_2 afforded 5.17g (89 %) of pure **113**. ^{1}H-NMR δ (ppm) = 5.80 (ddt, 2H, CH_2=C*H*); 4.95 (dd, 4H, C*H*$_2$=CH); 2.05 (dt, 4H, CH-C*H*$_2$); 1.43 (m, 4H, CH_2-C*H*$_2$-CH_2); 1.00 (t, 6H, C*H*$_3$); 0.65-0.74 (8H, Ge-C*H*$_2$). ^{13}C-NMR δ (ppm) = 138.9 (CH_2=*C*H); 114.4 (*C*H_2=CH); 37.8 (CH-*C*H_2); 24.7 (CH_2-*C*H_2-CH_2); 11.5 (CH_2-*C*H_2-Ge); 9.0(*C*H_3); 4.3 (*C*H_2-CH_3). HR-MS: $(M-1)^+$ = 271.1445; 241 ($C_{12}H_{23}Ge$)

72 %; 201 $(C_9H_{19}Ge)^+$ 100 %. Anal. Found: H, 10.61; C, 62.36. $C_{14}H_{28}Ge$. Calc.: H, 10.49; C, 62.52.

Cognate synthesis of bis(3-butenyl)-diethylgermanium (**114**). (5,5-diethyl-5-germana-1,8-nonadiene)

Diene **114** was prepared following the procedure described above. Yield: 77 %. ^{1}H-NMR δ (ppm) = 5.95 (ddt, 2H, CH_2=C*H*); 4.95 (dd, 4H, C*H*$_2$=CH); 2.10 (dt, 4H, CH-C*H*$_2$); 1.05 (t, 6H, C*H*$_3$); 0.90-0.60 (8H, Ge-C*H*$_2$). ^{13}C-NMR δ (ppm) = 141.6 (CH_2=*C*H); 112.8 (*C*H_2=CH); 29.3 (CH-*C*H_2); 11.1 (*C*H_3); 8.9 (*C*H_2-CH_3); 4.4 (CH_2-*C*H_2-Ge). HR MS: $(M-1)^+$ = 241.0953; 213 ($C_{10}H_{19}Ge$) 25 %; 197 ($C_9H_{17}Ge$) 53 %; 187 ($C_8H_{17}Ge$) 100 %; 185 ($C_8H_{15}Ge$) 73 %. Anal. Found: H, 10.26; C, 59.67. $C_{12}H_{24}Ge$. Calc.: H, 10.04; C, 59.83.

Cognate synthesis of bis(4-pentenyl)-dimethylgermanium (**115**). (6,6-dimethyl-6-germana-1,10-undecadiene)

Diene **115** was prepared following the procedure described above. Yield: 55 %. ^{1}H-NMR δ (ppm) = 5.89 (ddt, 2H, CH_2=C*H*); 4.95 (dd, 4H, C*H*$_2$=CH); 2.04 (dt, 4H, CH-C*H*$_2$); 1.44 (m, 4H, CH_2-C*H*$_2$-CH_2); 0.70 (m, 4H, Ge-C*H*$_2$); 0.07 (s, 6H, Ge-C*H*$_3$). ^{13}C-NMR δ (ppm) = 138.9 (CH_2=*C*H); 114.4 (*C*H_2=CH); 37.5 (CH-*C*H_2); 24.6 (CH_2-*C*H_2-CH_2); 15.0 (CH_2-*C*H_2-Ge); -4.2 (*C*H_3-Ge). HR-MS: $(M-1)^+$ = 241.1019; 227 ($C_{11}H_{21}Ge$) 26 %; 173 $(C_7H_{15}Ge)^+$ 100 %. Anal. Found: H, 10.55; C, 57.83. $C_{12}H_{24}Ge$. Calc.: H, 10.04; C, 59.83.

ADMET polymerization of diene **113**: synthesis of polymer **116**

Monomer **113**, (1.00 g, 3.72 mmol) and catalyst **26** (12 mg, ca. 16 μmol) were weighed in an argon-purged drybox and placed into a 25 mL round bottomed flask equipped with a Teflon™ high vacuum valve and a stir bar. The flask was stirred for five minutes in the box, sealed, and taken to a high vacuum Schlenk line, where the reaction mixture was stirred for ca. 48 hours (or until ethylene evolution stopped). Polymerization was terminated by exposing the flask contents to the atmosphere. The crude polymer was taken up in $CDCl_3$ and precipitated from ice-cold methanol. The viscous liquid was dried under vacuum for 24 hours. Attempts to remove catalyst residues by dissolution in $CHCl_3$ followed by filtration through different adsorbents (silica gel, alumina and activated charcoal) were fruitless. Yield 82 %. ^{1}H-NMR δ (ppm) = 5.40 (2H); 2.00 (4H); 1.42 (4H); 1.00 (t, 6H); 0.74 (8H). ^{13}C-NMR δ (ppm) = 130.4 (olefin, *trans*), 129.8 (olefin, *cis*), 36.6 (allylic, *trans*), 31.3 (allylic, *cis*), 25.4, 11.6, 9.0, 4.4. M_n (GPC) = 14 800, M_w/M_n (GPC) = 1.79. T_d (TGA, onset) = 299 °C. $T_{10\%}$ (TGA) = 353 °C. T_g (DSC) = -89 °C.

Cognate polymerization of diene **114**: synthesis of polymer **117**

Diene **114** was polymerized following the procedure described above. Polymer **117** was not purified prior to characterization. Yield: 91 %. ^{1}H-NMR δ (ppm) 5.42, 5.30 (2H); 2.05 (4H); 1.00 (4H); 0.65-0.85 (8H). ^{13}C-NMR δ (ppm) = 131.6 (olefin, *trans*), 131.3 (olefin, *cis*), 28.0 (allylic, *trans*), 22.6 (allylic, *cis*), 11.9, 9.0, 4.5. M_n (GPC) = 18

000, M_w/M_n (GPC) = 1.42. T_d (TGA, onset) = 428 °C. $T_{10\%}$ (TGA) = 428 °C. T_g (DSC) = -98 °C.

Cognate polymerization of diene **115**: synthesis of polymer **118**

Diene **115** was polymerized following the procedure described above, but using catalyst **28**. Yield: 75 %. ^{1}H-NMR δ (ppm) = 5.38 (2H); 2.01 (4H); 1.37 (4H); 0.60-0.80 (4H); 0.04 (s, 6H) ^{13}C-NMR δ (ppm) = 130.4 (olefin, *trans*), 129.8 (olefin, *cis*), 36.4 (allylic, *trans*), 31.0 (allylic, *cis*), 25.4, 25.3, 15.3, 15.1, -4.0, -4.2. M_n (GPC) = 5 300, M_w/M_n (GPC) = 2.31. T_d (TGA, onset) = 244 °C. $T_{10\%}$ (TGA) = 290 °C. T_g (DSC) = Not observable.

REFERENCES

Armstrong, S. K. J. Chem. Soc. Perkin Trans. 1 **1998,** 371.

Balcar, H.; Sedlacek, J. *Macromol. Rapid Commun.* **1994**, *15*, 771.

Balcar, H.; Sedlacek, J.; Pacovska, M.; Blechta, V. *Coll. Czech Chem. Commun.* **1995**, *60*, 489.

Banks, R. L. *CHEMTECH* **1986,** *16,* 112.

Banks, R. L.; Bailey, G. C. *Ind. Eng. Chem., Prod. Res. Dev.* **1964,** *3,* 170.

Barnes, D. L.; Eilerts, N. W.; Heppert, J. A.; Huang, W. H.; Morton, M. D. *Polyhedron* **1994,** *13,* 1267.

Bell, A. *J. Mol. Catal.* **1992,** *76,* 165.

Birot, M.; Pillot, J.-P.; Donogues, J. *Chem. Rev.* **1995,** *95,* 1443.

Brandli, C.; Ward, T. R. *Helv. Chim. Acta* **1998,** *81,* 1616.

Braunstein, P.; Morise, X. *Organometallics* **1998**, *17*, 540.

Brefort, J. L.; Corriu, R. J. P.; Guerin, C.; Hener, B. J. L. *J. Organomet. Chem.* **1994,** *464,* 133.

Brzezinska, K.; Wolfe, P. S.; Watson, M. D.; Wagener, K. B. *Macromol. Chem. Phys.* **1996,** *197,* 2065.

Brzezinska K. R.; Wagener K. B.; Burns, G. T. *J. Poly. Sci. A: Polym. Chem.* **1999,** *37,* 849.

Calderon, N. *Chem. Eng. News* **1967,** *45,* 51.

Calderon, N.; Chen, H. Y.; Scott, K. W. *Tetrahedron Lett.* **1967a,** 3327.

Calderon, N.; Oftstead, E. A.; Judy, W. A. *J. Polymer Sci., A-1* **1967b,** *5*, 2209.

Carothers, W. H. *J. Am. Chem. Soc.* **1929,** *51*, 2548.

Cho, O.-K.; Kim, Y.-H.; Choi, K.-Y.; Choi, S.-K. *Macromolecules* **1990,** *23,* 12.

Crabtree, R. H. *The Organometallic Chemistry of the Transition Metals*; Wiley-Interscience: New York, **1994**, p. 270.

Cummins, C. C.; Beachy, M. D.; Schrock, R. R.; Vale, M. G.; Sankaran, V.; Cohen, R. E. *Chem. Mat.* **1991,** *3,* 1153.

Cummings, S. K.; Ginsburg, E.; Miller, R. D.; Portmess, J. D.; Smith, D. W. in *Sep-Growth Polymers for High Performance Materials;* Hedrick, J. L., Labadie, J. W. Eds.; ACS Symposium Series; Washington, DC, **1996**.

Davidson, T. A.; Wagener, K. B. Acyclic Diene Metathesis (ADMET) Polymerization. In *Synthesis of Polymers;* Schluter, A.-D. Ed.; Materials Science and Technology Series; Wiley-VCH: Wienheim, **1999**, p 105.

Devylder, N.; Hill, M.; Molloy, K. C.; Price, G. J. *Chem. Commun.* **1996,** 711.

Dias, E. L.; Grubbs, R. H. *Organometallics* **1998,** *17,* 2758.

Dias, E. L.; Nguyen, S. T.; Grubbs, R. H. *J. Am. Chem. Soc.* **1997,** *119,* 3887.

Dietz, S. D.; Eilert, N. W; Heppert, J. A.; Morton, M. D. *Inorg. Chem.* **1993,** *32,* 1698.

Dodd, H. T.; Rutt, K. J. *J. Mol. Catal.* **1982,** *15,* 103.

Dodd, H. T.; Rutt, K. J. *J. Mol. Catal.* **1988,** *47,* 33.

Eleuterio, H. S. US Patent No. 3,074,918; **1957**.

Elsenbroich, C.; Salzer, A. *Organometallics: A Concise Introduction*; VCH: New York, **1992**.

Feldman, J.; Murdzek, J. S.; Davis, W. M.; Scrock, R. R. *Organometallics* **1989,** *8,* 2260.

Feldman, J.; Schrock, R. R. *Prog. Inorg. Chem.* **1991,** *39,* 1.

Finkelshtein, E. Sh.; Portnykh, E. B.; Ushakov, N. V.; Gringolts, M. L.; Yamposky, Y. P. *Macromol. Chem. Phys.* **1997,** *198,* 1085.

Flory, P. J. *Principles of Polymer Chemistry*; Cornell University Press: Ithaca, NY, **1953**.

Foucher, D. A.; Edwards, M.; Burrow, R. A.; Lough, A. J.; Manners, I. *Organometallics* **1994,** *13,* 4959.

Furstner, A. *Topic Catal.* **1997,** *4,* 285.

Giger, T.; Wigger, M.; Audetat, S.; Benner, S.A. *Synlett* **1998,** 688.

Grubbs, R. H.; Chang, S. *Tetrahedron* **1998,** *54,* 4413.

Grubbs, R. H.; Khosravi, E. Ring Opening Metathesis Polymerization (ROMP) and Related Processes. In *Synthesis of Polymers;* Schluter, A.-D. Ed.; Materials Science and Technology Series; Wiley-VCH: Wienheim, **1999**, p 65.

Hagihara, N.; Sonogashira, K.; Takahashi, S. *Adv. Polym. Sci.* **1981,** *41,* 149.

Hayashi, T.; Uchimaru, Y.; Reddy, N. P.; Tanaka, M. *Chem. Lett.* **1992,** 647.

Imori, T.; Tilley, T. D. *Polyhedron* **1994,** *13,* 2231.

Imori, T.; Lu, V.; Cai, H.; Tilley, T. D. *J. Am. Chem. Soc.* **1995,** *117,* 9931.

Ivin, K. J.; Milligan, B. D. *Makromol. Chem. Rapid Commun.* **1987,** *8,* 269.

Ivin, K. J.; Mol, J. C. *Olefin Metathesis and Metathesis Polymerization*; Academic Press: San Diego, CA, **1997**, 472 pp.

Jousseaume, B.; Chanson, E. *Synthesis* **1987**, 55.

Kawakami, T.; Suimoto, T.; Shibata, I.; Baba, A.; Matsuda, H.; Sonoda, N. *J. Org. Chem.* **1995**, *60,* 2677.

Kelsey, D. R.; Handlin, D. L.; Narayana, M.; Scardino, B. M. *J. Poly. Sci. A: Polym. Chem.* **1997,** *35,* 3027.

Kershner, J. L.; Fanwick, P. E.; Rothwell, I. P.; Huffman, J. C. *Inorg. Chem.* **1989a,** *29,* 780.

Kershner, J. L.; Torres, E. M.; Fanwick, P. E.; Rothwell, I. P.; Huffman, J. C. *Organometallics* **1989b,** *8,* 1424.

Klosiewicz, D. W. US Patent No. 4,657,981; **1987**.

Leusink, A. J.; Noltes, J. G.; Budding, H. A.; van der Kerk, G. J. M. *Recueil Trav. Chim.* **1964,** *83,* 609.

Lindmark-Hamberg, M.; Wagener, K. B. *Macromolecules* **1987,** *20,* 2949.

Lu, V.; Tilley, T. D. *Macromolecules* **1996,** *29,* 5763.

Manners, I. *Angew. Chem. Int. Ed. Engl.* **1996,** *35,* 1602.

Masuda, T.; Hamano, T.; Higashimura, T.; Ueda, T.; Muramatsu, H. *Macromolecules* **1988,** *21,* 281.

Masuda, T.; Higashimura, T. *Adv. Polym. Sci.* **1986,** *81,* 121.

Masuda, T.; Mishima, K.; Fujimori, J.-I.; Nishida, M.; Muramatsu, H.; Higashimura, T. *Macromolecules* **1992,** *25,* 1401.

Miller, R. D.; Michl, J. *Chem. Rev.* **1989,** *89,* 1359.

Miller, R. D.; Sooriyakumaran, R. *J. Polym. Sci. Polym. Chem. Ed.* **1987,** *25,* 111.

Mochida, K.; Chiba, H. *J. Organomet. Chem.* **1994,** *473,* 45.

Mochida, K.; Hayakawa, M.; Tsuchikawa, T.; Yokoyama, Y.; Wakasa, M.; Hayashi, H. *Chem. Lett.* **1998a,** 91.

Mochida, K.; Maeyama, S.; Wakasa, M.; Hayashi, H. *Polyhedron* **1998b,** *17,* 3963.

Mochida, K.; Ohkawa, T.; Kawata, H.; Watanabe, A.; Ito, O.; Masuda, M. *Bull. Chem. Soc. Jpn.* **1996,** *69,* 2993.

Mochida, K.; Shibayama, N.; Goto, M. *Chem. Lett.* **1998c,** 339.

Nakayama, Y.; Mashima, K.; Nakamura, A. *Macromolecules* **1993,** *26,* 6267.

Nakayama, Y.; Saito, H.; Nakamura, A. *Chem. Lett.* **1996,** 691.

Nel, J. G.; Wagener, K. B.; Boncella, J. M. *Polym. Prepr. (Am. Chem. Soc. Div. Polym. Chem.)* **1989,** *30*(2), 130.

Neumann, W. P.; Pedain, J. *Liebigs Ann. Chem.* **1964a,** *672,* 34.

Neumann, W. P.; Pedain, J. *Tetrahedron Lett.* **1964b,** *36,* 2461.

Nguyen, S. T.; Grubbs, R. H.; Ziller, J. W. *J. Am. Chem. Soc.* **1993,** *115,* 9858.

Noltes, J. G.; van der Kerk, G. J. M. *Recueil Trav. Chim.* **1961,** *80,* 623.

Noltes, J. G.; van der Kerk, G. J. M. *Recueil Trav. Chim.* **1962,** *81,* 41.

Nubel, P. O.; Lutman, C. A.; Yokelson, H. B. *Macromolecules* **1994,** *27,* 7000.

Nugent, W. A.; Feldman, J.; Calabrese, J. C. *J. Am. Chem. Soc.* **1995,** *117,* 8992.

Odian, G. *Principles of Polymerization,* 3 ed.; Wiley Interscience: New York, **1991**, 768 pp.

O'Gara, J. E.; Portmess, J. D.; Wagener, K. B. *Macromolecules* **1993,** *26,* 2837.

Okano, M.; Matsumoto N.; Arakawa, M.; Tsuruta, T.; Hamano, H. *Chem. Commun.* **1998,** 1799.

Peckham, T. J.; Massey, J. A.; Edwards, M.; Manners, I.; Foucher, D. A. *Macromolecules* **1996,** *29,* 2396.

Pomogailo, A. D.; Savost'yanov, V. S. *Synthesis and Polymerization of Metal-Containing Monomers*; CRC Press: Boca Raton, FL, **1994**.

Quignard, F.; Leconte, M.; Basset, J.-M. *J. Mol. Catal.* **1985,** *28,* 27.

Quignard, F.; Leconte, M.; Basset, J.-M. *J. Mol. Catal.* **1986,** *36,* 13.

Quignard, F.; Leconte, M.; Basset, J.-M. *Inorg. Chem.* **1987,** *26,* 4272.

Randall, M. L.; Snapper, M. L. *J. Molec. Catal. A. Chem.* **1998,** *133,* 29.

Reddy, N. P.; Yamashita, H.; Tanaka, M. *J. Chem. Soc. Chem. Commun.* **1995,** 2263.

Rehahn, M. *Acta Polym.* **1998,** *49,* 201.

Reichl, J. A.; Popoff, C. M.; Gallagher, L. A.; Remsen, E. E.; Berry, D. H. *J. Am. Chem. Soc.* **1996**, *118*, 9430.

Schrock, R. R. *J. Am. Chem. Soc.* **1974,** *96,* 6796.

Schrock, R. R. *J. Am. Chem. Soc.* **1975,** *97,* 6577.

Schrock, R. R. *Science* **1983,** *219,* 13.

Schrock, R. R. *Acc. Chem. Res.* **1990,** *23,* 158.

Schrock, R. R. Ring Opening Metathesis Polymerization. In *Ring-Opening Polymerization;* Bruneile, D. J. Ed.; Hanser: Munich, **1993**, p 129.

Schrock, R. R.; DePue, R. T.; Feldman, J.; Yap, K. B.; Yang, D. C.; Davis, W. M.; Park, L.; DiMare, M.; Schoefield, M.; Anhaus, J.; Walborsky, E.; Evitt, E.; Krüger C.; Betz, P. *Organometallics*, **1990a,** *9,* 2262.

Schrock, R. R.; DePue; R. T.; Feldman, J.; Schaverien, C. J.; Dewan, J. C.; Liu, A. H. *J. Am. Chem. Soc.* **1988,** *110,* 1423.

Schrock, R. R.; Murdzek, J. S.; Bazan, G. C.; Robbins, J.; DiMare, M.; O'Regan, M. *J. Am. Chem. Soc.* **1990b,** *112,* 3875.

Schuster, M.; Blechert, S. *Angew. Chem. Int. Ed.* **1997,** *36,* 2037.

Schwab, P.; Grubbs, R. H.; Ziller, J. W. *J. Am. Chem. Soc.* **1996,** *118,* 100.

Sharp, P. R.; Holmes, S. J.; Schrock, R. R. *J. Am. Chem. Soc.* **1981,** *103,* 965.

Shibata, K.; Weinert, C. S.; Sita, L. R. *Organometallics* **1998,** *17,* 2241.

Sita, L. R. *Organometallics* **1992,** *11,* 1442.

Sita, L. R. *Acc. Chem. Res.* **1994,** *27,* 191.

Smith, D. W.; Wagener, K. B. *Macromolecules* **1991,** *24,* 6073.

Steiger, D.; Weder, C.; Smith, P. *Macromolecules* **1999,** *32,* 5391.

Tallarico, J. A.; Bonitatebus, P. J.; Snapper, M. L. *J. Am. Chem. Soc.* **1997,** *119,* 7157.

Tao, D.; Wagener, K. B. *Macromolecules* **1994,** *27,* 1281.

Thorn-Csanyi, E.; Klockmann, O. *Synth. Met.* **1999,** *101,* 664.

Thorn-Csanyi, E.; Timm, H. *J. Mol. Catal.* **1985,** *28,* 37.

Tilley, T. D. *Acc. Chem. Res.* **1993,** *26,* 22.

Tindall, D.; Pawlow, J. H.; Wagener, K. B. Recent Advances in ADMET Chemistry. In *Alkene Metathesis in Organic Synthesis*; Furstner, A., Ed.; Springer-Verlag: Berlin, **1998**, p 183.

Tindall, D.; Wagener, K. B.; Brzezinska, K. R. *Polym. Prepr. (Am. Chem. Soc. Div. Polym. Chem.)* **1999,** *218*(2), 413.

Trefonas, P.; West, R. *J. Polym. Sci.* **1985,** *23,* 2099.

Truett, W. L.; Johnson, D. R.; Robinson, I. M.; Montague, B. A. *J. Am. Chem. Soc.* **1960,** *82,* 2337.

van Schalkwyk, C.; Vosloo, H. C. M.; du Plessis, J. A. K. *J. Mol. Catal. A. Chem.* **1998,** *133*, 167.

Vosloo, H. C. M.; Dickinson, A. J.; du Plessis, J. A. K. *J. Mol. Catal. A. Chem.* **1997,** *115*, 199.

Wagener, K. B.; Boncella, J. M.; Nel, J. G.; Duttweiler, R. P.; Hillmyer, M. A. *Makromol. Chem.* **1990,** *191,* 365.

Wagener, K. B.; Boncella, J. M.; Nel, J. G. *Macromolecules* **1991,** *24,* 2694.

Wagener, K. B.; Brzezinska, K.; Anderson, J. D.; Dilocker, S. *J. Poly. Sci. A: Polym. Chem.* **1997a,** *35,* 3441.

Wagener, K. B.; Brzezinska, K.; Anderson, J. D.; Younkin, T. R.; Steppe, K.; DeBoer, W. *Macromolecules* **1997b,** *30,* 7363.

Wagener, K. B.; Patton, J. *Macromolecules* **1993,** *26,* 249.

Walba, D. M.; Keller, P.; Shao, R. F.; Clark, N. A.; Hillmyer, M.; Grubbs, R. H. *J. Am. Chem. Soc.* **1996,** *118,* 2740.

West, R. *J. Organomet. Chem.* **1986,** *300,* 327.

Wolfe, P. S. Ph.D. Dissteration. University of Florida, **1997**.

Woo, H.-G.; Park, J.-M.; Song, S.-J.; Yang, S.-Y.; Kim, I.-S.; Kim; W.-G. *Bull. Korean Chem. Soc.* **1997,** *18,* 1291.

Yokoyama, Y.; Hayakawa, M.; Azemi, T.; Mochida, K. *J. Chem. Soc., Chem. Commun.* **1995,** 2275.

Zou, W. K.; Yang, N.-L. *Polym. Prepr. (Am. Chem. Soc. Div. Polym. Chem.)* **1992,** *33*(2), 188.

BIOGRAPHICAL SKETCH

Fernando José Gómez Fernández was born in Santiago de Cali, Colombia, on December 26, 1973. He attended his kindergarten, elementary, middle, and high school at Colegio San Antonio Maria Claret, a private Catholic institution where his high school teacher, Mr. Francisco Trujillo, first introduced him to chemistry. Fernando graduated from high school in June of 1989, and began college work at Universidad del Valle.

In the fall of 1992 Fernando visited the University of Florida in Gainesville as an international exchange student, conducting research on metathesis depolymerization in the group of Professor Kenneth Wagener. This experience would positively mark his scientific inclinations. Upon his return to Universidad del Valle, Fernando conducted research in free-radical chemistry in the group of Professor Luz Marina Jaramillo and graduated in August 1995.

Fernando rejoined Professor Wagener's group at the University of Florida in the fall of 1995, where he investigated metal-containing polymers and classical metathesis catalytic systems as part of his graduate research. After receiving his Ph. D. from the University of Florida, Fernando joined the research group of Professor Robert Waymouth at Stanford University, Palo Alto, California, where he began research on metallocene and polyolefin chemistry.